Dopamine Kinetics in a *Drosophila* Model of Parkinson Disease

Eve Privman Champaloux
Potsdam, NY

B.S. in Chemistry, University of Rochester, 2009
B.S. in Neuroscience, University of Rochester, 2009

A Dissertation presented to the Graduate Faculty of the University of Virginia in Candidacy for the Degree of Doctor of Philosophy

Department of Chemistry
Neuroscience Graduate Program
Medical Scientist Training Program

University of Virginia
August 2016

Dedicated to Bronislava Privman with special thanks to my friends, family, and all of the flies who made this work possible.

Abstract

Parkinson disease (PD) is a neurodegenerative movement disorder, with motor symptoms caused by the death of dopaminergic cells in the central nervous system. RING finger protein 11 (RNF11) has been identified in vulnerable neurons of the substantia nigra in Parkinson disease patients, and localized to the Lewy bodies of humans with idiopathic disease. In order to study the effects of RNF11 on dopamine neurotransmission, it was necessary to improve the techniques to detect dopamine at a millisecond time scale in *Drosophila*. Pulsed light stimulations were used alongside Michaelis-Menten modeling to characterize release and uptake of dopamine upon optogenetic stimulation. In order to avoid the electrochemical defect at the switching potential caused by blue light, a red light activated channelrhodopsin, CsChrimson, was characterized and used to measure from a novel region of the central nervous system, the protocerebrum. Using these new techniques, we tested the hypothesis that RNF11 modulates dopamine neurotransmission in *Drosophila* larvae. We identified RNF11 as a protein that may be a target for timely intervention and pharmacological prevention of Parkinson disease progression.

Table of Contents

Table of Figures

Chapter 1: Introduction

Parkinson Disease (PD)

Diagnosis of PD

Parkinson disease (PD) is the most common neurodegenerative movement disorder. It is characterized by the progressive death of dopaminergic neurons. The diagnosis of PD is made symptomatically, since there are no standard ways of confirming diagnosis before autopsy.(Beitz, 2014) Diagnostic symptoms include unilateral tremor, rigidity, masked facial expressions, and gait instability. Non-specific prodromal symptoms such as sleep disturbance, constipation, bladder dysfunction, obesity, and depression can precede clinical diagnosis by decades.(Hawkes et al., 2010) Imaging cannot currently be used to diagnose PD, but some modalities may have limited efficacy in distinguishing it from multisystem atrophy and essential tremor.(Gazewood et al., 2013)

Dopaminergic neurons are found throughout the human body. In the central nervous system, dopaminergic neuron cell bodies are largely clustered in the substantia nigra, ventral tegmental area, posterior and rostral hypothalamus, arcuate nucleus, zona incerta, preoptic area, periventricular nucleus, and the olfactory bulb. From there the dopaminergic cells innervate the brain diffusely via the mesocortical, mesolimbic, and mesostriatal pathways.(Björklund and Dunnett, 2007) Dopamine is also released into the extracellular space in the retina from amacrine cells during the day. The dopamine diffuses away from the amacrine cells to activate cone cells and inhibit rod cells during light hours.(West et al., 2015) Loss of dopaminergic neurons from the substantia nigra pars

compacta causes many of the hallmark symptoms used to diagnose PD, including slowness, rigidity, postural instability, and a pill-rolling resting tremor.(Braak and Del Tredici, 2008)

About half of the body's dopamine is produced in the enteric nervous system.(Eisenhofer et al., 1997) Gastric myenteric plexus cells can suffer similar pathology as central dopaminergic cells in the case of Parkinson disease, developing Lewy bodies.(Hawkes et al., 2010; Pellegrini et al., 2015) In fact, constipation is a peripheral symptom of Parkinson disease that can precede diagnosis by decades.(Singaram et al., 1995; Lin et al., 2014) In Chapter 3 we discuss early changes in dopaminergic cell function that may provide a drug target for early intervention in PD.

Pathology of PD

Microscopic pathological findings of PD include intraneuronal, fibrillar alpha-synuclein inclusions called Lewy bodies and dystrophic neurites called Lewy neurites.(Cookson, 2009; Moon and Paek, 2015) The first sites where Lewy bodies could be found in a patient with PD are the anterior olfactory structures, the dorsal motor nucleus of the vagal nerve, and the enteric nervous system.(Braak and Del Tredici, 2008) The disease seems to begin in distal axons and proceed retrogradely, and there may be separate mechanisms for axon damage and cell death in PD.(Cheng et al., 2010) This has led some to hypothesize that there may be a prion-like spread of misfolded alpha-synuclein.(Tyson et al., 2015) Since the nose and gut are gateways to the body and their corresponding neuronal structures are early sites of PD pathology, it is

thought that environmental damage can cause alpha-synuclein misfolding, which then spreads in a retrograde fashion to the rest of the CNS.(Klingelhoefer and Reichmann, 2015)

Current Treatments for PD

The current available treatments for PD are symptomatic.(Cookson, 2009) They fall into four main categories: L-DOPA, dopamine agonists, MAO-B inhibitors, and deep brain stimulation. Human induced pluripotent stem cell transplants are also being investigated as a method of replacing the damaged dopaminergic neurons, but neuronal stem cell therapy still has many hurdles to overcome before clinical implementation.(Li et al., 2015) For the non-motor symptoms of PD there are adjunct therapies that can be used to improve quality of life as the disease progresses such as amitryptyline for depression without dementia, cholinesterase inhibitors for dementia, polyethylene glycol for constipation, and clozapine for psychosis.(Miyasaki et al., 2006; Zesiewicz et al., 2010)

Levodopa (L-DOPA) remains the most effective drug for treating the symptoms of PD.(Barbeau, 1969; Miyasaki et al., 2002) L-DOPA is the metabolic precursor of dopamine and can cross the blood-brain barrier. It can be used in combination with carbidopa to decrease its peripheral metabolism. However, early use of L-DOPA can lead to abnormal involuntary movements called dyskinesias developing earlier in the disease course.(Gazewood et al., 2013)

Dopamine agonists such as pramipexole and ropinirole stimulate dopamine receptors and can be used instead of levodopa/carbidopa to avoid

dyskinesias. Non-ergot dopamine agonists can cause side effects such as sleepiness and hallucinations and therefore have poorer medication compliance. Ergot-derived dopamine agonists like bromocriptine carry the risk of serosal fibrosis and cardiac side-effects, and are therefore avoided as first-line treatments.(Gazewood et al., 2013)

Monoamine oxidase (MAO-B) inhibitors like selegiline can also be used as monotherapy in early PD. MAO-B inhibitors function by slowing the breakdown of dopamine, leaving more available for repackaging and signaling. Selegiline can be used in combination with L-DOPA to reduce motor fluctuations caused by medications wearing off between doses.(Pahwa et al., 2006)

Deep brain stimulation (DBS) may be considered to improve motor function in patients for whom pharmacological intervention is no longer sufficient.(Pahwa et al., 2006) In up to 53% of patients, there is symptomatic relief when a stimulating electrode is lowered into the thalamic brain tissue, even before the DBS is applied, due to microscopic tissue ablation or local adenosine release.(Chang et al., 2012) DBS dramatically reduces the need for medication to control motor symptoms, which can help limit dyskinesia and other side-effects.(Beitz, 2014) However, the implantation of a DBS electrode requires a major open neurosurgical procedure, and therefore carries the risk of complications such as bleeding, infection, and confusion.(Doshi, 2011; Suzuki et al., 2015)

The ideal therapy for PD would slow disease progression, reduce disability, and minimize complications and side-effects.(Miyasaki et al., 2002)

This would require both a decrease in dopaminergic cell death and a preservation of cell function. In order to achieve these goals, early disease processes need to be studied, like those described in Chapter 3.

Genetic Factors in PD

Just over 10% of PD cases have a known genetic cause. Proteins that have been implicated in the pathogenesis of PD include alpha-synuclein, PINK1, and Parkin.(Lesage and Brice, 2009; Varga et al., 2014). Alpha-synuclein is a small protein that is found in presynaptic cell terminals. Its function is poorly understood, and may involve synaptic vesicle release. It is concentrated in Lewy bodies and Lewy neuritis in PD brain tissue.(Cookson, 2009) Mutations in the alpha-synuclein gene on chromosome 4 are known to cause autosomal dominant familial PD. The first gene found to cause PD was the A53T mutation in alpha-synuclein in the late 1990s.(Polymeropoulos et al., 1997)

PTEN-Induced Kinase 1 (PINK1) and Parkin are proteins involved in the proper turnover of damaged mitochondria, known as mitophagy.(Von Stockum et al., 2015) Homozygous PINK1 mutations in the PARK6 locus can confer autosomal recessive PD.(Valente et al., 2004) Homozygous Parkin mutations in the PARK2 locus confer autosomal recessive juvenile PD.(Kitada et al., 1998) Heterozygous mutations of either PINK1 or Parkin can increase the risk of late-onset PD.(Lesage and Brice, 2009) Parkin mutations cause earlier onset disease, because it functions downstream of PINK1 in the mitophagy pathway.

Since diagnosis is almost always symptomatic and symptoms of PD do not manifest until 60-80% of dopaminergic neurons are already dead, the early

changes that lead to the pathology are poorly understood.(Cheng et al., 2010) It is vital to study these early cellular changes in order to prevent the progression of the disease as our understanding of the genetics improves, increasing the chances that earlier diagnosis will some day be possible. In Chapter 3 of this work, we describe early changes to dopamine neurotransmission caused by Really Interesting New Gene (RING) finger protein 11 (RNF11).

RING finger protein 11 (RNF11)

RNF11 and A20 Regulate NF-κB

RING finger protein 11 (RNF11) is an E3 ubiquitin ligase that functions as part of the A20 ubiquitin-editing complex to regulate NF-κB.(Seki et al., 1999) Persistent NF-κB activation is a hallmark of neurodegenerative disease.(Glass et al., 2010) NF-κB is an evolutionarily conserved transcription factor that is known for its regulation of the immune response to stimuli such as cytokines, growth factors, bacterial lipopolysaccharide (LPS), and viral infection.(Hayden and Ghosh, 2008; Herrington et al., 2015) NF-κB is a dimer comprised of 15 different combinations of Rel family members, the most abundant being the p50/p65 heterodimer.(Huxford and Ghosh, 2009) NF-κB directly interacts with DNA in over to promote transcription of target genes, including prosurvival genes.

Figure 1.1 shows how the deubiquitination enzyme complex A20 functions to dampen the signaling cascade that leads to NF-κB activation by IL-1 receptor activation. NF-κB, shown as the p50/p65 heterodimer, is held inert within the cytoplasm by IκB proteins. When IκB proteins are phosphorylated by IKKβ, they become ubiquitinated and undergo proteasomal degration. IKKβ phosphorylation

of IκB requires a complex of proteins whose function involves the TRAF6/Ubc13/Uev1A complex catalyzing the synthesis of K63 polyubiquitin chains. A20 is a deubiquitination enzyme complex that disassembles the K63 polyubiquitin chains, dampen IKKβ phosphorylation of IκB, which traps NF-κB in the cytoplasm where it cannot promote target gene expression.(Chen and Sun, 2009) In order to inhibit the NF-κB pathway, A20 complexes with three other proteins: TAX1BP1 and the two E3 ubiquitin ligases Itch and RING finger protein 11 (RNF11). The overall function of this suppression of the NF-κB pathway by A20, also known as tumor necrosis factor alpha-induced protein 3 ($TNFAIP_3$)**,** is to ensure that inflammatory signaling pathways are only activated in a transient fashion.(Shembade et al., 2009) A20 inhibits NF-κB activation in human neurons.(Pranski et al., 2012)

In *Drosophila* there are two main innate immune pathways involving the three known NF-κB homologues Relish (Rel), Dorsal (dl), and Dorsal-related immunity factor (Dif). Gram-negative bacterial lipopolysaccharide activates the Rel immune deficiency pathway, while Gram-positive bacteria and fungi activate the dl/Dif Toll pathway.(Meyer et al., 2014) The dl/Dif pathway signals through MyD88 like the mammalian pathway described in Figure 1.1. Spatzle (spz) is a secreted cytokine in *Drosophila*, which acts as the ligand for the Toll receptor, mediating innate immunity and dorsoventral patterning during embryonic development. Spz binding to the toll receptor recruits a protein complex similar to the TRAF6/Ubc13/Uev1A complex, which dephosphorylates Cactus/IκB, allowing the dl/Dif to translocate to the nucleus and activate target gene transcription.

There is some evidence that dl and Dif may form heterodimers like mammalian p65/p50.(Valanne et al., 2011)

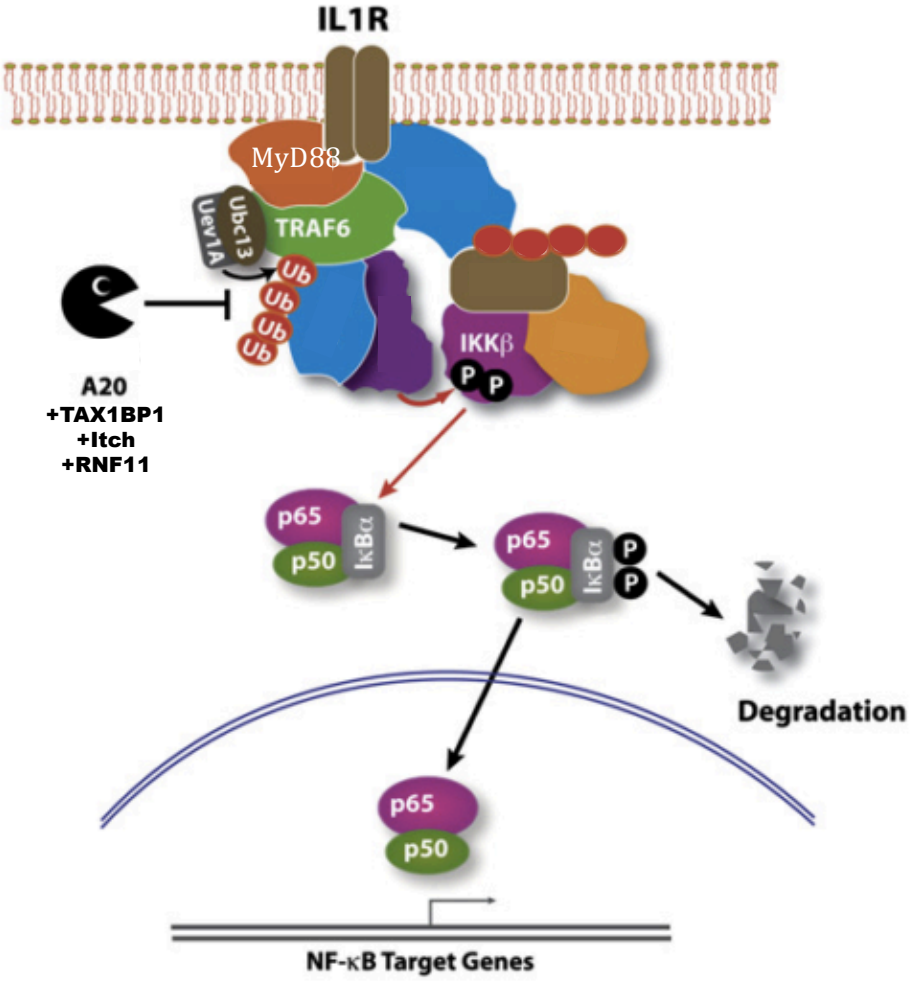

Figure 1.1 - A20 control of NF-κB activity. A20 (black pacman) deubiquitinates the K63 polyubiquitin chains (orange). This dampens IKKβ phosphorylation of IκB. which traps NF-κB in the cytoplasm where it cannot promote target gene expression. Adapted from Chen and Sun.(Chen and Sun, 2009)

RNF11 and Parkinson Disease

Recent work has indicated a role for RNF11 in Parkinson disease (PD) pathology. RNF11 variants in the PARK10 locus may increase susceptibility for PD.(Lesage and Brice, 2009) RNF11 gene transcription is decreased in brain tissue affected by neurodegenerative diseases, as found in a multi-cohort meta-

analysis. This decrease is not correlated with age, making RNF11 an unchanging candidate as a biomarker of neurodegeneration.(Li et al., 2014)

RNF11 expression is restricted to neurons in rat and human tissue. RNF11 protein expression is low in white matter, and is enriched in the somatodendritic compartments in many brain regions. There is high immunoreactivity in the apical dendrites of cortical pyramidal cells, the cell bodies and processes of the globus pallidus, and throughout the neurons of the amygdala. There is also expression of RNF11 in both dopaminergic and non-dopaminergic neurons and processes of the substantia nigra. In human PD tissue, RNF11 colocalizes with α-synuclein, Lewy bodies, and Lewy neurites. (Anderson et al., 2007)

The downregulated neuronal RNF11 expression in human PD tissue is associated with increased expression of activated NF-κB.(Pranski et al., 2013b) Viral RNF11 knockdown protected against dopaminergic neuronal cell death in rats exposed to the 6-OHDA model of PD and RNF11 overexpression enhanced toxicity. The enhanced toxicity from RNF11 overexpression corresponded to downregulation of NF-κB transcribed antioxidants glutathione synthetase and superoxide dismutase 1, anti-apoptotic factor BCL2, brain derived neurotrophic factor (BDNF), and tumor necrosis factor alpha (TNF-α). Therefore the decreased expression of RNF11 found in surviving neurons is a compensatory response to PD pathology.(Pranski et al., 2013a)

RNF11 is also overexpressed in some cancers and has been shown in the oncology literature to modulate ubiquitination events.(Santonico et al., 2014)

Ubiquitination of vesicles is important for vesicle trafficking.(Chen and Sun, 2009) RNF11 RNA and protein has also been found in exosomes, and RNF11 localizes to complexes that mediate endocytosis and endosome trafficking.(Pisitkun et al., 2004; Gonzales et al., 2009; Hong et al., 2009; Kostaras et al., 2014) It is therefore possible that RNF11 could modulate vesicular neurotransmitter release or membrane expression of dopamine transporters in a non-NF-κB dependent manner.

RNF11 has been shown to affect dopaminergic neuronal survival in the context of neurodegeneration. However, the effect of RNF11 on the ability of living dopaminergic neurons to release and uptake dopamine has not been established. Chapter 3 describes experiments in which we knock down or overexpress RNF11 in dopaminergic cells in order to understand the effect of RNF11 on dopamine release and uptake at an early time point in development. In order to address this question, *Drosophila melanogaster* is used as a model organism for its ease of genetic manipulation and largely conserved neurotransmitter systems.

Drosophila melanogaster

Drosophila as a Model Organism

Drosophila melanogaster, the fruit fly, has been used in scientific research as a genetic model organism for over 100 years and there is a long-standing tradition of open collaboration and reagent sharing within the field.(Rubin, 2015) *Drosophila* is small, easy to care for, and has a short life cycle that makes it possible to rear large quantities cheaply in controlled laboratory conditions. The

dopamine neurotransmitter system is largely conserved from flies to mammals, making it an important model organism for neurological drug testing and development.(Pandey and Nichols, 2011) Dopamine neurotransmission in the fruit fly is important for olfactory learning and memory. However, detailed studies of dopamine kinetics in *Drosophila* have been limited by the difficulty of measuring from such small tissue. Genetic and pharmacological manipulations of dopamine release and uptake can be assessed in the fruit fly using fast scan cyclic voltammetry.

Drosophila **Neuroanatomy**

The *Drosophila* central nervous system consists of the brain and the ventral nerve cord. The brain is divided into the central brain and the more lateral optic lobes. Within the central brain, there are multiple neuropil with distinct functions. For example the antennal lobes receive input from external chemosensory neurons.(Wright, 2013) The main targets of dopaminergic innervation in the central brain are the mushroom bodies and the central complex.(Mao and Davis, 2009; Pech et al., 2013) The central complex is located centrally and is involved in sensory integration, movement, courtship, and olfactory learning.(Kahsai and Winther, 2011) The mushroom bodies are paired structures that are involved in olfactory learning and memory, sleep, temperature regulation, and decision-making.(Bang et al., 2011) Dopamine has roles in modulating many of the behaviors in these higher order brain regions.

Dopaminergic neurons have been characterized in larval and adult *Drosophila* using histochemistry and immunocytochemistry. Dopaminergic

neurons are largely interneurons that are found in bilateral clusters throughout the CNS of the fly.(Monastirioti, 1999) Figure 1.2 is a summary of the work of Monastirioti showing the location of dopaminergic neurons in the larval and adult CNS. The largest cluster of dopaminergic neurons, the PAM cluster, develops during the pupal stage and does not label well with GFP when using the th-GAL4 driver. Recently, the R58E02-GAL4 driver line has been described for targeting the PAM cluster and helping elucidate its function in appetitive sucrose learning and memory via its inputs into the mushroom body, which is important for future work in adult *Drosophila* described in Chapter 4.(Liu et al., 2012; Yamagata et al., 2015)

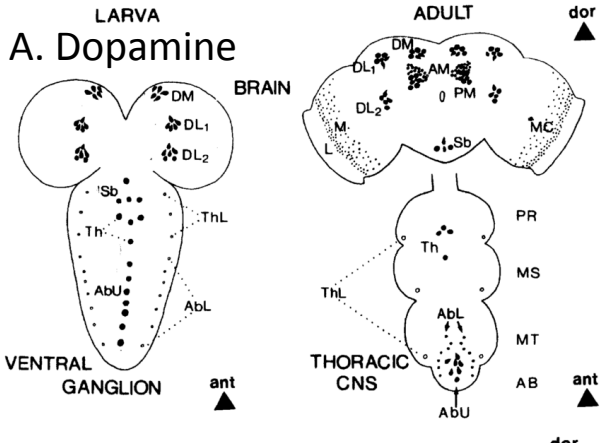

Figure 1.2 - Neuroanatomy of dopaminergic neurons in *Drosophila* larval and adult central nervous systems. Dopaminergic neurons in the larval and adult fly central nervous system. Cell bodies are black dots and stippling indicates areas of innervation. Key to abbreviations: AB=abdominal neuromere, AbL=lateral abdominal segments, AbU= medial abdominal segments, AM=anteriomedial, DL=dorsolateral protocerebrum, DM=dorsomedial protocerebrum, L=lamina, M=medulla, MC=cellular medulla, MS=medothoracic neuromere, MT=metathoracic neuromere, PM=posteriomedial aka PAM cluster, PR=prothoracic neuromere, Sb=subesophageal Th=medial prothoracic segment, ThL=lateral thoracic segments. Adapted from Monastirioti.(Monastirioti, 1999)

Amine neurotransmitters that are released can circulate in the hemolymph and regulate systemic functions such as digestion and circulation. Dopamine and

serotonin are involved in the regulation of feeding.(Neckameyer and Bhatt, 2012; Gasque et al., 2013; Lemaitre and Miguel-Aliaga, 2013) Additionally, the fly heart is known to respond to the bath application of dopamine, serotonin, and octopamine with a change in rate that differs with life stage.(Wolf and Rockman, 2011) However, these experiments have not been carried out in intact animals using physiologic levels of neurotransmitters or the newest cardiac imaging systems. Since *Drosophila* is such a versatile model organism for studying developmental cardiac abnormalities, it is important to understand how amine neurotransmitters affect the rate and contractility of the heart. In Chapter 4, we describe in detail our experiments using optogenetic stimulation of amine neurotransmitter release in intact *Drosophila* pupae while monitoring heart rate and contractility using optical coherence microscopy.(Alex et al., 2015) These experiments may be important in understanding the early cardiac effects of sympathetic pathology in PD.(Hawkes et al., 2010)

Drosophila Models of Parksinon Disease

Approximately 80% of known human disease genes have *Drosophila* orthologues.(Wolf and Rockman, 2011; Yamamoto et al., 2014) *Drosophila* have been used to model and study the underlying mechanisms of many neurological conditions including fragile X syndrome, Parkinson disease, Alzheimer disease, and some spinocerebellar ataxias.(Morales et al., 2002; Hirth, 2010) *Drosophila* exhibit many of the hallmarks of neurological disease such as neurodegeneration, protein aggregation, movement disorders, and sleep

disturbances when relevant genes are mutated, knocked down, or overexpressed.(Lu and Vogel, 2009; McGurk et al., 2015)

PD can be modeled in *Drosophila* using pharmacological or genetic factors. Pharmacologically, pesticides like rotenone and paraquat can be chronically fed to *Drosophila* to induce age-dependent loss of dopaminergic neurons and a decline in locomotion.(Varga et al., 2014) These pesticides function by inhibiting mitochondrial complex I or inducing oxidative stress, and are associated with the development of PD in humans, such as in farm workers with chronic exposure.(Tanner et al., 2011)

Genetically, the GAL4/UAS system can be used to express RNAi that will knock down *Drosophila* genes whose human homologue mutants are known to cause PD like PINK1. The *Drosophila* PINK1 protein has a mitochondrial targeting motif and a kinase domain which exhibits 60% similarity to human PINK1.(Park et al., 2006) dPINK1 knockdown induces significant dopaminergic cell death within the first ten days of adult life post eclosion (hatching from pupa) that can be rescued by expression of human PINK1 protein, indicating a conservation of function. Panneuronal knockdown of PINK1 also induces degeneration of retinal neurons in *Drosophila*.(Wang et al., 2006)

Alternatively, flies expressing mutant forms of endogenous proteins can be used to model PD in *Drosophila*. Flies expressing mutant forms of PINK1 have been generated; however they exhibit less dopaminergic cell death (~10% by day 30 post eclosion) than RNAi knockdown flies. These mutants have been used to show that Parkin and PINK1 act in a common pathway for normal

mitochondrial turnover in dopaminergic neurons and that Parkin functions downstream of PINK1 in PD pathology.(Park et al., 2006)

Flies expressing mutant human proteins can also be used as a model of PD. *Drosophila* lack endogenous α-synuclein.(Cookson, 2009) Expression of mutant disease-causing α-synuclein induces a PD phenotype in *Drosophila*, which recapitulates many salient aspects of PD, including selective degeneration of dopaminergic neurons, Lewy body-like inclusions, and motor deficits. However, this methodology leads to inconsistent results in terms of neuronal loss depending on where in the genome the exogenous construct is inserted.(Whitworth, 2011) Therefore, it is better to use knockdown of endogenous proteins like PINK1 when modeling PD in *Drosophila*.

Dopaminergic Neurotransmission in Drosophila

Neurotransmission

In order to use *Drosophila* as a model to understand PD, it is important to highlight the ways in which dopaminergic neurotransmission is evolutionarily conserved between humans and *Drosophila*. In the central nervous system, neurons communicate through chemical signals by exocytotic release of neurotransmitters from synaptic vesicles. Exocytosis occurs at the synapse, an approximately 100 nm space between the axon and dendrite of two neurons. The released neurotransmitters diffuse from the site of release to pre- and-post synaptic receptors. For some neurotransmitters, receptors are located both within the confines of the synapse and at extra-synaptic sites. The diffusion of a neurotransmitter to activate targets outside of the synapse is referred to as

volume transmission.(Fuxe et al., 2007) The binding of the neurotransmitter to a receptor causes intracellular changes to the cell, usually from the flow of ions through an opened channel or the activation of coupled G-proteins. Neurotransmitters are cleared from the extracellular space through diffusion, metabolism, and transporter-mediated reuptake into cells. Neurons can also communicate via direct electrical coupling through gap junctions formed from connexin proteins.(Hormuzdi et al., 2004)

Amine Neurotransmitters

Biogenic amines are neurotransmitters synthesized from the amino acids tyrosine, tryptophan, or histidine.(Monastirioti, 1999) They typically act as both neurotransmitters and neuromodulators, and the physiological relevance to normal human function and disease states is still being elucidated for many of these compounds.(Hardie and Hirsh, 2006) The best-characterized amine neurotransmitters are dopamine, serotonin, epinephrine, norepinephrine, octopamine, tyramine, and histamine. The synthesis of these neurotransmitters is summarized in Figure 1.3. Epinephrine and norepinephrine have not been found in fruit flies and their functions are thought to be largely carried out by octopamine and tyramine.(Selcho et al., 2012)

Many of these neurotransmitters and neuromodulators have highly conserved functions between *Drosophila* and humans.(Yamamoto and Seto, 2014) In both mammals and *Drosophila*, dopamine has a role in sleep, motor function, and learning and memory.(Kume et al., 2005; Selcho et al., 2009; Varga et al., 2014) The enzymes Ebony and Tan can beta-alanate dopamine. Orthologs

of these enzymes have not been found in the mammalian genome. However, a regulator of Ebony levels in flies, *dysbindin*, has a human homolog that is a known schizophrenia susceptibility gene.(Yamamoto and Seto, 2014) Serotonin has a conserved role in the modulation of sensory systems, feeding, and heart rate.(Huser et al., 2012) Octopamine and Tyramine are often studied in terms of their similarity to the mammalian adrenergic system. They regulate the fight or flight response as well as motivation and aggression. Additionally, they have roles in modifying heart rate, fat metabolism, respiration, and muscle contraction via release from type-II neuromuscular boutons.(Roeder, 2005; Lange, 2009; Selcho et al., 2012)

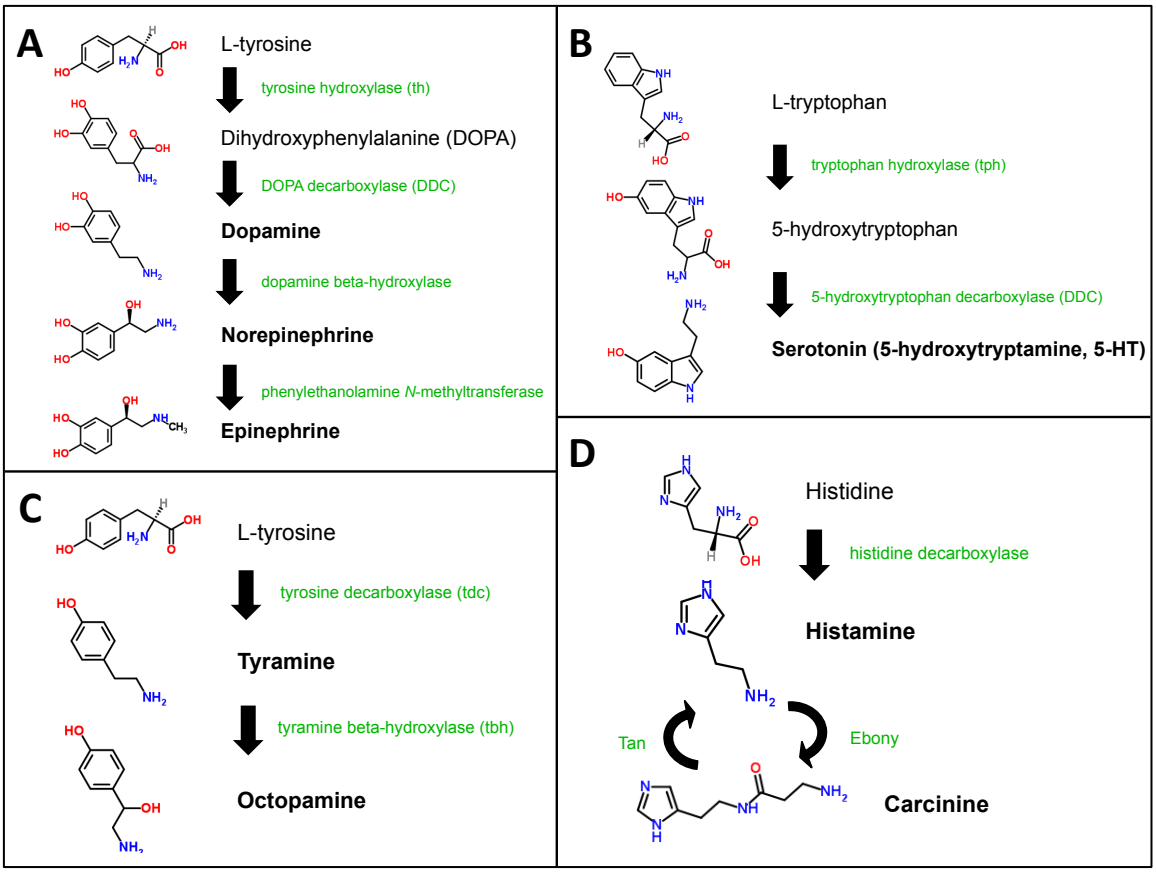

Figure 1.3 - Synthesis of the amine neurotransmitters. (A) dopamine, norepinephrine, and epinephrine; (B) serotonin; (C) octopamine and tyramine; and (D) histamine and carcinine. Chemical drawings from chemspider.com.

Receptors and Autoreceptors

Monoamine neurotransmission occurs in much the same way as most neurotransmission in the central nervous system in both humans and *Drosophila*. A neuron is depolarized from the influx of positively charged cations through ion channels in the dendrites, cell body, and axon. As the depolarization sweeps towards the synapse at the end of the axon, voltage-gated calcium channels open at the presynaptic membrane, allowing calcium influx to stimulate the fusion of synaptic vesicles with the presynaptic membrane. These synaptic vesicles release their stored neurotransmitters into the synaptic cleft. From there, the neurotransmitters diffuse across the synapse to excite post-synaptic receptors.

This will cause excitation, inhibition, or more complex physiological effects in the post-synaptic neuron.

Once released into the synapse, neurotransmitters are exposed to the extracellular milieu. If exposed to a current, dopamine can be reversibly oxidized to dopamine-*o*-quinone.(Jackson et al., 1995) Neurotransmitters can be removed from the extracellular space by diffusing away, being taken up into the pre-synaptic cell to be recycled and reused for neurotransmission, or being broken down by enzymes in the extracellular space or in the cytoplasm.

Neurotransmitters can be removed from the synaptic cleft by reuptake into the pre-synaptic cell by sodium/chloride symporters. Dopamine is taken up in flies by the *Drosophila* homologues of the human serotonin transporter (SERT) and dopamine transporter (DAT), known as dSERT and dDAT.(Corey et al., 1994; Pörzgen et al., 2001) dDAT also transports tyramine and to a lesser extent octopamine, but does not transport serotonin. dDAT exhibits cocaine and antidepressant sensitivities similar in mechanism to human reuptake inhibition.(Pörzgen et al., 2001) However, the robustness of the response is not perfectly conserved. Human DAT and SERT have similar affinity for cocaine, while dSERT has a five-fold higher affinity for cocaine than mammalian SERT.(Corey et al., 1994) Additionally, dDAT exhibits robust response to antidepressant medication unlike human DAT, which is only moderately affected by reuptake inhibition of tricyclic antidepressants. This implicates dDAT as a more primordial monoamine transporter than the specialized function of human DAT.(Pörzgen et al., 2001)

Once taken up into the presynaptic cell or after being newly synthesized in the cytoplasm, dopamine is packaged into secretory vesicles by vesicular monoamine transporters (VMAT). Humans encode two VMAT genes: VMAT1 and VMAT2, while *Drosophila* have only one: dVMAT. dVMAT functions as a vesicular packaging transporter for dopamine, serotonin, and octopamine in *Drosophila*. It is inhibited by reserpine just like human VMAT.(Martin and Krantz, 2014)

Once a neurotransmitter has diffused across the synaptic cleft, it will bind to post-synaptic receptors. These receptors for monoamine neurotransmitters primarily act as G-protein coupled receptors. They mediate complex intracellular effects through postsynaptic signaling cascades, often involving changing levels of cAMP and/or calcium.(Blenau and Baumann, 2001)

Dopamine receptors in both humans and *Drosophila* fall into two main families. *Drosophila* express two D1-like receptors, dDA1 and DAMB, and one D2-like receptor, D2R. D1-like receptors activate adenyl cyclase, increasing intracellular cAMP levels. D2-like receptors inhibit adenylyl cyclase and the formation of cAMP.(Qi and Lee, 2014) They are known to mediate behaviors in the *Drosophila* such as temperature-based preference, wakefulness, ethanol response, locomotion, copulation, sucrose preference, and olfactory learning.(Selcho et al., 2009; Bang et al., 2011; Berry et al., 2012; Marella et al., 2012; Crickmore and Vosshall, 2013)

Presynaptic receptors known as autoreceptors or heteroreceptors, can feed back on the signal to increase or decrease future neurotransmission at the

synapse. Autoreceptors are typically G-protein coupled-receptors sensitive to the neurotransmitter released by the cell in which they are located. They can work via second messenger systems to inhibit the future synthesis or release of the neurotransmitter, thus acting as a negative feedback system. Heteroreceptors are sensitive to neurotransmitters released by adjacent cells, and can influence neurotransmission via ligands not produced by the presynaptic cell. The D2 dopamine receptor functions as an autoreceptor in *Drosophila*.(Vickrey and Venton, 2011)

Pharmacology

A variety of drugs can be useful tools in understanding the release, uptake, and synthesis of dopamine in *Drosophila*.(Titlow et al., 2013; Yamamoto and Seto, 2014) In general, neurotransmission can be blocked using tetrodotoxin to stop the flow of sodium ions through voltage-gated sodium channels.(Ross et al., 2014) Amine neurotransmission can also be deceased using a drug like reserpine, which irreversibly blocks VMAT, thus stopping the packaging of the neurotransmitters into vesicles for exocytotic release. Reserpine significantly decreases stimulated dopamine release from *Drosophila* CNS tissue at a concentration of 100 μM for 30 minutes.(Vickrey et al., 2009) The uptake of dopamine through the dopamine transporter (DAT) can be selectively blocked using nisoxetine, which has an IC_{50} value of about 5.6 μM for dDAT, but an IC_{50} value of 5000 μM for dSERT.(Pörzgen et al., 2001) Nisoxetine will slow the rate of dopamine uptake in *Drosophila* CNS tissue after 15 minutes at 20 μM.(Privman and Venton, 2015) Mazindol is a slightly more potent dDAT blocker,

with an IC_{50} of 4.4 μM, but it is less specific with a 3.9 μM IC_{50} for dSERT.(Pörzgen et al., 2001) Cocaine has a higher affinity for dSERT than dDAT. Dopamine and serotonin synthesis can be blocked by feeding larval *Drosophila* with 6.6 μM NSD-1015 for two days.(Vickrey et al., 2009) Serotonin synthesis can be selectively blocked by 100 μM parachlorophenylalanine (PCPA), which inhibits tph.(Borue et al., 2010; Privman and Venton, 2015) Neurotransmitter synthesis can be generally increased by chronic feeding or bath application of synthetic precursors like tyramine in the case of octopamine neurotransmission or L-DOPA in the case of dopamine.(Riemensperger and Isabel, 2011; Majdi et al., 2015)

While the synthesis pathways and receptors are highly conserved evolutionarily, it is important to note that the intracellular enzymes used to break down monoamine neurotransmitters in humans, monoamine oxidase (MAO) and catechol-o-methyl transferase (COMT), have not been found in *Drosophila*. Mammalian dopamine catabolism is mediated to a lesser extent by n-acetyltransferase (NAT). In *Drosophila*, NAT has been proposed as a method of extracellular catecholamine metabolism, as has the N-beta-alanyl-dopamine synthetase Ebony.(Suh and Jackson, 2008; Ueno and Kume, 2014) In mammals, dopamine is broken down to homovanillic acid, which has been detected biochemically in *Drosophila*.(Freeman et al., 2013) Therefore, it is likely that dopamine metabolic pathways do exist in *Drosophila*.(Yamamoto et al., 2014)

Genetic Tools for Studying *Drosophila* Neurotransmission

The GAL4/UAS System

The 4 chromosomes of *Drosophila* were the first complex genome to be sequenced.(Adams, 2000) Due to the detailed understanding of the *Drosophila* genome, genetic targeting can be achieved by using the GAL4/UAS system.(Brand and Perrimon, 1993) The GAL4 gene encodes the yeast transcription-activating factor Gal4, which binds to and drives the expression of an enhancer, Upstream Activation Sequence (UAS). The UAS responder element can control the expression of an ectopic gene of interest. *Drosophila* GAL4 lines express the Gal4 protein in subsets of tissues, while reporter lines express UAS along with the desired gene to be expressed in subsets of cells. When the driver and reporter fly lines are crossed, the offspring will express Gal4 in subsets of cells, which will then drive the expression of the UAS and its associated gene in those cells of interest.(Duffy, 2002) In order to express exogenous proteins in dopaminergic cells, GAL4 driver lines have been used to target the dopamine synthesis enzymes tyrosine hydroxylase (TH) and DOPA decarboxylase (DDC) (Figure 1.3).

Optogenetic Control of Neurotransmission

Since neurotransmission requires the influx of positively charged cations through ion channels, it can be controlled by the genetic expression of exogenous ion channels.(Nagel et al., 2003; Lima and Miesenböck, 2005; Deisseroth and Feng, 2006; Liu et al., 2012) Light, chemicals, or heat can control these channels. Targeted expression of these channels in specific subsets of cells can be accomplished using the GAL4/UAS system.(Brand and Perrimon, 1993)

Optogenetics is a technique developed in 2006, in which light can be used in live tissue to control the activity of excitable cells.(Deisseroth and Feng, 2006) Optogenetics involves the genetic insertion of light sensitive cation channels like Channelrhodopsin-2, a seven transmembrane cation channel from algae. When expressed using the Gal4/UAS system, the channelrhodopsin will be synthesized in the subpopulation of cells containing the GAL4 driver. Channelrhodopsin requires all-*trans*-retinal, an aldehyde derivative of vitamin A, as a cofactor for proper protein function.(Bamann et al., 2008) Regular *Drosophila* cornmeal food contains some Vitamin A, but it is common to add 10-50 mM all-*trans*-retinal to the food that the *Drosophila* eat in order to ensure proper expression.

Cannelrhodopsin is inserted into the cell membrane. When blue light is shone onto the complex, the all-*trans*-retinal absorbs a photon and undergoes a conformation change to 13-cis-retinal.(Bamann et al., 2008) The maximum absorbance is 470-480 nm. This opens a 6-angstrom pore in the non-specific cation channel, allowing positively changed ions to flow into the neuron. The inward flow of positive cations causes the cell to depolarize, triggering a neuronal action potential.

Channelrhodopsin takes about 10 milliseconds to close, as the retinal eases back from 13-*cis* to all-*trans*. Fast light pulses are used to stimulate channelrhodopsin in rodents, for example 20 ms at 20 Hz.(Nagel et al., 2003) However, all of the previous work that had been done using FSCV in *Drosophila* has used long, continuous blue laser light stimulations of 1-10 seconds.(Borue et al., 2009, 2010; Vickrey et al., 2009; Vickrey and Venton, 2011) This discrepancy

in the methodology is most likely due to poor expression of channelrhodopsin in the fruit fly. Shorter, pulsed stimulations are preferable, because longer stimulations can cause tissue heating and damage, reducing the viability of the tissue over the course of a multiple stimulation experiment. To that end, pulsed optogenetic stimulations were used for the first time to characterize the release and Michaelis-Menten uptake kinetics from dopamine and serotonin cells in the larval *Drosophila* VNC.(Xiao et al., 2014) Tonic firing rates between 1 and 25 Hz have been measured using electrophysiology for dopaminergic neurons in *Drosophila*.(Marella et al., 2012)

When performing pulsed stimulation experiments, it is possible to model the extracellular concentration of a neurotransmitter as a balance between the release and clearance. The increase in extracellular neurotransmitter from release due to a pulsed stimulation is a discontinuous process that depends on the frequency of the stimulation and the amount of neurotransmitter released with each stimulation pulse. The clearance of the neurotransmitter from the extracellular space is a continuous process that can be described mathematically using Michaelis-Menten kinetics.(Garris et al., 1994; Garris and Wightman, 1995; Jones et al., 1995; Harun et al., 2014; Xiao et al., 2014) This model assumes that clearance happens primarily through the uptake of neurotransmitter through dedicated transport proteins and that the amount of neurotransmitter released is constant with each stimulus pulse, which may not hold true *in vivo*.(Privman and Venton, 2015) In order to study the sub-second dynamics of dopamine release

and uptake in *Drosophila* a fast, sensitive, spatially resolved method of dopamine detection must be employed.

Detecting Dopamine in *Drosophila*

Fast Scan Cyclic Voltammetry

Fast scan cyclic voltammetry (FSCV) is an analytical electrochemical technique pioneered by R. Mark Wightman in the early 1980s. FSCV can be used *in vitro*, *in vivo*, and *ex vivo* to study electrically active analytes such as anime neurotransmitters.(Garris et al., 1994; Jackson et al., 1995; Cooper and Venton, 2009) Due to their chemical structure, anime neurotransmitters undergo oxidation and reduction reactions in aqueous solution at characteristic applied voltages. Current is measured as a function of applied voltage as the redox reactions occur at the surface of a carbon fiber microelectrode, providing information about the identity and quantity of the analyte.(Garris and Wightman, 1995)

Fast scan cyclic voltammetry (FSCV) uses a carbon fiber microelectrode (CFME) that is approximately 7 um in diameter.(Jacobs et al., 2011) Analytes are detected on a millisecond time scale and the sensitivity of the technique for amine neurotransmitters puts the limit of detection within the nanomolar physiological range.(Bath et al., 2000) The potential that will cause oxidation and reduction of a molecule is dependent on its molecular structure. Therefore, FSCV can be used to distinguish between different anime neurotransmitters based on their structural electrochemical properties, as long as they differ in the potential of their oxidantion or reduction peaks by at least 200 mV.(Swamy and Venton,

2007) Combined, the speed, selectivity, and sensitivity of FSCV make it ideal for measuring neurotransmission in real time.

FSCV Data Collection and Analysis

An advantage to FSCV is the ease with which CFMEs can be synthesized in the lab at a relatively low cost. CFMEs are made by pulling a T-650 carbon fiber in a glass capillary to form a glass seal with a 50 um long cylinder of carbon (or however long the electrode is trimmed) extending out to be exposed to the extracellular milieu as seen in Figure 1.4A. The glass seal is reinforced with epoxy, which is baked in order to ensure proper hardening.(Huffman and Venton, 2008)

Different waveforms allow for better resolution of different analytes. For dopamine, a triangular waveform is used as seen in Figure 1.4B. The electrode is maintained at a low voltage holding potential of -0.4 V in between scans. This allows analytes to adsorb to the surface of the electrode if they are positively charged at the pH of the solution. The pKa of dopamine is around 9, so it is positively charged at physiological pH and obeys adsorption-dependent kinetics.(Armstrong and Barlow, 1976)

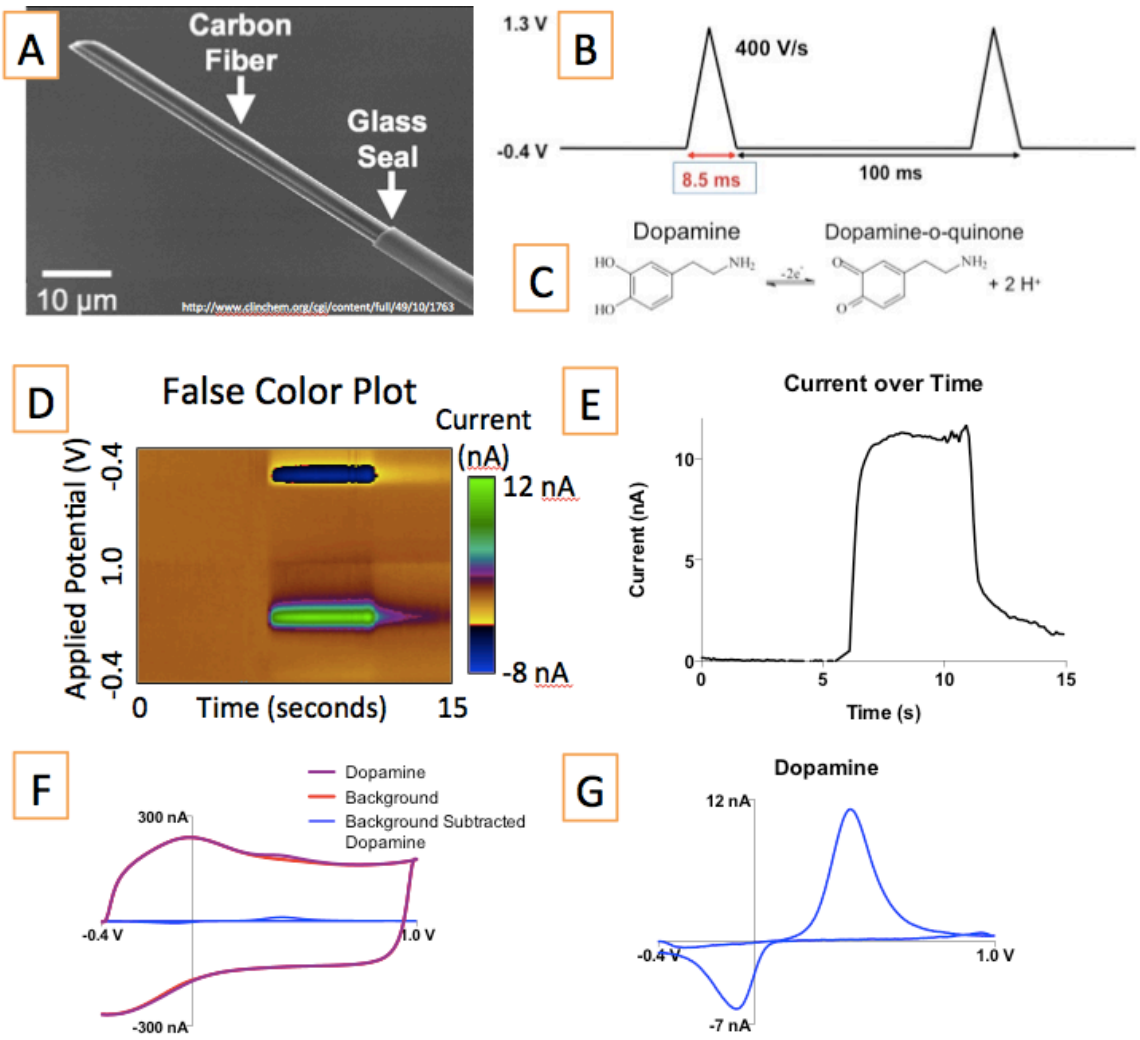

Figure 1.4 - Fast scan cyclic voltammetry for the detection of dopamine. (A) Carbon fiber microelectrode with a 7 um tip diameter.(Adapted from http://www.clinchem.org/cgi/content/full/49/10/1763) (B) Example waveform of the applied potential for dopamine FSCV (not to scale). (C) Oxidation of dopamine to dopamine-ortho-quinone. (D) False color plot with time on the x-axis, applied potential on the y-axis, and measured current in false color. Note the green oxidation of dopamine and dark blue reduction. (E) Peak oxidation current of dopamine over time. (F) Background subtraction is needed to distinguish the signal caused by dopamine from the relatively large background charging current. (G) Enlarged view of the dopamine cyclic voltammogram.

The electrode is rapidly scanned from the negative holding to a switching potential of 1.3 V and back down again (Figure 1.4B). This is repeated every 100 ms. As the potential increases, monoamine neurotransmitters are oxidized and as the potential ramps back down towards the holding potential, oxidized

analytes can reduce back to their equilibrium forms. Dopamine oxidizes to dopamine-ortho-quinone (Figure 1.4C) and reduces back at approximately 0.2 V, but due to the speed with which the potential is being scanned, the oxidation peak appears around 0.6 V and the reduction peak appears around -0.2 V (Figure 1.4G). Typical voltages for FSCV experiments are within the -0.6 to +1.5 V range to avoid the oxidation of water at larger positive voltages and the reduction of oxygen at larger negative voltages.

The electrode is scanned from the holding potential to the switching potential and back, which causes a current at the electrode from multiple sources. We are interested in measuring the oxidation and reduction of analytes at the surface of the electrode. However, it is important to understand the other reactions can occur and must be accounted for when analyzing the data. The surface of the electrode has electroactive functional groups that oxidize and reduce in response to the changing potential.(McCreery, 2008) Oxidation and reduction reactions of both the analyte and the electrode surface result in Faradaic currents, or currents that follow Faraday's Law.(Takmakov et al., 2010) Since the current is directly proportional to the number of reacting molecules, the background current from the electrode surface remains constant over time.(Roberts et al., 2013) Therefore, changes in current caused by changes in analyte concentration at the surface of the electrode are calculated from the total measured current using background subtraction (Figure 1.4D-G). This subtracted current is proportional to the amount of analyte present at the surface of the

electrode within physiological concentration ranges, and are therefore used to extrapolate analyte concentration at the tip of the carbon fiber microelectrode.

Background-subtracted currents can be examined in the form of a cyclic voltammogram (Figure 1.4G). Cyclic voltammograms contain information that is important for confirming the identity of the analyte. The voltages at which the oxidation and reduction peaks occur and the peak height ratios are characteristic of certain analytes, in this case dopamine. The unknown concentration of an analyte can be calculated from the peak oxidation current using cyclic voltammograms of known concentrations of analyte measured with the same electrode in a controlled calibration before the experiment.(Sinkala et al., 2013)

Background subtracted currents are visualized as they change over time using a false color plot (Figure 1.4D). Color plots provide information about the concentration of analyte present at the surface of the electrode over time. The y-axis of a color plot is voltage, with the middle of the y-axis representing the switching potential, and the top and bottom of the y-axis representing the holding potentials. The x-axis of a color plot is time, with 10 scans per second being graphed sequentially. The color scale of a color plot represents current. These false color plots were designed to be readable by people with and without colorblindness, with green indicating positive oxidation currents, yellow indicating baseline currents, and blue indicating negative reduction currents. Figure 1.4D shows an example of a color plot for dopamine, which was introduced *in vitro* at the surface of carbon fiber microelectrode. Note the green oxidation currents around 0.6 V and blue reduction currents around -0.2 V, which appear as

dopamine is introduced in the solution at 5 seconds, and which rapidly disappear from the color plot when dopamine is flushed from the electrode surface using buffer solution at 9 seconds. The reduction current for dopamine is smaller than the oxidation current because desorption of dopamine-*o*-quinone from the electrode surface occurs with faster kinetics than dopamine.(Jacobs et al., 2014) The current can be examined over time as a horizontal slice through the color plot, as represented in Figure 1.4E. A vertical slice through the color plot will yield a current versus voltage plot that is essentially an unfolded cyclic voltammogram.

FSCV in *Drosophila*

Fast scan cyclic voltammetry (FSCV) has been used extensively to monitor neurotransmission in mammals such as mice and rats. FSCV is especially used in the caudate putamen to monitor dopamine, serotonin, and adenosine neurotransmission.(Hashemi et al., 2009) The technique can be used *ex vivo* in brain slices and *in vivo* in anesthetized as well as in awake, behaving animals.(Robinson et al., 2003; Ross et al., 2014) FSCV has been extended to non-human primates to study rewards pathways in the striatum(Ariansen et al., 2012) and even to human patients with essential tremor to monitor adenosine as they receive deep brain stimulation treatment.(Chang et al., 2012)

FSCV measurements done *in vivo* are interpreted in much the same way as those taken *in vitro*. Current versus time plots can be examined to determine how quickly the analyte disappears from the surface of the electrode, the kinetics of which can be affected *in vivo* by processes such as diffusion, metabolism, and active uptake. When studying the *Drosophila* CNS *ex vivo*, the tissue remains

viable for more than 90 minutes when cultured in the proper buffers.(Borue et al., 2010) In *Drosophila*, the rapid release of serotonin and dopamine requires both synthesis of new neurotransmitter and uptake of recycled neurotransmitter.(Borue et al., 2010; Xiao and Venton, 2015) Therefore, when using stimulated release methods, neurons require multiple minutes between stimulations to recover their stores of neurotransmitter in both *Drosophila* and rats.(Bunin et al., 1998) The tissue needs to rest between stimulated releases or the signal will decrease sharply over time and confound the results of the study. In Chapter 4 we will discuss preliminary experiments in the adult *Drosophila* brain that highlight advantages of FSCV over monitoring dopaminergic neuronal function using live GCaMP imaging.

In *Drosophila melanogaster*, neurotransmitter levels were historically studied using immunohistochemistry, which is only an estimate of tissue levels and not an indication of functional neurotransmitter levels.(Borue et al., 2010) Electrochemical detection has been used to study amine neurotransmitters in *Drosophila* since 2009. In larvae, the Venton lab characterized stimulated release and reuptake of endogenous dopamine and serotonin from the ventral nerve cord using Channelrhodopsin-2.(Borue et al., 2009, 2010; Vickrey et al., 2009, 2013; Vickrey and Venton, 2011) Additionally, the kinetics of dopamine uptake have been modeled in the larval ventral nerve cord using exogenously applied dopamine.(Vickrey et al., 2013) In adult *Drosophila*, the Ewing group applied high concentrations of exogenous dopamine to brain tissue and found that methylphenidate (Ritalin) blocks the effects of cocaine at the dopamine

transporter.(Makos et al., 2009b, 2010; Berglund et al., 2013) The Campusano group used chronoamperometry to measure an efflux of biogenic amines from the *Drosophila* central brain upon stimulation of nicotinic acetylcholine receptors, implicating nicotine-mediated octopamine release in the startle response.(Fuenzalida-Uribe et al., 2013) The Ewing group also recently used amperometry to measure optogenetically-stimulated octopamine release from the type II neuromuscular varicosities in the larval *Drosophila* body wall. Due to the fast time resolution of amperometry and the large bouton size of 1-3 μm, measurements were made from single varicosities and single vesicle release events were characterized to determine the amount of octopamine released per vesicle.(Majdi et al., 2015)

While amperometry has a significantly better time resolution than fast-scan cyclic voltammetry, amperometry is unable to distinguish similar molecules based on their chemical characteristics, such as dopamine and serotonin. FSCV provides information about the characteristic oxidation and reduction potentials for the anime neurotransmitters, which allows them to be distinguished from one another.(Swamy and Venton, 2007; Makos et al., 2009a; Denno et al., 2014, 2016) Therefore, amperometry is useful for studying systems like the neuromuscular junction, which are isolated from other nervous tissue and are known to be octopaminergic. However, amperometry is less useful for central nervous system studies where it can be difficult to determine which of the anime neurotransmitters is being released.

These previous electrochemical studies in *Drosophila* have methodological drawbacks that would limit the study of PD. Two major regions of functional dopamine innervation in the adult Drosophila are the mushroom bodies and the central complex, both of which are located in the medial protocerebrum of the fly brain (Figure 1.2). The central complex has been compared in function to the basal ganglia of humans, where the loss of dopaminergic innervation causes some of the hallmark motor symptoms of PD.(Wessnitzer and Webb, 2006; Bouabid et al., 2015) These adult brain regions develop from the larval medial protocerebrum, where the DM, DL1, and DL2 clusters and later in development the PAM clusters of neurons send their projections in order to modulate behaviors such as olfactory learning and memory. In order to fully study PD in the *Drosophila* model, it is vital to extend the technique of FSCV dopamine monitoring to the medial protocerebrum. In Chapter 2, dopamine release and uptake are characterized in this new brain region in larvae. In Chapter 4, preliminary experiments recording from the central complex and mushroom bodies of adult flies as well as methodological hurdles are also discussed.

Stimulated neurotransmitter release can be improved using new red light activated channelrhodopsins instead of Channelrhodopsin-2. Blue light can change the surface properties of the microelectrode due to the photoelectric effect.(Vickrey et al., 2009; Bass et al., 2013) CsChrimson is a newly published channelrhodopsin that is activated by red light with a wavelength of 617 nm.(Klapoetke et al., 2014) It causes about a twenty-fold greater depolarization

than Channelrhodopsin-2 and would be more appropriate for behavioral work due to its stimulation spectrum outside of the normal visual range of a fruit fly.(Klapoetke et al., 2014) Chapter 2 describes in detail the first published use of CsChrimson for the direct measurement of stimulated dopamine release from heterozygous fruit flies.(Privman and Venton, 2015) Chapter 4 describes experiments involving activation of dopaminergic neurons through the opaque cuticle of a *Drosophila* pupa in order to study heart rate changes, which requires the deeper tissue penetration provided by red light stimulation of CsChrimson. These new methods can also be used to study PD in *Drosophila* by investigating the role of RNF11 in dopamine release and uptake at an early time point in development, as discussion in Chapter 3.

This dissertation describes the effect of RNF11 on dopaminergic neurotransmission in *Drosophila* as a model of PD. Chapter 2 focuses on the methodological improvements that have been contributed in a published, first-author work (Privman and Venton, 2015), including improved optogenetic stimulation using CsChrimson and recordings demonstrating the differences in dopamine kinetics between the VNC and the protocerebrum of larval *Drosophila*. Chapter 3 describes the exciting finding that RNF11 affects dopamine signaling early in the development of *Drosophila*. Chapter 4 describes the characterization of amine neurotransmitter effects on the cardiac function of *Drosophila*, which also has relevance to changes that happen early in the disease progression of PD. The final chapter discuses future directions for this work, including the use of adult *Drosophila* to understand dopamine changes that occur once PD has

progressed to symptomatic stage. Taken together, this work expands our understanding of early dopaminergic changes that occur in PD, provides an interesting new target for pharmacological intervention early in PD development, and improves the utility of *Drosophila* as a model organism for PD by expanding the available tools for studying dopamine.

Chapter 1 References

Adams MD (2000) The Genome Sequence of Drosophila melanogaster. Science (80-) 287:2185–2195.

Alex A, Li A, Tanzi RE, Zhou C (2015) Optogenetic pacing in Drosophila melanogaster.

Anderson LR, Betarbet R, Gearing M, Gulcher J, Hicks A a, Stefánsson K, Lah JJ, Levey AI (2007) PARK10 candidate RNF11 is expressed by vulnerable neurons and localizes to Lewy bodies in Parkinson disease brain. J Neuropathol Exp Neurol 66:955–964.

Ariansen JL, Heien ML a V, Hermans A, Phillips PEM, Hernadi I, Bermudez M a, Schultz W, Wightman RM (2012) Monitoring extracellular pH, oxygen, and dopamine during reward delivery in the striatum of primates. Front Behav Neurosci 6:36.

Armstrong J, Barlow RB (1976) THE IONIZATION OF PHENOLIC AMINES , INCLUDING AND AN ASSESSMENT OF ZWITTERION CONSTANTS. Br J Pharmac 57:501–516.

Bamann C, Kirsch T, Nagel G, Bamberg E (2008) Spectral characteristics of the photocycle of channelrhodopsin-2 and its implication for channel function. J Mol Biol 375:686–694.

Bang S, Hyun S, Hong S-T, Kang J, Jeong K, Park J-J, Choe J, Chung J (2011) Dopamine signalling in mushroom bodies regulates temperature-preference behaviour in Drosophila. PLoS Genet 7:e1001346.

Barbeau a (1969) L-dopa therapy in Parkinson's disease: a critical review of nine years' experience. Can Med Assoc J 101:59–68.

Bass CE, Grinevich VP, Kulikova AD, Bonin KD, Budygin EA (2013) Terminal effects of optogenetic stimulation on dopamine dynamics in rat striatum. J Neurosci Methods 214:149–155.

Bath BD, Michael DJ, Trafton BJ, Joseph JD, Runnels PL, Wightman RM (2000) Subsecond adsorption and desorption of dopamine at carbon-fiber microelectrodes. Anal Chem 72:5994–6002.

Beitz JM (2014) Parkinson's disease: a review. Front Biosci S6:65–74.

Berglund EC, Makos MA, Keighron JD, Phan N, Heien ML, Ewing AG (2013) Oral administration of methylphenidate blocks the effect of cocaine on uptake at the Drosophila dopamine transporter. ACS Chem Neurosci 4:566–574.

Berry JA, Cervantes-Sandoval I, Nicholas EP, Davis RL (2012) Dopamine is required for learning and forgetting in Drosophila. Neuron 74:530–542.

Björklund A, Dunnett SB (2007) Dopamine neuron systems in the brain: an update. Trends Neurosci 30:194–202.

Blenau W, Baumann A (2001) Molecular and pharmacological properties of insect biogenic amine receptors: lessons from Drosophila melanogaster and Apis mellifera. Arch Insect Biochem Physiol 48:13–38.

Borue X, Condron B, Venton BJ (2010) Both synthesis and reuptake are critical for replenishing the releasable serotonin pool in Drosophila. J Neurochem 113:188–199.

Borue X, Cooper S, Hirsh J, Condron B, Venton BJ (2009) Quantitative evaluation of serotonin release and clearance in Drosophila. J Neurosci Methods 179:300–308.

Bouabid S, Tinakoua A, Lakhdar-Ghazal N, Benazzouz A (2015) Manganese Neurotoxicity: behavioral disorders associated with dysfunctions in the basal ganglia and neurochemical transmission. J Neurochem.

Braak H, Del Tredici K (2008) Invited Article: Nervous system pathology in sporadic Parkinson disease. Neurology 70:1916–1925.

Brand a H, Perrimon N (1993) Targeted gene expression as a means of altering cell fates and generating dominant phenotypes. Development 118:401–415.

Bunin MA, Prioleau C, Mailman RB, Wightman RM (1998) Release and uptake rates of 5-hydroxytryptamine in the dorsal raphe and substantia nigra reticulata of the rat brain. J Neurochem 70:1077–1087.

Chang S-Y, Kim I, Marsh MP, Jang DP, Hwang S-C, Van Gompel JJ, Goerss SJ, Kimble CJ, Bennet KE, Garris PA, Blaha CD, Lee KH (2012) Wireless Fast-Scan Cyclic Voltammetry to Monitor Adenosine in Patients With Essential Tremor During Deep Brain Stimulation. Mayo Clin Proc 87:760–765.

Chen ZJ, Sun LJ (2009) Nonproteolytic Functions of Ubiquitin in Cell Signaling. Mol Cell 33:275–286.

Cheng HC, Ulane C., Burke R. (2010) Clinical progression in Parkinson's disease and the neurobiology of Axons. Ann Neurol 67:715–725.

Cookson MR (2009) alpha-Synuclein and neuronal cell death. Mol Neurodegener 4:9.

Cooper SE, Venton BJ (2009) Fast-scan cyclic voltammetry for the detection of tyramine and octopamine. Anal Bioanal Chem 394:329–336.

Corey JL, Quick MW, Davidson N, Lester H a, Guastella J (1994) A cocaine-sensitive Drosophila serotonin transporter: cloning, expression, and electrophysiological characterization. Proc Natl Acad Sci U S A 91:1188–1192.

Crickmore MA, Vosshall LB (2013) Opposing dopaminergic and GABAergic neurons control the duration and persistence of copulation in Drosophila. Cell 155:881–893.

Deisseroth K, Feng G (2006) Next-generation optical technologies for illuminating

genetically targeted brain circuits. J … 26.

Denno ME, Privman E, Borman RP, Wolin DC, Venton BJ (2016) Quantification of Histamine and Carcinine in Drosophila melanogaster Tissues. ACS Chem Neurosci:acschemneuro.5b00326.

Denno ME, Privman E, Venton BJ (2014) Analysis of Neurotransmitter Tissue Content of Drosophila melanogaster in Different Life Stages. ACS Chem Neurosci.

Doshi PK (2011) Long-term surgical and hardware-related complications of deep brain stimulation. Stereotact Funct Neurosurg 89:89–95.

Duffy JB (2002) GAL4 system in Drosophila: a fly geneticist's Swiss army knife. Genesis 34:1–15.

Eisenhofer G, Aneman Å, Friberg P, Hooper D, Fåndriks L, Lonroth H, Hunyady B, Mezey E (1997) Substantial production of Dopamine in the human gastrointestinal tract. J Clin Endocrinol Metab 82:3864–3871.

Freeman A, Pranski E, Miller RD, Radmard S, Bernhard D, Jinnah H, Betarbet R, Rye DB, Sanyal S (2013) Sleep fragmentation and motor restlessness in a Drosophila model of Restless Leg Syndrome. Curr Biol 22:1142–1148.

Fuenzalida-Uribe N, Meza RC, Hoffmann H a, Varas R, Campusano JM (2013) nAChR-induced octopamine release mediates the effect of nicotine on a startle response in Drosophila melanogaster. J Neurochem:281–290.

Fuxe K, Dahlström A, Höistad M, Marcellino D, Jansson A, Rivera A, Diaz-Cabiale Z, Jacobsen K, Tinner-Staines B, Hagman B, Leo G, Staines W, Guidolin D, Kehr J, Genedani S, Belluardo N, Agnati LF (2007) From the Golgi–Cajal mapping to the transmitter-based characterization of the neuronal networks leading to two modes of brain communication: Wiring and volume transmission. Brain Res Rev 55:17–54.

Garris PA, Ciolkowski EL, Pastore P, Wightman RM (1994) Efflux of dopamine from the synaptic cleft in the nucleus accumbens of the rat brain. J Neurosci 14:6084–6093.

Garris PA, Wightman RM (1995) Regional differences in dopamine release, uptake, and diffusion measured by fast-scan cyclic voltammetry. In: Neuromethods: Voltammetric Methods in Brain Systems (A B, G B, RN A, eds), pp 179–220. Humana Press Inc.

Gasque G, Conway S, Huang J, Rao Y, Vosshall LB (2013) Small molecule drug screening in Drosophila identifies the 5HT2A receptor as a feeding modulation target. Sci Rep 3:1–8.

Gazewood JD, Richards DR, Clebak K (2013) Parkinson disease: An update. Am Fam Physician 87:267–273.

Glass CK, Saijo K, Winner B, Marchetto MC, Gage FH (2010) Mechanisms Underlying Inflammation in Neurodegeneration. Cell 140:918–934.

Gonzales PA, Pisitkun T, Hoffert JD, Tchapyjnikov D, Star RA, Kleta R, Wang NS, Knepper MA (2009) Large-Scale Proteomics and Phosphoproteomics of Urinary Exosomes. J Am Soc Nephrol 20:363–379.

Hardie SL, Hirsh J (2006) An improved method for the separation and detection of biogenic amines in adult Drosophila brain extracts by high performance liquid chromatography. J Neurosci Methods 153:243–249.

Harun R, Grassi CM, Munoz MJ, Torres GE, Wagner AK (2014) Neurobiological model of stimulated dopamine neurotransmission to interpret fast-scan cyclic voltammetry data. Brain Res:1–18.

Hashemi P, Dankoski EC, Petrovic J, Keithley RB, Wightman RM (2009) Voltammetric detection of 5-hydroxytryptamine release in the rat brain. Anal Chem 81:9462–9471.

Hawkes CH, Del Tredici K, Braak H (2010) A timeline for Parkinson's disease. Park Relat Disord 16:79–84.

Hayden MS, Ghosh S (2008) Shared Principles in NF-kappaB Signaling. Cell 132:344–362.

Herrington FD, Carmody RJ, Goodyear CS (2015) Modulation of NF- κ B Signaling as a Therapeutic Target in Autoimmunity. J Biomol Screen.

Hirth F (2010) Drosophila melanogaster in the Study of Human Neurodegeneration. CNS Neurol Disord - Drug Targets 9:504–523.

Hong BS, Cho J-H, Kim H, Choi E-J, Rho S, Kim J, Kim JH, Choi D-S, Kim Y-K, Hwang D, Gho YS (2009) Colorectal cancer cell-derived microvesicles are enriched in cell cycle-related mRNAs that promote proliferation of endothelial cells. BMC Genomics 10:556.

Hormuzdi SG, Filippov MA, Mitropoulou G, Monyer H, Bruzzone R (2004) Electrical synapses: a dynamic signaling system that shapes the activity of neuronal networks. Biochem Biophys Acta 1662:113–137.

Huffman ML, Venton BJ (2008) Electrochemical Properties of Different Carbon-Fiber Microelectrodes Using Fast-Scan Cyclic Voltammetry. Electroanalysis 20:2422–2428.

Huser A, Rohwedder A, Apostolopoulou A a, Widmann A, Pfitzenmaier JE, Maiolo EM, Selcho M, Pauls D, von Essen A, Gupta T, Sprecher SG, Birman S, Riemensperger T, Stocker RF, Thum AS (2012) The serotonergic central nervous system of the Drosophila larva: anatomy and behavioral function. PLoS One 7:e47518.

Huxford T, Ghosh G (2009) A structural guide to proteins of the NF-kappaB signaling module. Cold Spring Harb Perspect Biol 1:1–16.

Jackson B, Dietz S, Wightman R (1995) Fast-Scan Cyclic Voltammetry of 5-Hydroxytryptamine. Anal Chem 67:1115–1120.

Jacobs CB, Ivanov IN, Nguyen MD, Zestos AG, Venton BJ (2014) High temporal resolution measurements of dopamine with carbon nanotube yarn microelectrodes. Anal Chem 86:5721–5727.

Jacobs CB, Vickrey TL, Venton BJ (2011) Functional groups modulate the sensitivity and electron transfer kinetics of neurochemicals at carbon nanotube modified microelectrodes. Analyst 136:3557–3565.

Jones SR, Garris PA, Kilts CD, Wightman RM (1995) Comparison of dopamine uptake in the basolateral amygdaloid nucleus, caudate-putamen, and nucleus accumbens of the rat. J Neurochem 64:2581–2589.

Kahsai L, Winther AME (2011) Chemical neuroanatomy of the Drosophila central complex: distribution of multiple neuropeptides in relation to neurotransmitters. J Comp Neurol 519:290–315.

Kitada T, Asakawa S, Hattori N, Matsumine H, Yamamura Y, Minoshima S, Yokochi M, Mizuno Y, Shimizu N (1998) Mutations in the parkin gene cause autosomal recessive juvenile parkinsonism. Nature 392:605–608.

Klapoetke NC et al. (2014) Independent optical excitation of distinct neural populations. Nat Methods 11:338–346.

Klingelhoefer L, Reichmann H (2015) Pathogenesis of Parkinson disease—the gut–brain axis and environmental factors. Nat Rev Neurol 11:625–636.

Kostaras E, Pedersen NM, Stenmark H, Fotsis T, Murphy C (2014) SARA and RNF11 at the crossroads of EGFR signaling and trafficking., 1st ed. Elsevier Inc.

Kume K, Kume S, Park SK, Hirsh J, Jackson FR (2005) Dopamine is a regulator of arousal in the fruit fly. J Neurosci 25:7377–7384.

Lange AB (2009) Tyramine: from octopamine precursor to neuroactive chemical in insects. Gen Comp Endocrinol 162:18–26.

Lemaitre B, Miguel-Aliaga I (2013) The Digestive Tract of Drosophila melanogaster. Annu Rev Genet 47:377–404.

Lesage S, Brice A (2009) Parkinson's disease: from monogenic forms to genetic susceptibility factors. Hum Mol Genet 18:R48–R59.

Li MD, Burns TC, Morgan A a, Khatri P (2014) Integrated multi-cohort transcriptional meta-analysis of neurodegenerative diseases. Acta Neuropathol Commun 2:93.

Li W, Chen S, Li J-Y (2015) Human induced pluripotent stem cells in Parkinson's disease: A novel cell source of cell therapy and disease modeling. Prog Neurobiol 134:161–177.

Lima SQ, Miesenböck G (2005) Remote control of behavior through genetically targeted photostimulation of neurons. Cell 121:141–152.

Lin C-H, Lin J-W, Liu Y-C, Chang C-H, Wu R-M (2014) Risk of Parkinson's

disease following severe constipation: A nationwide population-based cohort study. Parkinsonism Relat Disord:1–5.

Liu C, Plaçais P-Y, Yamagata N, Pfeiffer BD, Aso Y, Friedrich AB, Siwanowicz I, Rubin GM, Preat T, Tanimoto H (2012) A subset of dopamine neurons signals reward for odour memory in Drosophila. Nature 488:512–516.

Lu B, Vogel H (2009) Drosophila Models of Neurodegenerative Diseases. Annu Rev Pathol 4:315–342.

Majdi S, Berglund EC, Dunevall J, Oleinick AI, Amatore C, Krantz DE, Ewing AG (2015) Electrochemical Measurements of Optogenetically Stimulated Quantal Amine Release from Single Nerve Cell Varicosities in Drosophila Larvae. Angew Chemie Int Ed 54:13609–13612.

Makos M, Kuklinski N, Heien M (2009a) Chemical measurements in Drosophila. TrAC Trends … 28:1223–1234.

Makos MA, Han K-A, Heien ML, Ewing AG (2010) Using in Vivo Electrochemistry to Study the Physiological Effects of Cocaine and Other Stimulants on the Drosophila melanogaster Dopamine Transporter. ACS Chem Neurosci 1:74–83.

Makos MA, Kim Y-C, Han K-A, Heien ML, Ewing AG (2009b) In vivo electrochemical measurements of exogenously applied dopamine in Drosophila melanogaster. Anal Chem 81:1848–1854.

Mao Z, Davis RL (2009) Eight different types of dopaminergic neurons innervate the Drosophila mushroom body neuropil: anatomical and physiological heterogeneity. Front Neural Circuits 3:5.

Marella S, Mann K, Scott K (2012) Dopaminergic Modulation of Sucrose Acceptance Behavior in Drosophila. Neuron 73:941–950.

Martin CA, Krantz DE (2014) Drosophila melanogaster as a genetic model system to study neurotransmitter transporters. Neurochem Int 73:71–88.

McCreery RL (2008) Advanced carbon electrode materials for molecular electrochemistry. Chem Rev 108:2646–2687.

McGurk L, Berson A, Bonini NM (2015) Drosophila as an In Vivo Model for Human Neurodegenerative Disease. Genetics 201:377–402.

Meyer SN, Amoyel M, Bergantinos C, de la Cova C, Schertel C, Basler K, Johnston LA (2014) An ancient defense system eliminates unfit cells from developing tissues during cell competition. Science (80-) 346:1258236–1258236.

Miyasaki JM, Martin W, Suchowersky O, Weiner WJ, Lang AE (2002) Practice parameter: initiation of treatment for Parkinson's disease: an evidence-based review: report of the Quality Standards Subcommittee of the American Academy of Neurology. Neurology 58:11–17.

Miyasaki JM, Shannon K, Voon V, Ravina B, Kleiner-Fisman G, Anderson K, Shulman LM, Gronseth G, Weiner WJ (2006) Practice parameter: Evaluation and treatment of depression, psychosis, and dementia in Parkinson disease (an evidence-based review): Report of the Quality Standards Subcommittee of the American Academy of Neurology. Neurology 66:996–1002.

Monastirioti M (1999) Biogenic amine systems in the fruit fly Drosophila melanogaster. Microsc Res Tech 45:106–121.

Moon HE, Paek SH (2015) Mitochondrial Dysfunction in Parkinson's Disease. Exp Neurobiol 24:103–116.

Morales J, Hiesinger PR, Schroeder AJ, Kume K, Verstreken P, Jackson FR, Nelson DL, Hassan B a (2002) Drosophila fragile X protein, DFXR, regulates neuronal morphology and function in the brain. Neuron 34:961–972.

Nagel G, Szellas T, Huhn W, Kateriya S, Adeishvili N, Berthold P, Ollig D, Hegemann P, Bamberg E (2003) Channelrhodopsin-2, a directly light-gated cation-selective membrane channel. Proc Natl Acad Sci 100:13940–13945.

Neckameyer WS, Bhatt P (2012) Neurotrophic actions of dopamine on the development of a serotonergic feeding circuit in Drosophila melanogaster. BMC Neurosci 13:26.

Pahwa R, Factor SA, Lyons KE, Ondo WG, Gronseth G, Bronte-Stewart H, Hallett M, Miyasaki J, Stevens J, Weiner WJ (2006) Practice parameter: Treatment of Parkinson disease with motor fluctuations and dyskinesia (an evidence-based review): Report of the Quality Standards Subcommittee of the American Academy of Neurology. Neurology 66:983–995.

Pandey UB, Nichols CD (2011) Human disease models in Drosophila melanogaster and the role of the fly in therapeutic drug discovery. Pharmacol Rev 63:411–436.

Park J, Lee SB, Lee S, Kim Y, Song S, Kim S, Bae E, Kim J, Shong M, Kim J-M, Chung J (2006) Mitochondrial dysfunction in Drosophila PINK1 mutants is complemented by parkin. Nature 441:1157–1161.

Pech U, Pooryasin A, Birman S, Fiala A (2013) Localization of the contacts between Kenyon cells and aminergic neurons in the Drosophila melanogaster brain using SplitGFP reconstitution. J Comp Neurol 521:3992–4026.

Pellegrini C, Antonioli L, Colucci R, Ballabeni V, Barocelli E, Bernardini N, Blandizzi C, Fornai M (2015) Gastric motor dysfunctions in Parkinson's disease: Current pre-clinical evidence. Parkinsonism Relat Disord 21:1407–1414.

Pisitkun T, Shen R-F, Knepper M a (2004) Identification and proteomic profiling of exosomes in human urine. Proc Natl Acad Sci U S A 101:13368–13373.

Polymeropoulos MH et al. (1997) Mutation in the α-Synuclein Gene Identified in

Families with Parkinson's Disease. Science (80-) 276:2045–2047.

Pörzgen P, Park SK, Hirsh J, Sonders MS, Amara SG (2001) The antidepressant-sensitive dopamine transporter in Drosophila melanogaster: a primordial carrier for catecholamines. Mol Pharmacol 59:83–95.

Pranski EL, Dalal N V, Van Sanford CD, Herskowitz JH, Gearing M, Lazo C, Miller GW, Lah JJ, Levey AI, Betarbet RS (2013a) RING finger protein 11 (RNF11) modulates susceptibility to 6- OHDA-induced nigral degeneration and behavioral deficits through NF-κB signaling in dopaminergic cells. Neurobiol Dis 54:264–279.

Pranski EL, Van Sanford CD, Dalal N V, Orr AL, Karmali D, Cooper DS, Costa N, Heilman CJ, Gearing M, Lah JJ, Levey AI, Betarbet RS (2012) Comparative distribution of protein components of the A20 ubiquitin-editing complex in normal human brain. Neurosci Lett 520:104–109.

Pranski EL, Van Sanford CD, Dalal N V, Orr AL, Karmali D, Cooper DS, Gearing M, Lah JJ, Levey AI, Betarbet RS (2013b) NF-κB activity is inversely correlated to RNF11 expression in Parkinson's disease. Neurosci Lett 547:16–20.

Privman E, Venton BJ (2015) Comparison of dopamine kinetics in the larval Drosophila ventral nerve cord and protocerebrum with improved optogenetic stimulation. J Neurochem 135:695–704.

Qi C, Lee D (2014) Pre- and Postsynaptic Role of Dopamine D2 Receptor DD2R in Drosophila Olfactory Associative Learning. Biology (Basel) 3:831–845.

Riemensperger T, Isabel G (2011) Behavioral consequences of dopamine deficiency in the Drosophila central nervous system. Proc ….

Roberts JG, Toups JV, Eyualem E, McCarty GS, Sombers L a. (2013) In situ electrode calibration strategy for voltammetric measurements in vivo. Anal Chem Chem 85:11568–11575.

Robinson DL, Venton BJ, Heien ML a V, Wightman RM (2003) Detecting subsecond dopamine release with fast-scan cyclic voltammetry in vivo. Clin Chem 49:1763–1773.

Roeder T (2005) TYRAMINE AND OCTOPAMINE: Ruling Behavior and Metabolism. Rev Lit Arts Am.

Ross AE, Nguyen MD, Privman E, Venton BJ (2014) Mechanical stimulation evokes rapid increases in extracellular adenosine concentration in the prefrontal cortex. J Neurochem 130:50–60.

Rubin G (2015) FlyBook: A Preface. Genetics 201:343.

Santonico E, Mattioni A, Panni S, Belleudi F, Mattei M, Torrisi MR, Cesareni G, Castagnoli L (2014) RNF11 is a GGA protein cargo and acts as a molecular adaptor for GGA3 ubiquitination mediated by Itch. Oncogene 34:1–14.

Seki N, Hattori A, Hayashi A, Kozuma S, Sasaki M, Suzuki Y, Sugano S, Muramatsu M a, Saito T (1999) Cloning and expression profile of mouse and human genes, Rnf11/RNF11, encoding a novel RING-H2 finger protein. Biochim Biophys Acta 1489:421–427.

Selcho M, Pauls D, El Jundi B, Stocker RF, Thum AS (2012) The Role of octopamine and tyramine in Drosophila larval locomotion. J Comp Neurol 520:3764–3785.

Selcho M, Pauls D, Han K-A, Stocker RF, Thum AS (2009) The role of dopamine in Drosophila larval classical olfactory conditioning. PLoS One 4:e5897.

Shembade N, Parvatiyar K, Harhaj NS, Harhaj EW (2009) The ubiquitin-editing enzyme A20 requires RNF11 to downregulate NF-kappaB signalling. EMBO J 28:513–522.

Singaram C, Gaumnitz E, Torbey C (1995) Dopaminergic defect of enteric nervous system in Parkinson's disease patients with chronic constipation. Lancet:861–864.

Sinkala E, McCutcheon JE, Schuck M, Schmidt E, Roitman MF, Eddington DT (2013) Electrode Calibration with a Microfluidic Flow Cell for Fast-scan Cyclic Voltammetry. Lab Chip 12:2403–2408.

Suh J, Jackson FR (2008) Drosophila Ebony Activity is Required in Glia for the Circadian Regulation of Locomotor Activity. Neuron 55:435–447.

Suzuki K, Miyamoto M, Miyamoto T, Hirata K (2015) Restless Legs Syndrome and Leg Motor Restlessness in Parkinson's Disease. Parkinsons Dis 2015:1–9.

Swamy BEK, Venton BJ (2007) Carbon nanotube-modified microelectrodes for simultaneous detection of dopamine and serotonin in vivo. Analyst 132:876–884.

Takmakov P, Zachek MK, Keithley RB, Bucher ES, McCarty GS, Wightman RM (2010) Characterization of local pH changes in brain using fast-scan cyclic voltammetry with carbon microelectrodes. Anal Chem 82:9892–9900.

Tanner CM et al. (2011) Rotenone, paraquat, and Parkinson's disease. Environ Health Perspect 119:866–872.

Titlow JS, Rufer JM, King KE, Cooper RL (2013) Pharmacological analysis of dopamine modulation in the Drosophila melanogaster larval heart. Physiol Rep 1:e00020.

Tyson T, Steiner JA, Brundin P (2015) Sorting Out Release, Uptake and Processing of Alpha-Synuclein During Prion-Like Spread of Pathology. J Neurochem.

Ueno T, Kume K (2014) Functional characterization of dopamine transporter in vivo using Drosophila melanogaster behavioral assays. Front Behav Neurosci 8:1–11.

Valanne S, Wang J-H, Rämet M (2011) The Drosophila Toll signaling pathway. J Immunol 186:649–656.

Valente EM et al. (2004) Hereditary early-onset Parkinson's disease caused by mutations in PINK1. Science 304:1158–1160.

Varga SJ, Qi C, Podolsky E, Lee D (2014) A new Drosophila model to study the interaction between genetic and environmental factors in Parkinson's disease. Brain Res 1583:277–286.

Vickrey TL, Condron B, Venton BJ (2009) Detection of endogenous dopamine changes in Drosophila melanogaster using fast-scan cyclic voltammetry. Anal Chem 81:9306–9313.

Vickrey TL, Venton BJ (2011) Drosophila Dopamine2-like receptors function as autoreceptors. ACS Chem Neurosci 2:723–729.

Vickrey TL, Xiao N, Venton BJ (2013) Kinetics of the dopamine transporter in Drosophila larva. ACS Chem Neurosci 4:832–837.

Von Stockum S, Nardin A, Schrepfer E, Ziviani E (2015) Mitochondrial dynamics and mitophagy in Parkinson's disease: A fly point of view. Neurobiol Dis.

Wang D, Qian L, Xiong H, Liu J, Neckameyer WS, Oldham S, Xia K, Wang J, Bodmer R, Zhang Z (2006) Antioxidants protect PINK1-dependent dopaminergic neurons in Drosophila. Proc Natl Acad Sci U S A 103:13520–13525.

Wessnitzer J, Webb B (2006) Multimodal sensory integration in insects--towards insect brain control architectures. Bioinspir Biomim 1:63–75.

West RJH, Furmston R, Williams CAC, Elliott CJH (2015) Neurophysiology of Drosophila Models of Parkinson's Disease. Parkinsons Dis 2015:1–11.

Whitworth AJ (2011) Drosophila models of Parkinson's disease., 1st ed. Elsevier Inc.

Wolf MJ, Rockman HA (2011) Drosophila, Genetic Screens, and Cardiac Function. Circ Res 109:794–806.

Wright NJD (2013) Evolution of the techniques used in studying associative olfactory learning and memory in adult Drosophila in vivo: a historical and technical perspective. Invert Neurosci.

Xiao N, Privman E, Venton BJ (2014) Optogenetic control of serotonin and dopamine release in Drosophila larvae. ACS Chem Neurosci 5:666–673.

Xiao N, Venton BJ (2015) Characterization of dopamine releasable and reserve pools in Drosophila larvae using ATP/P2X2 -mediated stimulation. J Neurochem 134:445–454.

Yamagata N, Ichinose T, Aso Y, Plaçais P-Y, Friedrich AB, Sima RJ, Preat T, Rubin GM, Tanimoto H (2015) Distinct dopamine neurons mediate reward signals for short- and long-term memories. Proc Natl Acad Sci 112:578–583.

Yamamoto S et al. (2014) A Drosophila Genetic Resource of Mutants to Study Mechanisms Underlying Human Genetic Diseases. Cell 159:200–214.

Yamamoto S, Seto ES (2014) Dopamine dynamics and signaling in Drosophila: an overview of genes, drugs and behavioral paradigms. Exp Anim 63:107–119.

Zesiewicz TA, Sullivan KL, Arnulf I, Chaudhuri KR, Morgan JC, Gronseth GS, Miyasaki J, Iverson DJ, Weiner WJ (2010) Practice parameter: Treatment of nonmotor symptoms of Parkinson disease: Report of the quality standards subcommittee of the American academy of neurology. Neurology 74:924–931.

Chapter 2: Comparison of Dopamine Kinetics in the Larval Drosophila Ventral Nerve Cord and Protocerebrum with Improved Optogenetic Stimulation

Abstract

Dopamine release and uptake have been studied in the *Drosophila* larval ventral nerve cord (VNC) using optogenetics to stimulate endogenous release. However, other areas of the central nervous system remain uncharacterized. Here, we compare dopamine release in the VNC and protocerebrum of larval *Drosophila.* Stimulations were performed with CsChrimson, a new, improved, red light-activated channelrhodopsin. In both regions, dopamine release was observed after only a single, 4 ms duration light pulse. Michaelis-Menten modeling was used to understand release and uptake parameters for dopamine. The amount of dopamine released ($[DA]_p$) on the first stimulation pulse is higher than the average $[DA]_p$ released from subsequent pulses. The initial and average amount of dopamine released per stimulation pulse is smaller in the protocerebrum than in the VNC. The average V_{max} of 0.08 μM/s in the protocerebrum was significantly higher than the V_{max} of 0.05 μM/s VNC. The average K_m of 0.11 μM in the protocerebrum was not significantly different from the K_m of 0.10 μM in the VNC. When the competitive dopamine transporter (DAT) inhibitor nisoxetine was applied, the K_m increased significantly in both regions while V_{max} stayed the same. This work demonstrates regional differences in dopamine release and uptake kinetics, indicating important variation in the amount of dopamine available for neurotransmission and neuromodulation. This work was published in the Journal of Neurochemistry.

Introduction

There are a vast array of genetic tools available to study *Drosophila melanogaster*, making it a powerful and convenient model organism.(Martin and Krantz, 2014) The basic mechanisms of neurotransmission are evolutionarily conserved, allowing for the study of human neurological diseases in *Drosophila*.(Pandey and Nichols, 2011) There are approximately 90 dopaminergic neurons in the larval *Drosophila* central nervous system, organized into clusters in the protocerebrum, subesophageal zone, and the ventral nerve cord (VNC).(Selcho et al., 2009) Each region mediates specific physiological responses and behaviors. Dopaminergic neurons in the VNC function in motor behaviors such as grooming and copulation, dopaminergic neurons in the protocerebrum control olfactory learning and memory, and dopaminergic neurons in the subesophageal ganglion trigger proboscis extension as part of the primary taste relay.(Yellman et al., 1997; Selcho et al., 2009; Marella et al., 2012; Crickmore and Vosshall, 2013) Direct measurements of endogenous dopamine have only been made in the larval VNC.(Borue et al., 2009; Vickrey et al., 2009; Xiao et al., 2014)

In *Drosophila* larvae, Channelrhodopsin-2 (ChR2) is a cation channel that has been used to evoke endogenous neurotransmitter release, which is measured using an implanted microelectrode.(Vickrey et al., 2009, 2013; Borue et al., 2010; Vickrey and Venton, 2011) Optogenetic stimulation can be used to excite subpopulations of neurons by targeting specific neurotransmitter synthesis pathways using the Gal4/UAS system.(Duffy, 2002; Nagel et al., 2003) ChR2

responds to blue light, which does not penetrate deeply into tissue and can cause an aberrant signal near the switching potential in electrochemical recordings (Figure 2.1).(Vickrey et al., 2009; Bass et al., 2013; Xiao et al., 2014) Recently, there has been interest in shifting from blue to red light activated channelrhodopsins.(Nagel et al., 2003; Lin et al., 2013; Klapoetke et al., 2014) Red light penetrates deeper and is less visible to flies, making it more useful in behavioral experiments. Klapoetke *et al* (2014) characterized the cation channel CsChrimson in *Drosophila*, controlling neuronal activation using short, low-intensity, red light stimulations.

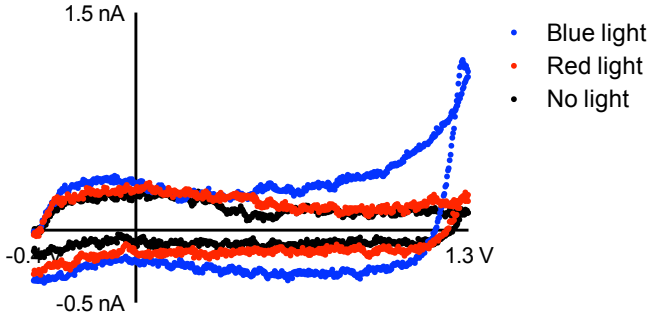

Figure 2.1 - Blue light directly affects the carbon fiber microelectrode. Blue (473 nm) or red (617 nm) light was applied to a carbon fiber microelectrode in buffer for 5 seconds. After background subtraction, the cyclic voltammograms were compared to the same electrode after being in buffer for 5 seconds without light. The red light did not cause direct errors at the carbon surface. However, the blue light caused a large error near the switching potential (1.3 V).

Dopamine is cleared from the extracellular space by uptake through *Drosophila* dopamine transporters (dDAT).(Pörzgen et al., 2001) dDAT regulation of extracellular dopamine has been studied by exogenously applying dopamine and then modeling the clearance using Michaelis-Menten kinetics.(Sabeti et al., 2002; Makos et al., 2009b, 2010; Berglund et al., 2013; Vickrey et al., 2013) Alternatively, stimulated endogenous dopamine release can be modeled to

extract Michaelis-Menten values. Studying endogenous dopamine is advantageous because physiological amounts are measured and the dopamine released per stimulation pulse can be modeled. In mammals, dopamine release and clearance kinetics vary by brain region due to differential terminal density and DAT expression and we hypothesize that distinct *Drosophila* neuropil will also have differences in release and uptake.(Wu et al., 2001)

Here, we compare dopamine release in the *Drosophila* larval VNC and protocerebrum. The amount of dopamine released was high with CsChrimson-mediated stimulations and it could be measured after a single, 4 ms pulse of red light. Stimulated dopamine release was larger in the VNC than the protocerebrum, and the regions exhibited different uptake kinetics.

Materials and Methods

Chemicals

All chemicals were purchased from Sigma-Aldrich (St. Louis, MO) and all solutions were made with Milli-Q water (Millipore, Billerica, MA). Dissections, recordings, and calibrations were performed in a simple physiological solution (131.3 mM NaCl, 3.0 mM KCl, 10 mM NaH_2PO_4 monohydrate, 1.2 mM $MgCl_2$ hexahydrate, 2.0 mM Na_2SO_4 anhydrous, 1.2 $CaCl_2$ dihydrate, 11.1 mM glucose, 5.3 mM trehalose, pH = 7.4). A concentrated stock solution of nisoxetine was made in buffer and added to the sample for a final concentration of 20 μM.

Electrochemical Measurements

Carbon fiber microelectrodes were fabricated from T-650 carbon fibers (a gift of Cytec Engineering Materials, West Patterson, NJ) as previously

described.(Jacobs et al., 2011) Electrodes were calibrated *in vitro* using a flow cell to alternatively apply buffer and buffer containing 1 μM dopamine to determine the unique response to 1 μM dopamine for each electrode. The amount of dopamine measured *in vivo* is then calculated using this calibration factor, since the measured peak oxidation current for dopamine increases linearly with dopamine concentration within the physiological range. Fast-scan cyclic voltammetry was performed using a ChemClamp potentiostat with a n=0.01 headstage (Dagan, Minneapolis, MN), PCI 6711 and 6052 computer interface cards (National Instruments, Austin, TX), and a home built break-out box. The TarHeel CV software (a gift of Mark Wightman, University of North Carolina) was used to collect and background subtract the data. Every 100 ms the electrode was scanned from -0.4 to 1.3 V at 400 V/s.

Tissue Preparation

Virgin females with UAS-CsChrimson (a chimera of CsChR and Chrimson; a gift of Vivek Jayaraman) inserted in attp18 were crossed with TH-GAL4 (a gift of Jay Hirsh).(Klapoetke et al., 2014) Resulting heterozygous larvae were shielded from light and raised on standard cornmeal food mixed 250:1 with 100 mM all-trans-retinal (Sigma-Aldrich, St. Louis, MO). A small amount of moistened Red Star yeast (Red Star, Wilwaukii, WI) was placed on top of the food to promote egg laying. The central nervous system of third instar wandering larvae of either sex were dissected out in buffer. Isolated VNCs were prepared and recorded from as previously described.(Borue et al., 2009) For the protocerebrum recordings, the CNS was placed on an uncoated Petri dish dorsal side down. A small slice of the

lateral optic lobe was removed using the tip of a 22-gauge hypodermic needle. The electrode was implanted from the lateral edge of the tissue into the dorsal medial protocerebrum. The electrode was allowed to equilibrate in the tissue for 10 minutes prior to data collection. A baseline recording was taken for 10 seconds prior to stimulation.

Stimulated Neurotransmitter Release

Red-orange light from a 617 nm fiber-coupled high-power LED with a 200 μm core optical cable (ThorLabs, Newton, NJ) was used to stimulate the CsChrimson ion channel. A commercial power meter (Coherent Incorporation, Santa Clara, CA) estimated the output power at 0.75 mW. The fiber was centered pointing at the brain region being monitored by the recording electrode and positioned 75-100 um from the sample using a micromanipulator. The light was modulated with Transistor-Transistor Logic (TTL) inputs to a T-cube LED controller (ThorLabs, Newton, NJ), which was connected to the breakout box. TTL input was driven by electrical pulses controlled by the TarHeel CV software, which was used to control frequency, pulse width, and number of pulses.

Statistics and Data Analysis

Data are presented as mean +/- standard error of the mean (SEM) displayed as error bars. GraphPad Prism 6 (GraphPad Software Inc, La Jolla, CA) was used to perform all statistics, including one-way and two-way ANOVA with Bonferonni post-hoc test. Stimulated changes in the extracellular concentration of dopamine were modeled as a balance between discontinuous release and continuous uptake.(Wu et al., 2001) A nonlinear regression with a simplex minimization

algorithm was used to fit the curves.(Garris and Wightman, 1995) The modeling software was stopped when the iteration number continued increasing without a change in the three floated parameters. The goodness of the fit was described using the square regression coefficient (R^2). The R^2 fitting values for the two-second stimulations in the VNC were 0.94+/-0.01 (n=19) and in the protocerebrum were 0.91+/-0.02 (n=8). The average values of kinetic parameters were obtained by fitting data from 2 second long stimulations with 4 ms pulses at 60 Hz.

Results

Dopamine release was stimulated by red light (617 nm) from dopaminergic neurons in th-Gal4;UAS-CsChrimson larvae. Changes in dopamine concentration were measured with fast-scan cyclic voltammetry. For the VNC measurements, the 7 μm diameter carbon-fiber microelectrode was positioned in the neuropil of the isolated VNC (Figure 2.2A). A false color plot shows all the data collected with the background-subtracted current plotted in false color, applied potential on the y-axis, and time on the x-axis. Figure 2.2B shows an example of a 2 s continuous stimulation in the VNC, where dopamine oxidation (green) and reduction (dark blue) were observed around the expected potentials of 0.6 V and -0.2 V, respectively.(Garris and Wightman, 1995) The cyclic voltammograms, a plot of current vs voltage, provide an electrochemical fingerprint to help identity dopamine (Figure 2.2C). The shape and location of the oxidation and reduction peaks in the cyclic voltammogram are different than other fly neurotransmitters, such as serotonin and octopamine. In addition, the

specific targeting of the dopaminergic synthetic pathway with the th-GAL4 driver helps provide confident identification of the released electroactive compound as dopamine. Repeated stimulations in the presence of the serotonin synthesis blocker PCPA did not significantly decrease the signal as it does for serotonin release, indicating that secondary serotonin release does not contribute significantly to the measured current (Figure 2.3).(Borue et al., 2009) The concentration of dopamine in the extracellular space of the VNC increased while the light was on, and then quickly returned towards baseline when the light was turned off (Figure 2.2D). This indicates that the dopamine is released as a consequence of the light stimulation and no downstream product due to dopamine release is detected that would appear after the light is turned off.

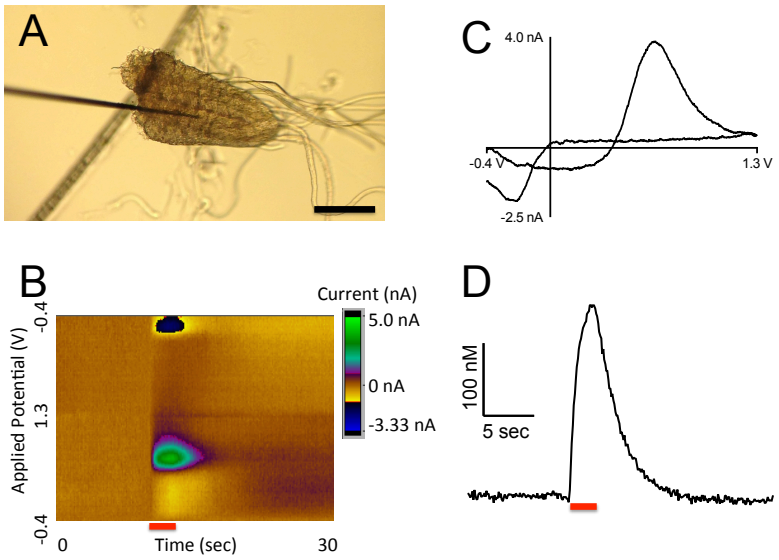

Figure 2.2 - CsChrimson stimulated dopamine release from the ventral nerve cord of larval *Drosophila.* (A) A 7 µm carbon fiber microelectrode inserted into the neuropil of an isolated VNC through a cut surface. Scale bar is 50 µm. (B) False color plot of dopamine release in the VNC. The red bar marks the duration of a 2 s continuous light stimulation. Note the oxidation of dopamine in green and the reduction in dark blue during the stimulation. (C) Cyclic voltammagram of dopamine has characteristic oxidation (0.6 V) and reduction (-0.2 V) peaks for dopamine. This plot is a vertical cut through the color plot at time

12 sec. (D) Concentration of dopamine over time. Red light was applied for 2 seconds (red bar) causing a peak extracellular dopamine concentration of 262 nM. This plot is a horizontal cut through the color plot at 0.6 V, with current converted to concentration using a precalibration factor unique to the recording electrode (see *Electrochemical Measurements* in Materials and Methods).

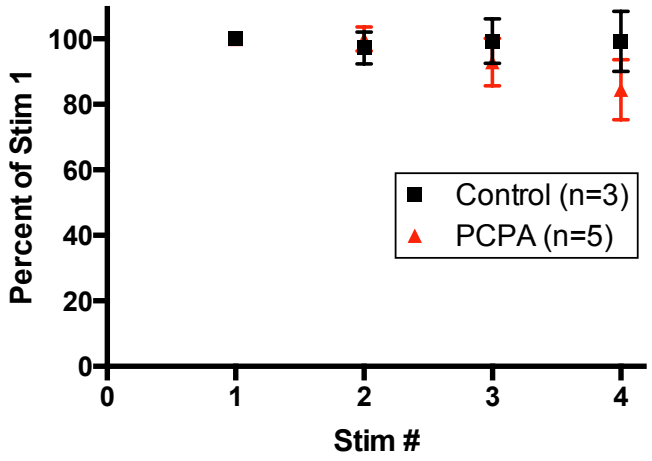

Figure 2.3 - Measured current does not significantly decrease in the presence of a serotonin synthesis blocker. VNC from th-GAL4;UAS-CsChrimson flies were dissected in either control buffer (n=3) or 100 μM para-chlorophenylalanine (PCPA; n=5). The electrode was inserted and the tissue was allowed to equilibrate for 10 minutes. 2 second long, 60 Hz pulsed red-light stimulations were repeated every 5 minutes. The tissue was incubated in either control or 100 μM PCPA buffer for the entirety of the experiment. Previous work indicates that repeated stimulations will reduce the serotonin signal to half its original amount within 4 stimulations.(Borue et al., 2009) A two-way ANOVA showed no significant main effect of stim # ($p=0.6289$) or drug treatment ($p=0.3342$), and no interaction ($p=0.5655$), indicating that serotonin does not contribute significantly to the measured signal. Data (mean +/- SEM) are normalized to the first stimulation to account for variation among animals.

Dopamine release and uptake were also monitored in a novel region of the *Drosophila* central nervous system: the protocerebrum. The carbon-fiber microelectrode was inserted into the medial protocerebrum through a lateral cut in the tissue (Figure 2.4A). Similarly to the VNC, extracellular dopamine concentration was evoked by 2 s continuous light and measured over time (Figure 2.4B and D). The identity of dopamine is confirmed by the cyclic voltammogram, which has oxidation and reduction peaks occurring at the same

potentials as in the VNC (Figure 2.4C). Note that the y-scale bar in Figure 2.2D is larger than in Figure 2.4D, because the measured dopamine release was larger in the VNC than in the protocerebrum.

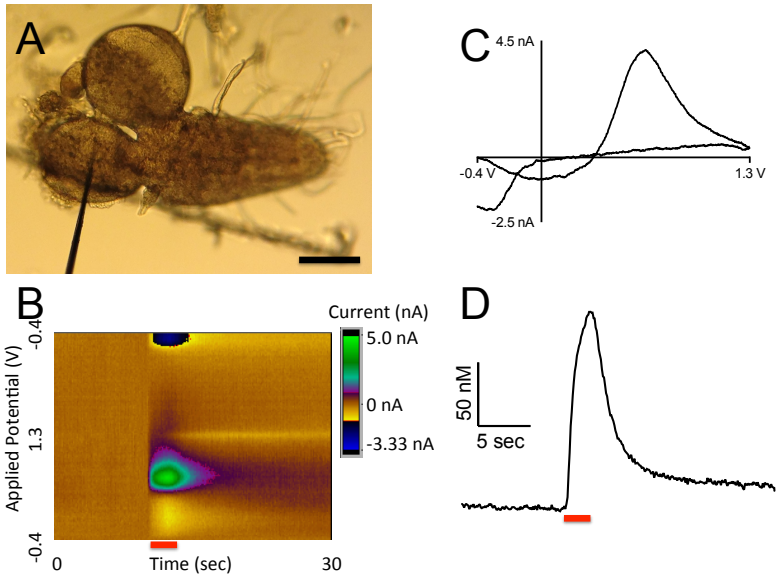

Figure 2.4 - CsChrimson stimulated release from the protocerebrum of larval *Drosophila*. (A) A 7 µm carbon fiber microelectrode inserted into the medial protocerebrum through a lateral cut in the central nervous system. Scale bar is 50 µm. (B) False color plot of dopamine release in the protocerebrum. Note the oxidation of dopamine in green and the reduction in dark blue as the red light is applied to the sample (red bar). (C) Cyclic voltammagram of dopamine as it is oxidized (0.6 V) and reduced (-0.2 V). (D) Concentration of dopamine over time. Red light was applied for 2 seconds (red bar) causing a peak extracellular dopamine concentration of 155 nM.

In previous studies using blue light to stimulate ChR2 mediated release, an error was observed at the switching potential due to the photoelectric effect.(Vickrey et al., 2009; Bass et al., 2013) With red light that error is eliminated (Figure 2.1), because the light is not of sufficient energy to interfere with the electrode. There is a slight decrease in current centered around 0 V in the cyclic voltammograms (Figure 2.2C, Figure 2.4C), but this peak is likely due to changes in pH or extracellular calcium concentrations due to the rapid,

simultaneous depolarization of many dopaminergic neurons.(Takmakov et al., 2010) The peak is not at the same potential as dopamine oxidation (0.6 V) or reduction (-0.2 V) and therefore does not interfere with dopamine detection.

In order to show that CsChrimson can be used to mimic different firing patterns, short pulses of red light were used to elicit dopamine release from the VNC and protocerebrum. Increasing concentrations of dopamine were detected with increasing number of pulses (Figure 2.5A). As the number of 4 ms light pulses increased from 1 to 120 at a frequency of 60 Hz, there was an increase in peak extracellular dopamine concentration (Figure 2.5B). However, the increase was not linear, indicating more dopamine was released for the first few pulses. A two-way ANOVA indicates a main effect of pulse number ($p<0.0001$, n=5-7) and brain region ($p<0.0001$, n=5-7), and no interaction. The protocerebrum releases less dopamine than the VNC. The data for each animal were then normalized to 2 second continuous stimulations to account for differences in release between animals (Figure 2.5C). The amount of dopamine release by pulsed stimulations was always less than or equal to the 2 s continuous stimulation. The normalized data reveal that the shape of the curves for the VNC and protocerbrum are similar. A two-way ANOVA indicates a main effect of pulse number ($p<0.0001$, n=5-7), but no effect due to brain region and no interaction.

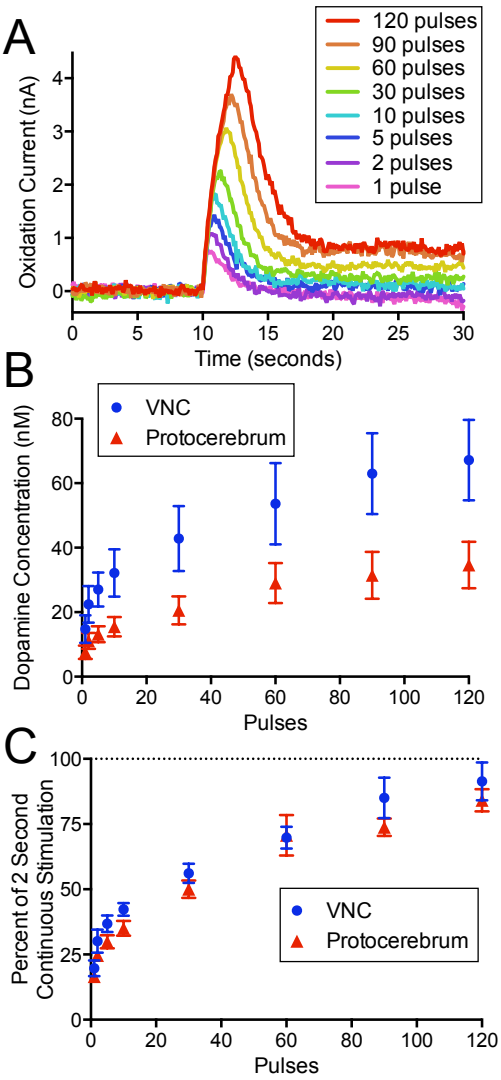

Figure 2.5 - Extracellular dopamine increases similarly in the VNC and protocerebrum with red light exposure. (A) The peak oxidation current of dopamine over time as dopamine release is stimulated by increasing numbers of consecutive 4 ms red light pulses at 60 Hz in the VNC. (B) The amount of extracellular dopamine increases with number of pulses in both the VNC (blue circles, n=5) and the protocerebrum (red triangles, n=7). (C) Data (mean +/- SEM) are normalized to a 2 s continuous light stimulation to account for variation between animals.

The effect of varying red light pulse frequency was tested in both regions, using frequencies of 10-120 Hz for 2 seconds total stimulus duration (Figure 2.6A, each pulse is 4 ms). For example there were 20 pulses at 10 Hz and 200 pulses at 100 Hz. The peak oxidation current for dopamine was normalized to a

two second continuous stimulation for each animal. Increasing the frequency of the light pulses (Figure 2.6B) increased the extracellular dopamine concentration in the VNC (one-way ANOVA, $p<0.0001$, $n=7$-9) and in the protocerebrum (one-way ANOVA, $p=0.0007$, $n=5$-7). The pulsed stimulation is no longer significantly different from the continuous stimulation (100%) above 80 Hz in the VNC and above 60 Hz in the protocerebrum ($p>0.05$, Bonferroni post-hoc t-tests). A two-way ANOVA indicates that there is a main effect of both frequency ($p<0.0001$) and brain region ($p<0.0001$), and no interaction. The normalized extracellular dopamine is significantly higher in the VNC than in the protocerebrum at 10 and 20 Hz ($p<0.01$, Bonferroni post-hoc tests).

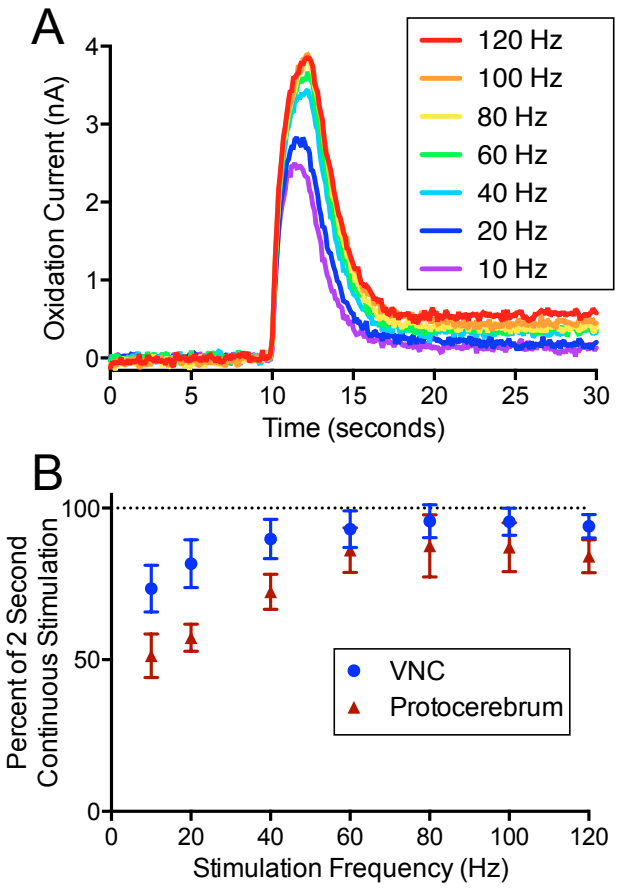

Figure 2.6 - Extracellular dopamine increases with increasing light pulse frequency and then plateaus in both the VNC and protocerebrum. (A) The

peak oxidation current of dopamine over time. Release is stimulated by different frequencies of 4 ms red light pulses for two seconds from the VNC. (B) The amount of extracellular dopamine detected in both the VNC (blue circles, n=7-9) and the protocerebrum (red triangles, n=5-7) increases with the frequency of red light pulses. Data (mean +/- SEM) are normalized to a 2 second continuous light stimulation to account for variation between animals.

Using the 60 Hz, 120 pulse pulsed stimulation data, we modeled the release and uptake of dopamine in the VNC (Figure 2.7A, average R^2=0.94) and protocerebrum (Figure 2.7B, average R^2=0.91). The model (in black) is a nonlinear regression with a simplex minimization algorithm, which regards the extracellular concentration of dopamine as a balance between the pulsed release of dopamine and its continuous uptake.(Garris and Wightman, 1995) The average dopamine released per pulse is assumed to be the same for all pulses. $[DA]_p$, V_{max}, and K_m are summarized in Figure 2.8. The dopamine released per pulse was significantly lower in the protocerebrum (n=8) than in the VNC (n=19) (unpaired t-test, p=0.0062), while the V_{max} was significantly higher in the protocerebrum than in the VNC (p=0.0447, unpaired t-test). The K_m was not significantly different between the two regions (p>0.05, unpaired t-test).

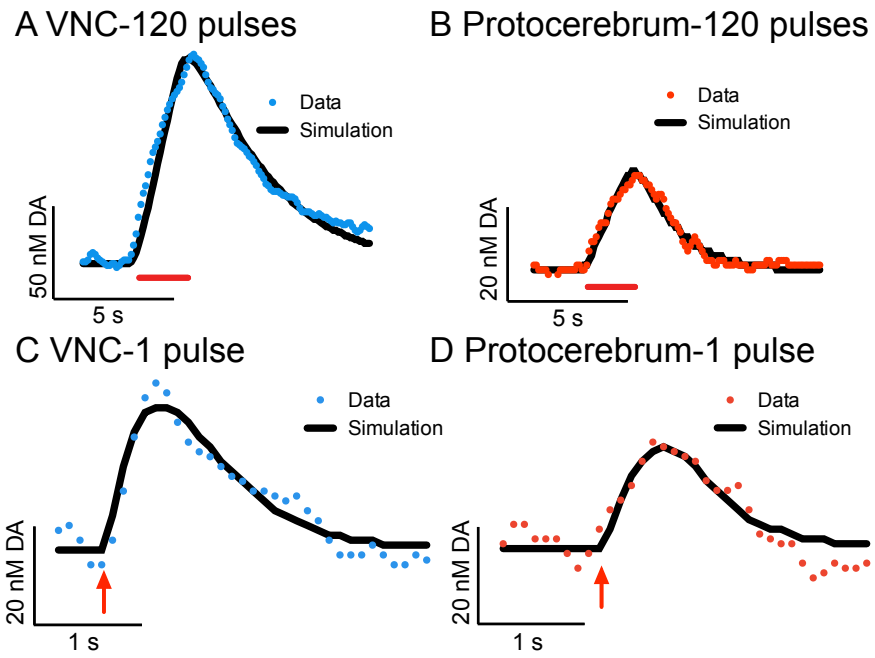

Figure 2.7 - Michaelis-Menten modeling of dopamine release in the VNC and protocerebrum. Raw data (color dots) are plotted with the corresponding Michaelis-Menten model of the data (black line): (A) An example trace from the VNC (blue), which was stimulated with 4 ms red light pulses at 60 Hz for 2 seconds (red bar). The $[DA]_p$ is 1.0 nM, V_{max} is 0.03 μM/s, and K_m is 0.07 μM. R^2 for fit is 0.98. (B) An example trace from the protocerebrum (red), which was stimulated with 4 ms red light pulses at 60 Hz for 2 seconds (red bar). The $[DA]_p$ is 0.3 nM, V_{max} is 0.09 μM/s, and K_m is 0.14 μM. R^2 for fit is 0.97. (C) An example trace from the VNC (blue), which was stimulated with a single 4 ms red light pulse (red arrow). The $[DA]_p$ is 25 nM, V_{max} is 0.04 μM/s, and K_m is 0.09 μM. R^2 for fit is 0.91. (D) An example trace from the protocerebrum (red), which was stimulated with a single 4 ms red light pulse (red arrow). The $[DA]_p$ is 18 nM, V_{max} is 0.08 μM/s, and K_m is 0.10 μM. R^2 is 0.89.

	$[DA]_p$ (nM)	V_{max} (μM/s)	K_m (μM)
Ventral nerve cord (1 pulse, n=4)	28 ± 12	0.04 ± 0.01	0.06 ± 0.02
Protocerebrum (1 pulse, n=5)	17 ± 3	0.11 ± 0.02	0.06 ± 0.01
Ventral Nerve Cord (120 pulses, 60 Hz, n=19)	0.93 ± 0.01	0.05 ± 0.01	0.10 ± 0.01
Protocerebrum (120 pulses, 60 Hz, n=9)	0.48 ± 0.01	0.08 ± 0.02	0.11 ± 0.02

Figure 2.8 - Kinetic values determined from Michaelis-Menten modeling. The dopamine released per pulse of red light ($[DA]_p$), V_{max}, and K_m of the VNC and protocerebrum with 1 (4 ms) pulse or 2 s stimulation (120 pulses, 4 ms, 60 Hz).

Because the pulse number data from Figure 2.5 indicated the first pulses release more dopamine than subsequent pulses, one pulse stimulations were

also modeled to gain a better understanding of the initial $[DA]_p$. The one pulse data are noisier, but the fits were still acceptable in the VNC (Figure 2.7C, average R^2=0.88) and protocerebrum (Figure 2.7D, average R^2=0.84). The resulting data, summarized in Figure 2.8, show that $[DA]_p$ values were significantly larger with one pulse stimulations than the average $[DA]_p$ with 120 pulses in both the VNC (p=0.0195, unpaired t-test) and protocerebrum (p=0.0322, unpaired t-test). For both regions, the initial $[DA]_p$ was about 30 times the average for the 2 second pulse train, indicating that $[DA]_p$ drops off dramatically with subsequent pulses. Figure 2.9 shows that for the data in both regions $[DA]_p$ drops off exponentially with pulse number, plateauing at 0.76 nM in the VNC and 0.41 nM in the protocerebrum. As expected, the number of pulses did not affect uptake values and K_m and V_{max} did not significantly differ in 1 pulse versus the longer stimulation data (p>0.05, unpaired t-tests).

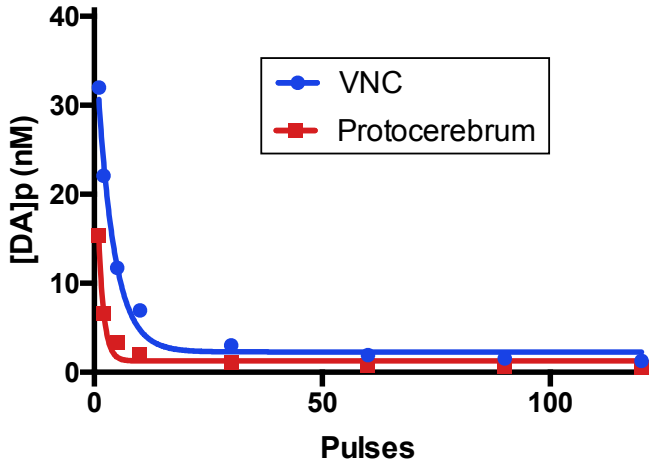

Figure 2.9 - Dopamine per pulse decays exponentially with increasing number of stimulation pulses. Data from the pulse number experiment (Figure 2.5) were modeled and the average dopamine per pulse was fit with a single phase exponential decay in Prism. The VNC data (blue) fit to the equation y=(1.99)*exp(-0.04*x)+0.76 with an R^2 value or 0.99. The protocerebrum data (red) fit to the equation y=(6.49)*exp(-0.18*x)+0.41 with an R^2 value of 0.97. The exponential decays for each data set are significantly different (extra sum-of-

squares F test, $p<0.0001$). $[DA]_p$ falls off faster in the protocerebrum than the VNC.

Finally, the effect of the dDAT blocker nisoxetine was measured in the VNC and protocerebrum. Nisoxetine was used at a concentration previously shown to impair the flux of dopamine through dDAT.(Pörzgen et al., 2001) In both regions, the clearance of stimulated extracellular dopamine was slowed 15 minutes after 20 μM nisoxetine application (Figure 2.10A, B). Two second long, 10 and 60 Hz stimulations were applied and the predrug and nisoxetine data were modeled as before. There was a significant main effect of drug on the apparent K_m (two-way ANOVA; $p=0.0310$, n=5-8), but not on V_{max} (two-way ANOVA; $p>0.05$, n=5-8) (Figure 2.10C). An increase in K_m and no change in V_{max} is consistent with nisoxetine acting as a competitive antagonist at dDAT.

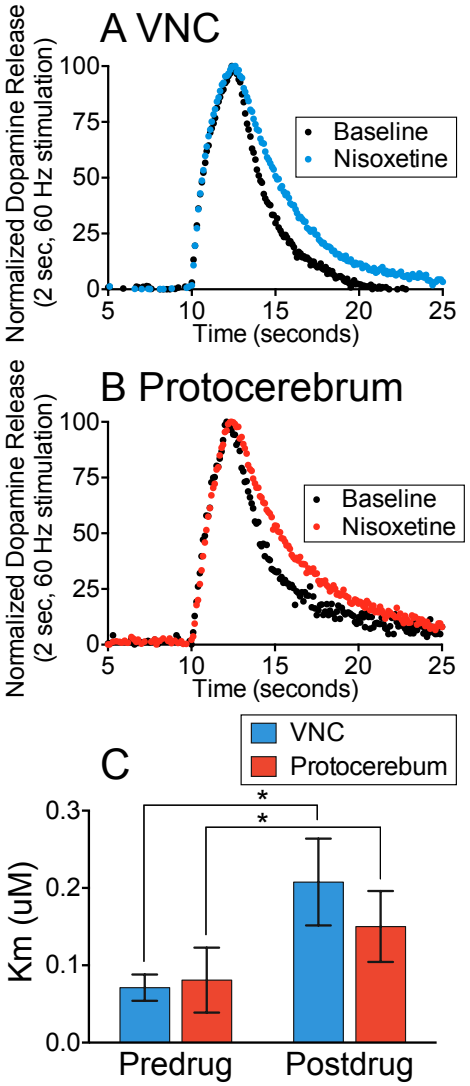

Figure 2.10 - Nisoxetine acts as a competitive inhibitor, decreasing the affinity of dDAT for dopamine in both the VNC and protocerebrum. (A,B) A pulsed stimulation (2 sec, 60 Hz, 4 ms pulses; black) was taken in each animal and then repeated after 20 µM nisoxetine was applied for 20 minutes (color) in the (A) VNC and (B) Protocerebrum. The uptake rate decreased when the pre- and post-drug data are normalized for height and plotted together. (C) The kinetics were modeled for pre- and post-nisoxetine traces for the VNC (n=8) and Protocerebrum (n=6). There was a significant main effect of drug on the K_m (two-way ANOVA; p=0.0310, n=5-8), but not on V_{max} and $[DA]_p$ (two-way ANOVA; p>0.05, n=5-8, not shown). Data are mean +/- SEM.

Discussion

We measured dopamine release stimulated by CsChrimson activation of dopamine neurons in two distinct regions of the larval *Drosophila* central nervous

system: the protocerebrum and VNC. Released dopamine could be measured after a single pulse of light using CsChrimson stimulation. The initial and average $[DA]_p$ is smaller in the protocerebrum than the VNC. The average K_m for uptake was the same in both regions, however the V_{max} was higher in the protocerebrum than in the VNC. Thus, although there is a lower amount of dopamine released in the protocerebrum after similar stimulation, there is a higher dopamine transporter density for clearance. The dDAT blocker nisoxetine acted as a competitive inhibitor, significantly increasing the K_m in both regions. Dopamine release and regulation by dDAT vary in different *Drosophila* neuropil, which leads to different amounts of dopamine available for signaling.

Dopamine Release in the VNC and Protocerebrum

Upon red light stimulation, CsChrimson expressed in the cell membranes of targeted cells will open, allowing an inward flow of cations that depolarizes the cell. Previous electrophysiological studies of CsChrimson have shown that repeated 5 ms pulsed stimulations at frequencies greater than 10 Hz do not reliably produce an action potential every time.(Klapoetke et al., 2014) However, with ChR2 it has been noted that increases in neurotransmitter release occur at higher stimulation frequencies than would be expected from the channel photocycle kinetics.(Bamann et al., 2008; Xiao et al., 2014) CsChrimson mediated release was frequency dependent up to 60 Hz in both regions, which is consistent with previous work in flies and mammals.(Wightman and Zimmerman, 1990; Xiao et al., 2014) CsChrimson kinetics were not limiting to the present study, likely because release comes from a population of neurons, which release

more dopamine with higher frequencies even if not every individual neuron produces an action potential with every stimulation pulse.

CsChrimson facilitated the measurement of stimulations with as little as a single pulse, in comparison to previous studies with ChR2, where at least 10 stimulation pulses were needed.(Xiao et al., 2014) In mammals, dopaminergic cells are known to fire spontaneously in average bursts of 3-4 spikes at approximately 14 Hz, so the ability to study short pulse trains is advantageous for mimicking neuronal burst firing.(Grace and Bunney, 1984) Shorter stimulations also avoid the effects of uptake.(Garris et al., 1994) The amount of dopamine released by small stimulations is much higher than expected if every pulse were to release the same amount of dopamine. For example, 1 pulse produced 20% of the signal elicited by 120 pulses in the VNC. The $[DA]_p$ for the initial stimulation is 30 times the average for a longer pulse train. Thus, the initial pulses in *Drosophila* produce more $[DA]_p$ than later stimulations in the train. This could be due to depletion of the dopamine pools with longer stimulation times or autoreceptor regulation.(Vickrey and Venton, 2011) Earlier research in mammals found that 4 pulses elicited 4 times the concentration of a single pulse in the presence of a dopamine uptake inhibitor, so $[DA]_p$ was assumed to be the same for each pulse.(Garris et al., 1994) However, recent work in mammals has also begun to recognize the heterogeneity in the amount of dopamine released during a long pulsed stimulation.(Taylor et al., 2015) Future models for longer pulse trains could model the changes in $[DA]_p$ and account for the exponential decay in

release. The uptake kinetics for single-pulse and longer trains were not different, so longer pulse trains can be used to examine uptake.

Dopamine released per pulse was significantly lower in the protocerebrum than in the VNC. This difference could be due to a lower density of dopaminergic synapses in the medial protocerebrum than in the compact, highly innervated neuropil of the VNC.(Selcho et al., 2009) In the medial protocerebrum there are projections from approximately 20 dopaminergic cells in three clusters (DM, DL1, and DL2) per lobe.(Pörzgen et al., 2001) In the VNC, there are approximately 22 neurons that send projections to the densely innervated, sheathed neuropil. Dopaminergic neurons acting in a neuromodulatory capacity, such as those in the protocerebrum, would have diffuse projections rather than forming direct synapses.(Selcho et al., 2009) The lower dopamine per pulse measured in the protocerebrum could therefore be due to fewer dopaminergic synapses or less releasable dopamine per synapse.

Uptake Kinetics in the VNC and Protocerebrum

The uptake kinetics of dopamine were obtained from the modeled pulsed stimulation data in the VNC and protocerebrum. Uptake of dopamine through dDAT is assumed to follow Michaelis-Menten kinetics. V_{max} is a function of the density of the transporters and K_m is a measure of the affinity of the transporter for dopamine. As expected, K_m and V_{max} were unaffected by the number of stimulation pulses. K_m was not significantly different in the VNC and protocerebrum, which indicates that dDAT has a consistent affinity for dopamine. V_{max} was significantly higher in the protocerebrum than in the VNC. More tightly

regulated neuromodulatory dopaminergic projections in the protocerebrum may account for the higher V_{max} due to more dense expression of dDAT for uptake.(Selcho et al., 2009) There may be N-terminal serine phosphorylation of DAT as there is in the rat that changes the transport speed or surface expression of DAT in different regions of the *Drosophila* brain.(Foster et al., 2002) Different splice variants of dopamine receptors may also be interacting with and stabilizing DAT differently in the presynaptic membrane of subsets of dopaminergic cells.(Sullivan et al., 2013) Good staining methods for dDAT have not been optimized, but future work can look into the expression levels of dDAT in different regions of the *Drosophila* brain.

The consequence of the varying uptake and release per pulse is that different amounts of dopamine are available for signaling in the protoecerbrum and the VNC. Lower extracellular concentrations of dopamine are present in the medial protocerebrum, reflected in its smaller release and faster uptake. The medial protocerebrum is active in sensory learning and memory, which may not require as much dopamine for activation due to receptor sensitivity in this region. Sensory learning and memory may also be less important in this wandering stage of larvae. On the other hand dopamine neurons in the VNC are primarily involved in motor regulation. Locomotion may require more dopamine signaling and may be more active in this stage of larvae.

Here, the average K_m in the VNC is 0.10 ± 0.01 μM, which is the same order of magnitude as previous work using Channelrhodopsin-2 to stimulate release (0.45 ± 0.13 μM). However, these values are an order of magnitude

lower than the previous work using dDAT transfected into MDCK cells (4.8 ± 0.4 μM) and exogenously applied dopamine in the VNC (1.3 ± 0.6 μM).(Pörzgen et al., 2001; Vickrey et al., 2013) The modeling of pulsed stimulations is more accurate, because it relies on physiological amounts of endogenous dopamine. The *Drosophila* VNC values for K_m are similar to literature values for rat DAT in the caudate putamen and nucleus accumbens (0.2 μM).(Jones et al., 1995) The V_{max} measured with CsChrimson (0.05 ± 0.01 μM/s) is also similar to that measured previously with ChR2 (0.12 ± 0.03 μM/s).

Effect of Transport Blockade in the VNC and Protocerebrum

Nisoxetine slowed clearance of stimulated extracellular dopamine in both the VNC and protocerebrum. The K_m significantly increased with nisoxetine treatment, while the V_{max} did not change. An increase in only K_m indicates that nisoxetine is acting as a competitive inhibitor at dDAT, similar to previous results from expressing dDAT in *Xenopus* oocytes.(Pörzgen et al., 2001) Nisoxetine is typically used as a competitive inhibitor of the human norepinephrine transporter (hNET), and dDAT is thought to be an evolutionary precursor to hNET.(Cheetham et al., 1996; Pörzgen et al., 2001) Norepinephrine has not been found in the *Drosophila*, which instead use octopamine for neurotransmission. Octopamine has a very different cyclic voltammagram from dopamine.(Denno et al., 2014) The dDAT has a higher maximal uptake velocity for dopamine than other biogenic amines, and nisoxetine is three orders of magnitude more specific for dDAT than for the serotonin transporter, the only other known transporter for amine clearance in *Drosophila*.(Pörzgen et al., 2001)

Therefore, the uptake inhibitor nisoxetine slowed dopamine clearance by acting as a competitive inhibitor of dDAT, affecting extracellular dopamine concentration in the expected manner in both regions of the larval CNS.

Advantages of CsChrimson Stimulation

This work demonstrates that red light stimulated CsChrimson can be used to study the release and uptake of dopamine in *Drosophila*. Traditionally, Channelrhodopsin-2 has been used for optical stimulation of neurons, but CsChrimson has several advantages over ChR2. CsChrimson is stimulated by red light instead of blue light. Blue light does not penetrate deeply into tissue due to scattering and absorption by endogenous chromophores.(Lin et al., 2013) Additionally, shining blue light on the carbon-fiber microelectrode surface causes a change in surface properties, resulting in an error that been documented in both mammals and flies.(Vickrey et al., 2009; Bass et al., 2013) Red light is lower in energy and does not affect the electrode surface. CsChrimson should facilitate future work studying tyramine and octopamine, which have oxidation potentials at the switching potential.(Cooper and Venton, 2009) An additional benefit of these flies is that they are heterozygous crosses between UAS-CsChrimson and th-Gal4 flies. This single cross is much easier and more stable than homozygous lines. The dopamine released per pulse, V_{max}, and K_m are all the same order of magnitude when using CsChrimson or Channelrhodopsin-2 to stimulate dopamine release from the VNC.(Xiao et al., 2014) Differences in the release and uptake can be accounted for by the unique properties of the channels: light penetration, membrane expression of the channel, and photocurrent

size.(Klapoetke et al., 2014) Stimulations with CsChrimson can be effectively and conveniently used to characterize the different kinetics of dopamine release and uptake in *Drosophila* neuropil.

Conclusions

We measured CsChrimson stimulated dopamine release in VNC and protocerebrum of the larval *Drosophila* central nervous system. Dopamine was measured after a single pulse of light using CsChrimson stimulation, an improvement over previous studies using Channelrhodopsin-2.(Vickrey et al., 2009; Xiao et al., 2014) There is a lower amount of dopamine released in the protocerebrum than in the VNC, and there is a higher maximum rate of clearance in the protocerebrum. The dDAT blocker nisoxetine acts as a competitive inhibitor, decreasing transporter affinity in both regions. Dopamine release and regulation differ in different *Drosophila* neuropil, which leads to different amounts of extracellular dopamine available for neurotransmission and neuromodulation.

Acknowledgements

We thank Paul Garris and Mark Wightman for providing software and Vivek Jayaraman, Sung-Soo Kim, and Jay Hirsh for providing fly strains. This work was funded by the NIH (MH085159). The authors declare no competing financial interests. EP collected the data and EP and BJV both designed experiments, interpreted data, and wrote the article.

Chapter 2 References

Bamann C, Kirsch T, Nagel G, Bamberg E (2008) Spectral characteristics of the photocycle of channelrhodopsin-2 and its implication for channel function. J Mol Biol 375:686–694.

Bass CE, Grinevich VP, Kulikova AD, Bonin KD, Budygin EA (2013) Terminal effects of optogenetic stimulation on dopamine dynamics in rat striatum. J Neurosci Methods 214:149–155.

Berglund EC, Makos MA, Keighron JD, Phan N, Heien ML, Ewing AG (2013) Oral administration of methylphenidate blocks the effect of cocaine on uptake at the Drosophila dopamine transporter. ACS Chem Neurosci 4:566–574.

Borue X, Condron B, Venton BJ (2010) Both synthesis and reuptake are critical for replenishing the releasable serotonin pool in Drosophila. J Neurochem 113:188–199.

Borue X, Cooper S, Hirsh J, Condron B, Venton BJ (2009) Quantitative evaluation of serotonin release and clearance in Drosophila. J Neurosci Methods 179:300–308.

Cheetham SC, Viggers JA, Butler SA, Prow MR, Heal DJ (1996) [3H]nisoxetine--a radioligand for noradrenaline reuptake sites: correlation with inhibition of [3H]noradrenaline uptake and effect of DSP-4 lesioning and antidepressant treatments. Neuropharmacology 35:63–70.

Cooper SE, Venton BJ (2009) Fast-scan cyclic voltammetry for the detection of tyramine and octopamine. Anal Bioanal Chem 394:329–336.

Crickmore MA, Vosshall LB (2013) Opposing dopaminergic and GABAergic neurons control the duration and persistence of copulation in Drosophila. Cell 155:881–893.

Denno ME, Privman E, Venton BJ (2014) Analysis of Neurotransmitter Tissue Content of Drosophila melanogaster in Different Life Stages. ACS Chem Neurosci.

Duffy JB (2002) GAL4 system in Drosophila: a fly geneticist's Swiss army knife. Genesis 34:1–15.

Foster JD, Pananusorn B, Vaughan R a. (2002) Dopamine transporters are phosphorylated on N-terminal serines in rat striatum. J Biol Chem 277:25178–25186.

Garris PA, Ciolkowski EL, Pastore P, Wightman RM (1994) Efflux of dopamine from the synaptic cleft in the nucleus accumbens of the rat brain. J Neurosci 14:6084–6093.

Garris PA, Wightman RM (1995) Regional differences in dopamine release, uptake, and diffusion measured by fast-scan cyclic voltammetry. In:

Neuromethods: Voltammetric Methods in Brain Systems (A B, G B, RN A, eds), pp 179–220. Humana Press Inc.

Grace AA, Bunney BS (1984) The control of firing pattern in nigral dopamine neurons: burst firing. J Neurosci 4:2877–2890.

Jacobs CB, Vickrey TL, Venton BJ (2011) Functional groups modulate the sensitivity and electron transfer kinetics of neurochemicals at carbon nanotube modified microelectrodes. Analyst 136:3557–3565.

Jones SR, Garris PA, Kilts CD, Wightman RM (1995) Comparison of dopamine uptake in the basolateral amygdaloid nucleus, caudate-putamen, and nucleus accumbens of the rat. J Neurochem 64:2581–2589.

Klapoetke NC et al. (2014) Independent optical excitation of distinct neural populations. Nat Methods 11:338–346.

Lin JY, Knutsen PM, Muller A, Kleinfeld D, Tsien RY (2013) ReaChR: a red-shifted variant of channelrhodopsin enables deep transcranial optogenetic excitation. Nat Neurosci 16:1499–1508.

Makos MA, Han K-A, Heien ML, Ewing AG (2010) Using in Vivo Electrochemistry to Study the Physiological Effects of Cocaine and Other Stimulants on the Drosophila melanogaster Dopamine Transporter. ACS Chem Neurosci 1:74–83.

Makos MA, Kim Y-C, Han K-A, Heien ML, Ewing AG (2009) In vivo electrochemical measurements of exogenously applied dopamine in Drosophila melanogaster. Anal Chem 81:1848–1854.

Marella S, Mann K, Scott K (2012) Dopaminergic Modulation of Sucrose Acceptance Behavior in Drosophila. Neuron 73:941–950.

Martin CA, Krantz DE (2014) Drosophila melanogaster as a genetic model system to study neurotransmitter transporters. Neurochem Int 73:71–88.

Nagel G, Szellas T, Huhn W, Kateriya S, Adeishvili N, Berthold P, Ollig D, Hegemann P, Bamberg E (2003) Channelrhodopsin-2, a directly light-gated cation-selective membrane channel. Proc Natl Acad Sci 100:13940–13945.

Pandey UB, Nichols CD (2011) Human disease models in Drosophila melanogaster and the role of the fly in therapeutic drug discovery. Pharmacol Rev 63:411–436.

Pörzgen P, Park SK, Hirsh J, Sonders MS, Amara SG (2001) The antidepressant-sensitive dopamine transporter in Drosophila melanogaster: a primordial carrier for catecholamines. Mol Pharmacol 59:83–95.

Sabeti J, Adams CE, Burmeister J, Gerhardt GA, Zahniser NR (2002) Kinetic analysis of striatal clearance of exogenous dopamine recorded by chronoamperometry in freely-moving rats. J Neurosci Methods 121:41–52.

Selcho M, Pauls D, Han K-A, Stocker RF, Thum AS (2009) The role of dopamine

in Drosophila larval classical olfactory conditioning. PLoS One 4:e5897.

Sullivan D, Pinsonneault JK, Papp a C, Zhu H, Lemeshow S, Mash DC, Sadee W (2013) Dopamine transporter DAT and receptor DRD2 variants affect risk of lethal cocaine abuse: a gene-gene-environment interaction. Transl Psychiatry 3:e222.

Takmakov P, Zachek MK, Keithley RB, Bucher ES, McCarty GS, Wightman RM (2010) Characterization of local pH changes in brain using fast-scan cyclic voltammetry with carbon microelectrodes. Anal Chem 82:9892–9900.

Taylor IM, Nesbitt KM, Walters SH, Varner EL, Shu Z, Bartlow KM, Jaquins-Gerstl AS, Michael AC (2015) Kinetic diversity of dopamine transmission in the dorsal striatum. J Neurochem 133:522–531.

Vickrey TL, Condron B, Venton BJ (2009) Detection of endogenous dopamine changes in Drosophila melanogaster using fast-scan cyclic voltammetry. Anal Chem 81:9306–9313.

Vickrey TL, Venton BJ (2011) Drosophila Dopamine2-like receptors function as autoreceptors. ACS Chem Neurosci 2:723–729.

Vickrey TL, Xiao N, Venton BJ (2013) Kinetics of the dopamine transporter in Drosophila larva. ACS Chem Neurosci 4:832–837.

Wightman RM, Zimmerman JB (1990) Control of dopamine extracellular concentration in rat striatum by impulse flow and uptake. Brain Res Rev 15:135–144.

Wu Q, Reith MEA, Wightman RM, Kawagoe KT, Garris PA (2001) Determination of release and uptake parameters from electrically evoked dopamine dynamics measured by real-time voltammetry. J Neurosci Methods 112:119–133.

Xiao N, Privman E, Venton BJ (2014) Optogenetic control of serotonin and dopamine release in Drosophila larvae. ACS Chem Neurosci 5:666–673.

Yellman C, Tao H, He B, Hirsh J (1997) Conserved and sexually dimorphic behavioral responses to biogenic amines in decapitated Drosophila. Proc Natl Acad Sci 94:4131–4136.

Chapter 3: RING Finger Protein 11 (RNF11) Modulates Dopamine Release and Uptake in *Drosophila*

Abstract

Recent work has indicated a role for RING finger protein 11 (RNF11) in Parkinson disease (PD) pathology, which involves the loss of dopaminergic neurons. However, the role of RNF11 in regulating dopamine neurotransmission has not been studied. In this work we tested the effect of RNAi knockdown or overexpression of RNF11 to change stimulated dopamine release in the larval *Drosophila* central nervous system. Dopamine release was stimulated using pulsed red light activation of CsChrimson and monitored in real time using fast-scan cyclic voltammetry at an electrode implanted in the isolated ventral nerve cord. RNF11 knockdown caused dopamine release to double, but there was no equivalent decrease in dopamine from RNF11 overexpression. RNF11 knockdown does not significantly increase stimulated serotonergic or octopaminergic release, indicating that the effect is dopamine specific. RNF11 RNAi flies had a higher V_{max} and RNF11 overexpressing flies had a lower V_{max} than control flies, indicating that RNF11 affects the rate of dopamine clearance. RNF11 knockdown increases the recycled releasable pool of dopamine. Nisoxetine, a DAT inhibitor, and flupenthixol, a D2 antagonist, do not affect RNF11 RNAi or overexpressing flies differently than control. Thus, we have identified that RNF11 causes early changes in dopamine neurotransmission and this is the first work to demonstrate that RNF11 affects both dopamine release and uptake. There is a decrease in RNF11 in human dopaminergic neurons

during PD and that decrease may be protective by increasing dopamine neurotransmission in the remaining cells.

Introduction

Recent work has indicated a role for Ring finger protein 11 (RNF11) in Parkinson disease (PD) pathology. RNF11 is an E3 ubiquitin ligase that functions as part of the A20 ubiquitin-editing complex. The A20 complex inhibits NF-κB activation in human neurons (Pranski et al., 2012) and persistent NF-κB activation is a hallmark of neurodegenerative disease.(Glass et al., 2010) RNF11 variants in the PARK10 locus may increase susceptibility for PD.(Lesage and Brice, 2009) RNF11 colocalizes with α-synuclein and Lewy bodies in PD tissue.(Anderson et al., 2007) RNF11 gene transcription is decreased in brain tissue affected by neurodegenerative diseases, as found in a multi-cohort meta-analysis.(Li et al., 2014) In rats with the 6-OHDA model of PD, viral RNF11 knockdown protected against dopaminergic neuronal cell death and RNF11 overexpression enhanced toxicity.(Pranski et al., 2013a) The enhanced toxicity from RNF11 overexpression corresponded to downregulation of NF-κB transcribed antioxidants glutathione synthetase and superoxide dismutase 1, anti-apoptotic factor BCL2, neurotrophic factor brain derived neurotrophic factor (BDNF), and tumor necrosis factor alpha (TNF-α). Therefore the decreased expression of RNF11 found in surviving neurons is thought to be a compensatory response to PD pathology.(Pranski et al., 2013a) This decrease is not correlated with age, making RNF11 an unchanging candidate as a biomarker of neurodegeneration.(Li et al., 2014) While RNF11 downregulation has been

discovered in the context of neurodegeneration, no studies have addressed the effect of RNF11 on neurotransmission.

Drosophila melanogaster is a powerful model organism for the study of neurodegeneration (Hirth, 2010) and can be used to study the effects of manipulating RNF11 expression levels on neurotransmission. A true homologue of RNF11, *CG32850*, has been identified in the *Drosophila melanogaster* genome. This *Drosophila* RNF11 has 87% positive sequence identity with the RING domain of the human protein.(Kitching et al., 2003) An A20 ubiquitin-editing complex has not been described in fruit flies. However, homologs for many NF-κB pathway proteins have been described (Khush and Lemaitre, 2000), so it is likely that *Drosophila* RNF11 works in concert with these proteins to edit ubiquitin and inhibit NF-κB function.

The goal of this study was to test the effect of RNF11 knockdown or overexpression on the release and clearance of dopamine in *Drosophila* larvae. The GAL4/UAS system was used to either overexpress RNF11 or knock it down using RNAi.(Brand and Perrimon, 1993) Fast scan cyclic voltammetry (FSCV) was used to measure dopamine release and uptake in the *Drosophila* ventral nerve cord (VNC).(Vickrey et al., 2009) Release was controlled optogenetically using the red light sensitive channelrhodopsin CsChrimson.(Privman and Venton, 2015) RNF11 RNAi flies release double the control level of dopamine, while RNF11 overexpressing flies did not release dopamine differently than control. This effect was specific to dopamine, as knocking down RNF11 in serotonergic or octopaminergic neurons did not alter release. Pulsed stimulations were

modeled to obtain the Michaelis-Menten kinetic parameters (Xiao et al., 2014), revealing that V_{max}, the maximum rate of dopamine uptake, increased in RNF11 RNAi flies and decreased in RNF11 overexpressing flies. These experiments are the first to demonstrate that RNF11 affects the ability of cells to release and uptake dopamine. Thus, the decrease in RNF11 during PD may also be leading to increased dopamine neurotransmission, which could be compensating for dopaminergic cell loss.

Materials and Methods

Chemicals

Chemicals and drugs were purchased from Sigma-Aldrich (St. Louis, MO) and solutions were made with Milli-Q water (Millipore, Billerica, MA). Dissections, recordings, and calibrations were performed in a simple physiological buffer (131.3 mM NaCl, 3.0 mM KCl, 10 mM NaH_2PO_4 monohydrate, 1.2 mM $MgCl_2$ hexahydrate, 2.0 mM Na_2SO_4 anhydrous, 1.2 $CaCl_2$ dihydrate, 11.1 mM glucose, 5.3 mM trehalose, pH = 7.4). A concentrated stock solution of nisoxetine was made in buffer and added to the sample for a final concentration of 20 μM. A 10 mM stock solution of flupenthixol was made in DMSO, diluted in buffer, and added to the sample for a final concentration of 5 μM flupenthixol. For nisoxetine and flupenthixol testing, a pre-drug baseline recording was taken and then the drug was bath applied for 15 minutes before post-drug recordings were taken. Flupenthixol is known to decrease the sensitivity of the electrode for dopamine, so the post-drug data were corrected with a calibration factor to account for the loss in signal.(Vickrey and Venton, 2011)

Electrochemical Measurements

Cylindrical carbon fiber microelectrodes were made using T-650 carbon fibers (a gift of Cytec Engineering Materials, West Patterson, NJ) as previously described.(Jacobs et al., 2011) Electrodes were calibrated *in vitro* using a flow cell to determine the electroactive surface area. The electrodes were each alternatively exposed to buffer and buffer containing 1 μM dopamine, serotonin, or octopamine to determine the response each neurotransmitter. This calibration factor was used to calculate the amount of neurotransmitter measured *in vivo* as peak oxidation current increases linearly with analyte concentration within the physiological range. Fast-scan cyclic voltammetry was performed using a ChemClamp potentiostat with an n=0.01 headstage (Dagan, Minneapolis, MN), PCI 6711 and 6052 computer interface cards (National Instruments, Austin, TX), and a home built break-out box. TarHeel CV software (a gift of Mark Wightman, University of North Carolina) was used to collect and background subtract the data. Every 100 ms the electrode was scanned from -0.4 to 1.3 V at 400 V/s for dopamine detection. For serotonin and octopamine detection, modified waveforms were used to minimize electrode fouling. For the serotonin waveform, the potential was held at 0.2 V, and then scanned up to 1.0 V, down to −0.1 V, and then back to 0.2 V at a rate of 1000 V/s every 100 ms.(Jackson et al., 1995; Borue et al., 2009) For octopamine detection, the potential was held at -0.4 V and scanned to 1.4 V at 100 V/s every 100 ms.(Pyakurel, Privman, and Venton, unpublished) The tissue content of dopamine was measured from 3 pooled larval

Drosophila ventral nerve cords using capillary electrophoresis coupled with FSCV as described previously.(Denno et al., 2014, 2016)

Tissue Preparation

Fly stocks were all prepared on a white genetic background. Virgin females with TH-GAL4,UAS-CD8-GFP were crossed with males with UAS-CsChrimson (control); UAS-CsChrimson,UAS-RNF11-RNAi (RNF11 knock down); or UAS-CsChrimson,UAS-RNF11 (RNF11 overexpression). All parents strains were kept balanced with cyo/sp;tm6b/sb to avoid crossing over and to aid in the visual identification of homozygous parent flies. For the serotonin experiments, the female virgin parents expressed TPH-GAL4 instead and for octopamine experiments they expressed TDC-GAL4. The resulting heterozygous offspring contain a driver targeting gene expression to dopaminergic cells (th-GAL4), serotonergic cells (tph-GAL4), or octopaminergic cells (tdc-GAL4); GFP for visualization of the cells; CsChrimson for optogenetic control of the cells(Klapoetke et al., 2014); and the genetic experimental condition (control, RNF11 RNAi, or RNF11 overexpression). Resulting heterozygous larvae were shielded from light and raised on standard cornmeal food mixed 250:1 with 100 mM all-trans-retinal. The VNC of a third instar wandering larva (either sex) was dissected out in buffer. Isolated VNCs were prepared and recorded from as previously described.(Borue et al., 2009) The electrode was allowed to equilibrate in the tissue for 10 minutes prior to data collection. A baseline recording was taken for 10 seconds prior to stimulation to facilitate background subtraction.

Stimulated Neurotransmitter Release

Red-orange light from a 617 nm fiber-coupled high-power LED with a 200 μm core optical cable (ThorLabs, Newton, NJ) was used to stimulate the CsChrimson ion channel. The power output at the fiber end was 0.75 mW and the fiber was centered positioned 75-100 μm from the ventral nerve cord using a micromanipulator. The light was modulated with Transistor-Transistor Logic (TTL) inputs to a T-cube LED controller (ThorLabs, Newton, NJ), which was connected to the breakout box. TTL input was driven by electrical pulses controlled by the TarHeel CV software, which was used to control the frequency (60 Hz), pulse width (4 ms), and number of pulses (120) in the stimulations.

Statistics and Data Analysis

Data are presented as mean +/- standard error of the mean (SEM) displayed as error bars. GraphPad Prism 6 (GraphPad Software Inc, La Jolla, CA) was used to perform all statistics, including one-way and two-way ANOVA with Bonferonni post-hoc tests. Stimulated changes in the extracellular concentration of dopamine were modeled as a balance between discontinuous release and continuous uptake.(Wu et al., 2001) A nonlinear regression with a simplex minimization algorithm was used to fit the curves.(Garris and Wightman, 1995) The modeling software was stopped when the iteration number continued increasing without a change in the three floated parameters: K_m, V_{max}, and dopamine release per light pulse ($[DA]_p$). The goodness of the fit was described using the square regression coefficient (R^2). The average R^2 for this work was 0.96 with a standard deviation of 0.02.

Results

RNF11 was overexpressed or knocked down with the constituently active Gal4/UAS system in *Drosophila* dopaminergic cells. The RNF11 RNAi used in these studies knock mRNA levels down to 62% when driven in muscle and the overexpression of RNF11 increased mRNA levels by 420%. Dopamine release was stimulated using red light to activate CsChrimson and extracellular dopamine concentrations were monitored in real time using FSCV. The pulsed optogenetic stimulation mimics the phasic neurotransmission that is important for reward and motivation in mammals.(Venton et al., 2003) Figure 3.1A shows that knocking down RNF11 caused a much larger amount of dopamine release than control or RNF11 overexpression flies. Figure 3.1B shows example cyclic voltammograms, which confirm dopamine was detected because of the characteristic oxidation peak at 0.6 V and reduction peak at -0.2 V. Figure 3.1C shows the average peak oxidation currents for the three genotypes. Peak extracellular dopamine concentration varies with genotype (one-way ANOVA, $p=0.0058$) and RNF11 RNAi flies have significantly larger dopamine release than control, about double the concentration of normal release (Bonferroni post hoc tests, $p<0.01$). There was no significant difference between the peak release for control and RNF11 overexpressing flies.

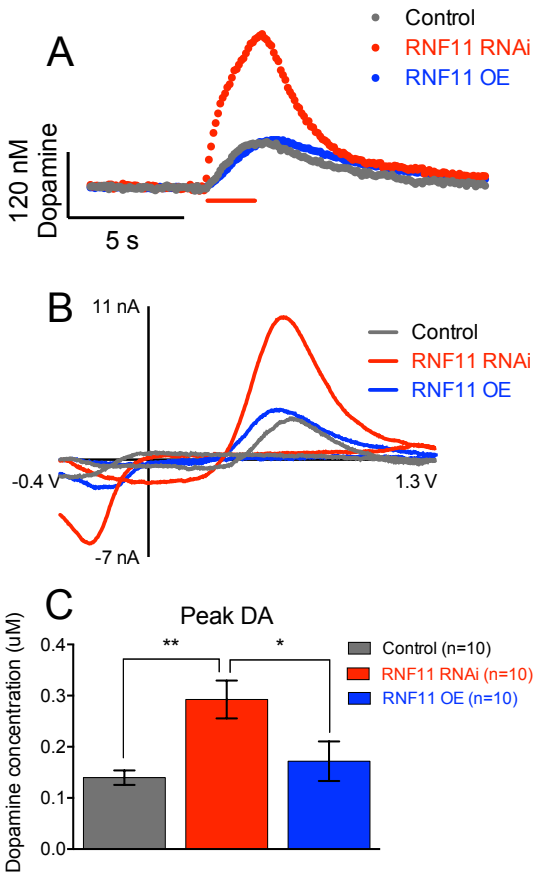

Figure 3.1 - Knocking down RNF11 with RNAi increases dopamine release. (A) Peak oxidation current of stimulated dopamine in isolated larval ventral nerve cords. The 2 s stimulation is marked by the red line (60 Hz, 120 pulses, 4 ms red light each pulse). The three genotypes plotted are control (grey, th-Gal4;UAS-CsChrimson), RNF11 knockdown (red, th-Gal4;UAS-RNF11 RNAi,UAS-CsChrimson), and RNF11 overexpressing (blue, th-Gal4;UAS-RNF11,UAS-CsChrimson). (B) Cyclic voltammograms showing characteristic oxidation peaks for dopamine at 0.6 V and reduction peaks at -0.2 V. (C) Average peak stimulated dopamine concentration changes with genotype (one-way ANOVA, $p=0.0019$). RNF11 RNAi flies have more release than control or RNF11 overexpressing flies (Bonferroni post-test, $p<0.01$, **), while RNF11 overexpression does not affect peak dopamine concentration ($p>0.05$). Data shown are mean ± SEM.

In order to check the specificity of this effect for dopaminergic neurons, RNF11 RNAi was expressed along with CsChrimson in serotonergic (tph-GAL4) or octopaminergic (tdc-GAL4) neurons. Neurotransmitter release was monitored using specialized waveforms for those neurotransmitters during a 2 s pulsed red

light stimulation. Knocking down RNF11 in serotonin neurons did not change stimulated serotonin levels (Figure 3.2A, t-test, p=0.8054); similarly, knocking down octopamine in RNF11 neurons did not change peak octopamine concentrations (Figure 3.2B, t-test, p=0.9345). Thus, RNF11 RNAi selectively increases dopamine release.

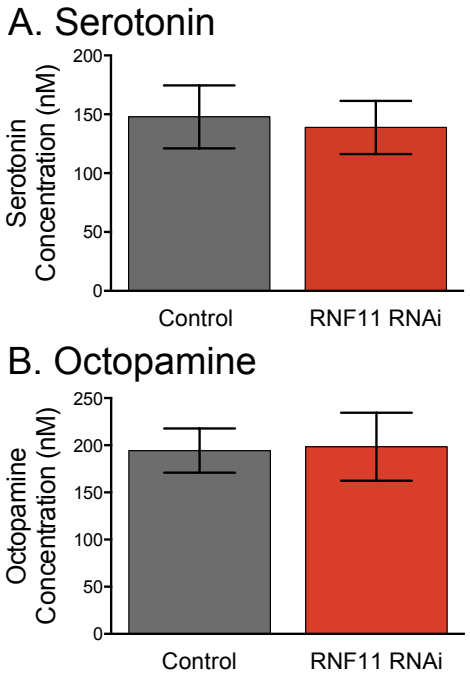

Figure 3.2 - Knocking down RNF11 with RNAi does not change peak serotonin or octopamine levels. RNF11 RNAi expressed in (A) serotonergic or (B) octopaminergic cells did not significantly change peak stimulated neurotransmitter levels (unpaired t-tests, p>0.05, n=4-6). Stimulation was 2 s,60 Hz, 120 pulses. Data are mean ± SEM.

In order to determine the extent to which dopamine release and uptake are affected by RNF11 knock down, the current versus time plots (examples shown in Figure 3.1A) were modeled using Michaelis-Menten kinetics (Figure 3.3).(Garris and Wightman, 1995; Wu et al., 2001) The parameters determined were the amount of dopamine released with each pulse of stimulating light ($[DA]_p$); V_{max}, the maximum rate of clearance by the dopamine transporter (DAT);

and Km, the affinity of DAT for dopamine. Dopamine released per pulse of light is affected by genotype (Figure 3.3A, one-way ANOVA, p=0.0006) and RNF11 knockdown significantly increases dopamine release per pulse compared to control (Bonferroni post hoc test, p<0.001), while RNF11 overexpression does not affect $[DA]_p$. V_{max} is also significantly affected by genotype (Figure 3.3B, one-way ANOVA, p<0.0001). RNF11 knockdown significantly increases V_{max} compared to control (post-hoc t-test, p<0.05) and RNF11 overexpression significantly decreases V_{max} compared to control (post-hoc t-test, p<0.05). K_m is not affected by genotype (Figure 3.3C, one-way ANOVA, p=0.3056).

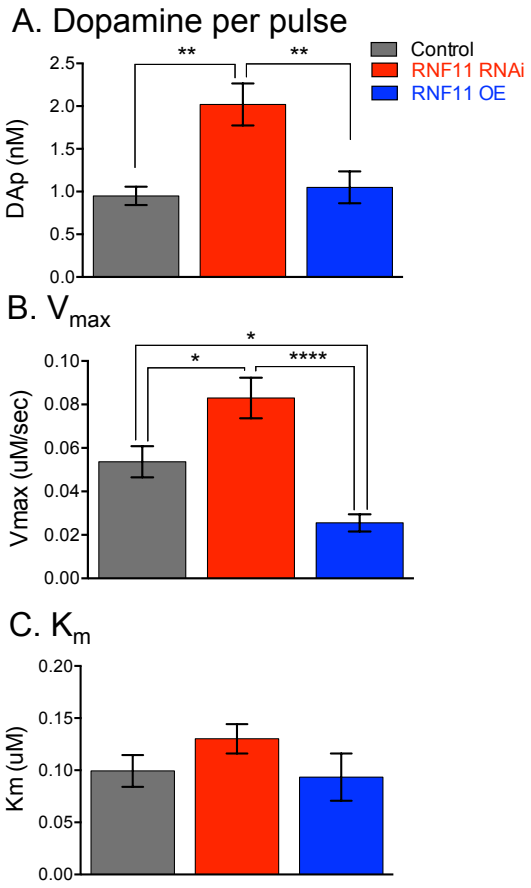

Figure 3.3 - RNF11 knockdown increases dopamine release and clearance. Dopamine release was modeled and release and uptake parameters determined. (A) Dopamine released per light stimulation pulse (120 pulse, 60 Hz, 4 ms pulse width stimulation) is affected by genotype (one-way ANOVA, p=0.0006).

Dopamine release is greater in RNF11 RNAi flies than control or RNF overexpressing flies (**, p<0.01). (B) V_{max} is significantly affected by genotype (one-way ANOVA, p<0.0001). RNF11 knockdown significantly increases V_{max} compared to control (*, p<0.05) and RNF11 overexpression (****, p<0.0001). RNF11 overexpression significantly decreases V_{max} compared to control (*, p<0.05). (C) K_m is not significantly affected by genotype (one-way ANOVA, p>0.5). Data shown are mean ± SEM and n=10.

The amount of dopamine release may be due to increases in the total pool of dopamine. Tissue content measurements were made to assess the dopamine pool using capillary electrophoresis coupled to FSCV (Figure 3.4). The dopamine content per larval central nervous system (CNS) was significantly affected by the genotype of the flies (one-way ANOVA, p=0.0003). Post hoc tests showed that the RNF11 RNAi tissues had significantly more dopamine than the RNF11 overexpressing tissue (p=0.0002). However, neither the RNF11 RNAi (p=0.1152) nor the overexpressing (p=0.0510) flies differed significantly from control. This indicates that tissue content did not increase as much as release.

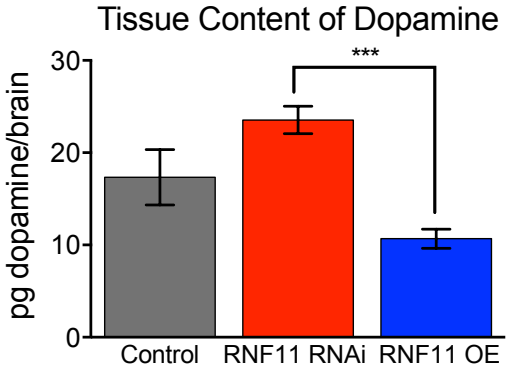

Figure 3.4 - RNF11 knockdown larval CNS have more dopamine tissue content than RNF11 overexpressing flies. Capillary electrophoresis coupled to FSCV was used to measure the tissue content of dopamine. The dopamine content was significantly affected by the genotype of the flies (one-way ANOVA, p=0.0003, n=6-9). Post hoc tests showed that the RNF11 RNAi tissues had significantly more dopamine than the RNF11 overexpressing tissue (p=0.0002). However, RNF11 RNAi did not differ from control (p=0.1152) nor did RNF11 overexpressing (p=0.0510). Data shown are mean ± SEM and n=6-9.

DAT typically clears released dopamine, although occasionally dopamine is also released by the transporter through reverse transport.(Pörzgen et al., 2001) DAT was competitively inhibited by bath application of 20 μM nisoxetine for 15 minutes. Figure 3.5A shows example data of the pre-drug baseline stimulation in an RNF11 RNAi VNC (orange) and the slowed dopamine uptake after nisoxetine (purple), as evidenced by the increased time to half the maximum concentration (t_{50}). Figure 3.5B summarizes the data from control, RNF11 RNAi, and RNF11 overexpressing flies. A two-way ANOVA showed a significant main effect of genotype ($p=0.0002$) and nisoxetine ($p=0.0012$), but no interaction. Post tests show a higher t_{50} for RNF11 overexpressing than both RNF11 RNAi and control. The percent increase in t_{50} from baseline upon application of nisoxetine was calculated for each genotype, and one-way ANOVA revealed no significant difference ($p=0.3558$). This indicates that nisoxetine is affecting dopamine uptake equally among the genotypes, despite the slower uptake in RNF11 overexpressing flies. These results also indicate that the larger dopamine releases seen in RNF11 RNAi flies cannot be accounted for by reverse transport through DAT.

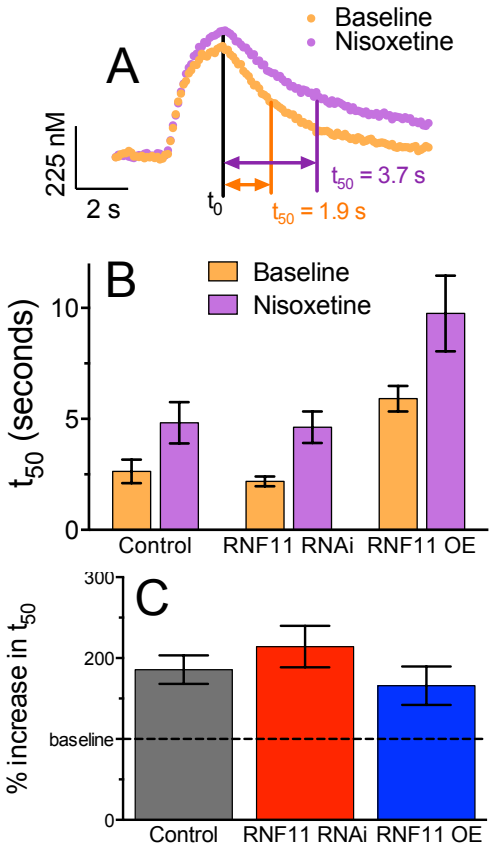

Figure 3.5 - Blocking DAT with nisoxetine causes slowed uptake in all three genotypes. (A) Peak oxidation current for dopamine was monitored over time before (orange) and 15 minutes after (purple) application of 20 µM nisoxetine. This example data shows an RNF11 RNAi VNC. (B) Nisoxetine caused an increase in t_{50}. A two-way ANOVA showed a significant main effect of genotype ($p=0.0002$, $n=4$) and nisoxetine ($p=0.0012$, $n=4$), but no interaction. (C) The fold increase from baseline upon application of nisoxetine was not significantly different among the different genotypes (one way ANOVA, $p=0.3558$). Data shown are mean ± SEM and $n=4$.

Extracellular dopamine levels can be controlled through negative feedback of the D2 dopamine autoreceptor. If RNF11 knockdown decreases D2 receptor levels in the presynaptic cell membrane, the cell would release more dopamine due to a lack of negative inhibition. D2 was blocked by bath application of 5 µM flupenthixol for 15 minutes.(Vickrey and Venton, 2011) Figure 3.6A shows example data of the pre-drug baseline in an RNF11 RNAi VNC (light green) and the post-drug increased dopamine release (dark green). Figure 3.6B summarizes

the data from control, RNF11 RNAi, and RNF11 overexpressing tissue. Stimulated dopamine release about doubled in all genotypes after flupenthixol bath application. A two-way ANOVA showed a significant main effect of genotype (p=0.0105) and flupenthixol (p=0.0007), but no interaction (p=0.2963). Post tests showed higher dopamine levels in RNF11 RNAi than both RNF11 overexpressing and control. The percent increase in dopamine concentration from baseline upon application of flupenthixol was calculated for each genotype, and one-way ANOVA revealed no significant difference (Figure 3.6C,p=0.0659, n=4-7). This indicates that D2 autoreceptors function similarly in all genotypes and RNF11 knockdown is not increasing dopamine by modulating D2 autoreceptor function.

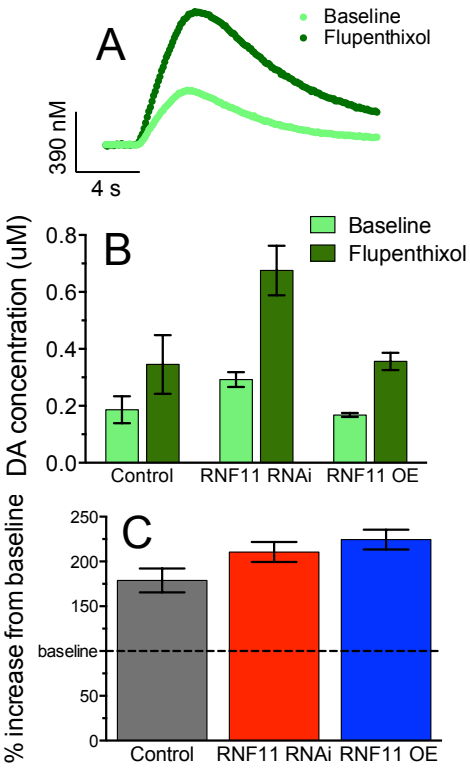

Figure 3.6 - Blocking the D2 autoreceptor with flupenthixol causes increased dopamine release in all three genotypes. Peak oxidation current for dopamine was monitored over time before, 15 minutes, and 30 minutes after the

application of 5 μM flupenthixol. (A) Example plot of the effect of 30 minutes of flupenthixol on dopamine release in an RNF11 RNAi larval CNS. (B) Flupenthixol caused an increase in peak oxidation current of dopamine within 15 minutes in all genotypes. Two way ANOVA revealed a main effect of genotype ($p=0.0006$) and flupenthixol ($p=0.0008$), but no interaction ($p=0.5800$). (C) There was no significant difference among the genotypes in fold increase of dopamine release from baseline upon flupenthixol exposure. (one way ANOVA, $p=0.0659$, p=4-7).

The turnover of dopamine was assessed by performing multiple stimulations in quick succession and determining what percentage of the dopamine release was maintained by recycling. Stimulations were performed every 30 s, which excludes the contribution of dopamine synthesis to the releasable pool, since synthesis occurs on the order of 5-10 minutes.(Xiao and Venton, 2015) Figure 3.7 shows that stimulated release decreases with multiple stimulations, but that RNF11 RNAi flies did not exhibit as large a decrease in dopamine as did control or RNF11 overexpressing flies. There was a significant main effect of both stimulation number (two-way ANOVA, $p<0.0001$) and genotype ($p<0.0001$), but no interaction ($p=0.1468$). Post hoc tests showed that RNF11 RNAi flies have a higher plateau than both control and RNF11 overexpressing flies ($p<0.0001$ for both). The data were fit to a single-phase exponential decay, which were significantly different (comparison of fits, $p<0.0001$). Control flies plateaued at 51% of the initial stimulated release, RNF11 overexpressing plateaued at 59%, and RNF11 RNAi flies plateaued at 75%. Thus, significantly more dopamine is being recycled for reuse in RNF11 RNAi flies than in control or RNF11 overexpressing flies.

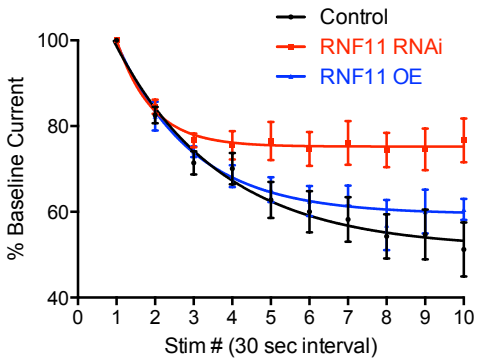

Figure 3.7 - Dopamine turnover is faster in RNF11 RNAi flies. Larval CNS was stimulated for 2 seconds every 30 seconds, and the peak oxidation current for dopamine was monitored. There was a significant main effect of both stimulation number ($p<0.0001$) and genotype ($p<0.0001$), but no interaction ($p=0.1468$, two-way ANOVA, $p=4$). Post hoc-tests showed that RNF11 RNAi flies have a higher plateau than both control and RNF11 overexpressing flies. The data for each genotype was fit to a single-phase exponential decay, which were significantly different (comparison of fits, $p<0.0001$).

Discussion

RNF11 downregulation has been implicated in the late pathogenesis of PD; however early effects of RNF11 depletion have not been studied. In addition, no study had examined the effect of RNF11 knockdown on dopamine release and clearance. Here we describe for the first time that knocking down RNF11 increases dopamine neurotransmission early in *Drosophila* development. This effect was specific for dopamine, as knocking down RNF11 in serotonin or octopamine neurons did not affect stimulated release. RNF11 RNAi larvae had faster rates of dopamine uptake and more dopamine available for rapidly repeated stimulations than control or RNF11 overexpressing flies, indicating that RNF11 knockdown promotes recycling of dopamine and maintenance of the releasable pool. RNF11 downregulation in neurodegenerative tissue has been postulated as a compensatory response to protect dopaminergic neurons from the insult of PD. Our work indicates that dopaminergic cells with downregulated

RNF11 have more phasic dopamine release. PD patients do not exhibit motor symptoms until a majority of the dopaminergic neurons are dead. Therefore downregulation of RNF11 may be a mechanism by which the remaining cells compensate for that loss to maintain the long, symptom-free progression that characterizes this movement disorder.

RNF11 knockdown specifically increases dopamine release

RNF11 RNAi flies had about half the normal levels of RNF11 expression and had significantly higher stimulated dopamine release than control flies. This doubling in release is about equivalent to blocking the D2 autoreceptors with flupenthixol, which shows that release is greatly affected by the RNF11 knockdown. However, the increase in release is not due to modulation of D2 autoreceptors, since application of flupenthixol doubled the release in RNF11 RNAi flies as well as controls. One explanation for greater release could be greater synthesis of dopamine. However, RNF11 RNAi flies did not have significantly higher dopamine levels than control flies. RNF11 knockdown flies did have significantly more larval dopamine tissue content than RNF11 overexpressing flies, indicating that synthesis might be somewhat affected by changing RNF11 levels, but the effect is certainly not a doubling of tissue content. RNF11 knockdown flies also have greater stimulated release when stimuli were closely applied, showing that they have more dopamine turnover to maintain a larger releasable pool. Thus, the main finding of this work is that RNF11 RNAi flies are able to increase dopamine release and maintain the

releasable pool, and this effect was not primarily mediated by D2 autoreceptors or synthesis.

To test the specificity of release, RNF11 RNAi knockdown was also performed in serotonergic or octopaminergic neurons. Stimulated release of serotonin or octopamine was not affected by RNF11 RNAi knockdown. This demonstrates that the effect of RNF11 knockdown is not universal to all neurotransmitters, but is more specific for dopamine. Dopamine, serotonin, and octopamine are all packaged into vesicles by the same mechanism: vesicular monoamine transporters. Humans encode two VMAT genes: VMAT1 and VMAT2, while *Drosophila* have only one: dVMAT.(Martin and Krantz, 2014) Since RNF11 RNAi affects only dopamine release, it is unlikely that the mechanism is through dVMAT, since that would also affect other amine neurotransmitters such as serotonin and octopamine.

While RNF11 knockdown flies had dramatically larger stimulated dopamine release, overexpressing RNAi by 4.2 fold did not significantly change the level of stimulated release. However, the tissue content of dopamine in RNF11 overexpressing flies was significantly lower than in RNF11 knockdown flies, and close to significantly lower ($p=0.0510$) than control flies. These data indicate that there is some compensation happening in the dopamine neurons that allows the RNF11 overexpressing flies to maintain normal stimulated release, even when the tissue content is somewhat lower. D2 autoreceptors do not appear to be responsible for this effect, as the magnitude of change with flupenthixol was not different than control or RNF11 RNAi flies. Interestingly, the

turnover of dopamine is similar to control, meaning the tissue can support the same level of release with RNF11 overexpression even though tissue levels are somewhat lower.

In humans, RNF11 functions as part of the deubiquitination enzyme complex A20 to dampen the signaling cascade that leads to NF-κB activation.(Pranski et al., 2013b) Overexpressing RNF11 leads to a decrease in NF-κB function and knocking down RNF11 increases NF-κB function.(Shembade et al., 2009) In this work we see effects on release, tissue content, and dopamine recycling in dopaminergic neurons with decreased RNF11, which may be due to increased NF-κB function. NF-κB has multiple targets and future studies would be needed to discern whether the increase in release works through NF-κB and how its downstream targets work together to affect release. However, we see a limited effect on release and tissue content with RNF11 overexpression. This may be due to NF-κB already functioning at a low baseline in healthy dopaminergic cells, and further downregulation having limited downstream effects.

RNF11 RNAi flies have increased dopamine uptake

RNF11 RNAi and overexpressing flies exhibit clear changes in dopamine uptake. RNF11 RNAi flies had significantly faster uptake than control flies and RNF11 overexpressing flies had a significantly slower uptake than control. The affinity of the transporter for dopamine did not change. A change in V_{max} often relates to the number of transporters expressed on the surface. A greater V_{max} in RNF11 RNAi flies may be due to greater dDAT expression, indicating that

RNF11 may affect the trafficking of dDAT. RNF11 could affect the surface levels of DAT by modulating the endocytic pathway.(Gabriel et al., 2013) Ubiquitination of vesicles is important for vesicle trafficking.(Chen and Sun, 2009) RNF11 RNA and protein has been found in exosomes, and RNF11 localizes to complexes that mediate endocytosis and endosome trafficking.(Pisitkun et al., 2004; Gonzales et al., 2009; Hong et al., 2009; Kostaras et al., 2014) RNF11 regulates the switch between recycling and degradation of endosomes.(Santonico et al., 2014) Therefore, its knockdown could lead to a higher proportion of DAT being recycled to the membrane rather than degraded in the endosome pathway. Our studies found faster uptake in RNF11 RNAi flies, which would be consistent with this faster endosome recycling mechanism, which is NF-κB independent. However, there are also NF-κB downstream pathways that could regulate uptake. Overexpressing RNF11 leads to less activated NF-κB and thus less transcription of BDNF. In mice with 50% of normal BDNF levels, the V_{max} of dopamine uptake was reduced (Bosse et al., 2013), which is consistent with the decrease V_{max} we observed in RNF11 overexpressing *Drosophila*. However, $BDNF^{+/-}$ mice also showed a decrease in dopamine release, which was not found in the RNF11 OE *Drosophila* model. Thus, the RNF11 effects on release and uptake cannot be explained by just one of the known downstream targets of NF-κB.

The turnover of dopamine within RNF11 RNAi flies is also faster, indicating that the mechanisms for dopamine repackaging and release are upregulated when RNF11 is knocked down. The increased uptake would lead to more dopamine being available for recycling, thus dopamine release is

maintained for closely repeated stimulations. This maintenance of the pool is not explained by the reverse transport of dopamine through DAT or through the downregulation of D2 dopamine autoreceptors. There is also a decrease in the uptake of dopamine in RNF11 overexpressing flies, allowing dopamine to be active in the extracellular space for longer. Release and turnover levels are maintained in RNF11 overexpressing flies, despite the lower tissue content and slower uptake. This normal releasable pool maintenance points to other mechanisms that are helping to maintain release in RNF11 overexpressing flies and determining this mechanism in the future would give more insight into the regulation of dopamine turnover. The increased tissue content, increased release, and faster turnover of dopamine seen in RNF11 RNAi flies could also occur due to a decreased metabolic breakdown of dopamine in the cytoplasm after uptake. The dopamine metabolic pathways are poorly characterized in *Drosophila;* however they would also likely metabolize serotonin and octopamine.(Suh and Jackson, 2008; Freeman et al., 2013; Ueno and Kume, 2014; Yamamoto et al., 2014) Therefore, metabolism is unlikely to be the cause of the dopamine release and turnover effects upon RNF11 knockdown.

Implications of RNF11 effects on dopamine neurotransmission in PD

RNF11 affects many pathways important to proper neuronal functioning that could make it important in the cellular response to PD. The insult in PD that specifically causes dopaminergic cells to begin dying is still not clear. However, there is a multi-decade compensation that is well known in PD, during which remaining neurons continue to support dopaminergic neurotransmission, even

with substantial loss of dopaminergic neurons.(Hawkes et al., 2010) RNF11 is downregulated in neurodegenerative diseases, including PD. Here we present the first evidence that RNF11 knockdown increased dopamine release and uptake, which may represent the mechanism by which dopaminergic cells maintain functional levels of dopamine despite the loss of a substantial percent of the local neuronal population. Future studies could examine the importance of RNF11 in PD by simultaneously manipulating RNF11 and known PD genes in *Drosophila*, such as *PINK1* and *parkin* (Park et al., 2006) to see the phenotypic effects of RNF11 on disease progression as well at the effects on dopamine neurotransmission. In addition, studies to change the levels of RNF11 knockdown could show the extent to which further decreases in RNF11 increase dopamine release and whether RNF11 could be a target for future PD therapies.

Conclusions

RNF11 has been implicated in the pathophysiology of human PD but its effect on dopamine neurotransmission was unknown. Here, we show that knocking down RNF11 causes a doubling of dopamine release, although RNF11 overexpression did not change release. This effect was dopamine specific, as RNF11 knockdown does not have a similar effect on the serotonergic or octopaminergic neurotransmitter pathways. RNF11 knockdown increased and RNF11 overexpression decreased the rate of dopamine uptake, showing that RNF11 affects both dopamine release and uptake. Future studies could identify the extent to which the effect of RNF11 is mediated by NF-κB or endosome recycling. These results are important for understanding PD, as the upregulation

of dopamine signaling in PD patients that have reduced RNF11 expression may explain why patients are asymptomatic despite neuron loss. RNF11 may also be a future biomarker or drug target for detecting or treating PD.

Acknowledgements

The authors would like to thank the Hirsh and Jayaraman labs for reagents and fly stocks, as well as Mark Wightman for the TarHeel CV software. Also, Karol Cichewicz for his help with fly selection. Funded by Biogen and NIH (MH085159).

Chapter 3 References

Anderson LR, Betarbet R, Gearing M, Gulcher J, Hicks A a, Stefánsson K, Lah JJ, Levey AI (2007) PARK10 candidate RNF11 is expressed by vulnerable neurons and localizes to Lewy bodies in Parkinson disease brain. J Neuropathol Exp Neurol 66:955–964.

Borue X, Cooper S, Hirsh J, Condron B, Venton BJ (2009) Quantitative evaluation of serotonin release and clearance in Drosophila. J Neurosci Methods 179:300–308.

Bosse KE, Maina FK, Birbeck JA, France MM, Joseph JP, Colombo ML, Mathews TA (2013) Aberrant striatal dopamine transmitter dynamics in brain- derived neurotrophic factor-deficient mice. J Neurochem 120:385–395.

Brand a H, Perrimon N (1993) Targeted gene expression as a means of altering cell fates and generating dominant phenotypes. Development 118:401–415.

Chen ZJ, Sun LJ (2009) Nonproteolytic Functions of Ubiquitin in Cell Signaling. Mol Cell 33:275–286.

Denno ME, Privman E, Borman RP, Wolin DC, Venton BJ (2016) Quantification of Histamine and Carcinine in Drosophila melanogaster Tissues. ACS Chem Neurosci:acschemneuro.5b00326.

Denno ME, Privman E, Venton BJ (2014) Analysis of Neurotransmitter Tissue Content of Drosophila melanogaster in Different Life Stages. ACS Chem Neurosci.

Freeman A, Pranski E, Miller RD, Radmard S, Bernhard D, Jinnah H, Betarbet R, Rye DB, Sanyal S (2013) Sleep fragmentation and motor restlessness in a Drosophila model of Restless Leg Syndrome. Curr Biol 22:1142–1148.

Gabriel LR, Wu S, Kearney P, Bellvé KD, Standley C, Fogarty KE, Melikian HE (2013) Dopamine transporter endocytic trafficking in striatal dopaminergic neurons: differential dependence on dynamin and the actin cytoskeleton. J Neurosci 33:17836–17846.

Garris PA, Wightman RM (1995) Regional differences in dopamine release, uptake, and diffusion measured by fast-scan cyclic voltammetry. In: Neuromethods: Voltammetric Methods in Brain Systems (A B, G B, RN A, eds), pp 179–220. Humana Press Inc.

Glass CK, Saijo K, Winner B, Marchetto MC, Gage FH (2010) Mechanisms Underlying Inflammation in Neurodegeneration. Cell 140:918–934.

Gonzales PA, Pisitkun T, Hoffert JD, Tchapyjnikov D, Star RA, Kleta R, Wang NS, Knepper MA (2009) Large-Scale Proteomics and Phosphoproteomics of Urinary Exosomes. J Am Soc Nephrol 20:363–379.

Hawkes CH, Del Tredici K, Braak H (2010) A timeline for Parkinson's disease.

Park Relat Disord 16:79–84.

Hirth F (2010) Drosophila melanogaster in the Study of Human Neurodegeneration. CNS Neurol Disord - Drug Targets 9:504–523.

Hong BS, Cho J-H, Kim H, Choi E-J, Rho S, Kim J, Kim JH, Choi D-S, Kim Y-K, Hwang D, Gho YS (2009) Colorectal cancer cell-derived microvesicles are enriched in cell cycle-related mRNAs that promote proliferation of endothelial cells. BMC Genomics 10:556.

Jackson B, Dietz S, Wightman R (1995) Fast-Scan Cyclic Voltammetry of 5-Hydroxytryptamine. Anal Chem 67:1115–1120.

Jacobs CB, Vickrey TL, Venton BJ (2011) Functional groups modulate the sensitivity and electron transfer kinetics of neurochemicals at carbon nanotube modified microelectrodes. Analyst 136:3557–3565.

Khush RS, Lemaitre B (2000) Genes that fight infection: What the Drosophila genome says about animal immunity. Trends Genet 16:442–449.

Kitching R, Wong MJ, Koehler D, Burger AM, Landberg G, Gish G, Seth A (2003) The RING-H2 protein RNF11 is differentially expressed in breast tumours and interacts with HECT-type E3 ligases. Biochim Biophys Acta - Mol Basis Dis 1639:104–112.

Klapoetke NC et al. (2014) Independent optical excitation of distinct neural populations. Nat Methods 11:338–346.

Kostaras E, Pedersen NM, Stenmark H, Fotsis T, Murphy C (2014) SARA and RNF11 at the crossroads of EGFR signaling and trafficking., 1st ed. Elsevier Inc.

Lesage S, Brice A (2009) Parkinson’s disease: from monogenic forms to genetic susceptibility factors. Hum Mol Genet 18:R48–R59.

Li MD, Burns TC, Morgan A a, Khatri P (2014) Integrated multi-cohort transcriptional meta-analysis of neurodegenerative diseases. Acta Neuropathol Commun 2:93.

Martin CA, Krantz DE (2014) Drosophila melanogaster as a genetic model system to study neurotransmitter transporters. Neurochem Int 73:71–88.

Park J, Lee SB, Lee S, Kim Y, Song S, Kim S, Bae E, Kim J, Shong M, Kim J-M, Chung J (2006) Mitochondrial dysfunction in Drosophila PINK1 mutants is complemented by parkin. Nature 441:1157–1161.

Pisitkun T, Shen R-F, Knepper M a (2004) Identification and proteomic profiling of exosomes in human urine. Proc Natl Acad Sci U S A 101:13368–13373.

Pörzgen P, Park SK, Hirsh J, Sonders MS, Amara SG (2001) The antidepressant-sensitive dopamine transporter in Drosophila melanogaster: a primordial carrier for catecholamines. Mol Pharmacol 59:83–95.

Pranski EL, Dalal N V, Van Sanford CD, Herskowitz JH, Gearing M, Lazo C,

Miller GW, Lah JJ, Levey AI, Betarbet RS (2013a) RING finger protein 11 (RNF11) modulates susceptibility to 6- OHDA-induced nigral degeneration and behavioral deficits through NF-κB signaling in dopaminergic cells. Neurobiol Dis 54:264–279.

Pranski EL, Van Sanford CD, Dalal N V, Orr AL, Karmali D, Cooper DS, Costa N, Heilman CJ, Gearing M, Lah JJ, Levey AI, Betarbet RS (2012) Comparative distribution of protein components of the A20 ubiquitin-editing complex in normal human brain. Neurosci Lett 520:104–109.

Pranski EL, Van Sanford CD, Dalal N V, Orr AL, Karmali D, Cooper DS, Gearing M, Lah JJ, Levey AI, Betarbet RS (2013b) NF-κB activity is inversely correlated to RNF11 expression in Parkinson's disease. Neurosci Lett 547:16–20.

Privman E, Venton BJ (2015) Comparison of dopamine kinetics in the larval Drosophila ventral nerve cord and protocerebrum with improved optogenetic stimulation. J Neurochem 135:695–704.

Santonico E, Mattioni A, Panni S, Belleudi F, Mattei M, Torrisi MR, Cesareni G, Castagnoli L (2014) RNF11 is a GGA protein cargo and acts as a molecular adaptor for GGA3 ubiquitination mediated by Itch. Oncogene 34:1–14.

Shembade N, Parvatiyar K, Harhaj NS, Harhaj EW (2009) The ubiquitin-editing enzyme A20 requires RNF11 to downregulate NF-kappaB signalling. EMBO J 28:513–522.

Suh J, Jackson FR (2008) Drosophila Ebony Activity is Required in Glia for the Circadian Regulation of Locomotor Activity. Neuron 55:435–447.

Ueno T, Kume K (2014) Functional characterization of dopamine transporter in vivo using Drosophila melanogaster behavioral assays. Front Behav Neurosci 8:1–11.

Venton BJ, Zhang H, Garris P a., Phillips PEM, Sulzer D, Wightman RM (2003) Real-time decoding of dopamine concentration changes in the caudate-putamen during tonic and phasic firing. J Neurochem 87:1284–1295.

Vickrey TL, Condron B, Venton BJ (2009) Detection of endogenous dopamine changes in Drosophila melanogaster using fast-scan cyclic voltammetry. Anal Chem 81:9306–9313.

Vickrey TL, Venton BJ (2011) Drosophila Dopamine2-like receptors function as autoreceptors. ACS Chem Neurosci 2:723–729.

Wu Q, Reith MEA, Wightman RM, Kawagoe KT, Garris PA (2001) Determination of release and uptake parameters from electrically evoked dopamine dynamics measured by real-time voltammetry. J Neurosci Methods 112:119–133.

Xiao N, Privman E, Venton BJ (2014) Optogenetic control of serotonin and dopamine release in Drosophila larvae. ACS Chem Neurosci 5:666–673.

Xiao N, Venton BJ (2015) Characterization of dopamine releasable and reserve pools in Drosophila larvae using ATP/P2X2 -mediated stimulation. J Neurochem 134:445–454.

Yamamoto S et al. (2014) A Drosophila Genetic Resource of Mutants to Study Mechanisms Underlying Human Genetic Diseases. Cell 159:200–214.

Chapter 4: Conclusions and Future Directions

This thesis describes work that improves the utility of *Drosophila* as a model organism for PD by expanding the available tools for studying dopamine neurotransmission. Using those tools, we have shown a new way to regulate dopamine release, through RNF11, that could be an interesting new target for pharmacological intervention early in PD development. These studies pave the way for many new exciting avenues of scientific inquiry, such as understanding how dopaminergic cells adapt to the insult of Parkinson disease and studying the role of monoamine neurotransmitters in sensory integration and sensory learning and memory. This chapter describes possible future directions for this work, including some preliminary work that provides a proof of concept for these new directions.

Measurements in adult brains and VNCs

In Chapter 2, I addressed some of the methodological drawbacks that limit the study of PD using *Drosophila* as a model organism. In order to study PD in the *Drosophila* model, we used the technique of FSCV to monitor dopamine in the medial protocerebrum for the first time. Dopamine release and uptake were characterized in this new brain region in larvae. By extending the new red light activated CsChrimson channel for use in this context, we paved the way for future experiments in deep adult tissues such as the middle brain. (Privman and Venton, 2015) The mushroom bodies and the central complex are highly innervated by dopaminergic neurons and are located in the medial protocerebrum of the fly brain. The central complex is comparable in function to

the basal ganglia of humans, where the loss of dopaminergic innervation causes some of the hallmark motor symptoms of PD. (Wessnitzer and Webb, 2006; Bouabid et al., 2015) These adult brain regions develop from the larval medial protocerebrum, where the DM, DL1, and DL2 clusters and later in development the PAM clusters of neurons send their projections in order to modulate behaviors such as olfactory learning and memory. The next step will be to make recordings from the central complex and mushroom bodies of adult flies, which will require overcoming additional methodological hurdles.

The first recordings in larval *Drosophila* were taken from the isolated ventral nerve cord. (Borue et al., 2009; Vickrey et al., 2009) The adult ventral nerve cord can also be isolated and recordings can be made from the abdominal ganglion, where many of the dopaminergic neurons are concentrated. (Monastirioti, 1999) However, the abdominal ganglion is only about 50 by 50 by 20 um (Boerner and Duch, 2010), making it difficult to target with a traditional 7 um diameter, 50 um long cylinder CFME (Figure 1A). Figure 1 demonstrates example data of a successful recording from an adult *Drosophila* VNC using a traditional CFME as a proof of concept. However, a smaller electrode is desirable to localize more precisely and reliably within the neuropil. If these methodological barriers can be overcome, the role of dopamine in modulating VNC behaviors such as grooming and copulation (Yellman et al., 1997; Crickmore and Vosshall, 2013) can be further elucidated, and the role of dopamine in maintaining proper movement in the context of Parkinson disease can be investigated.

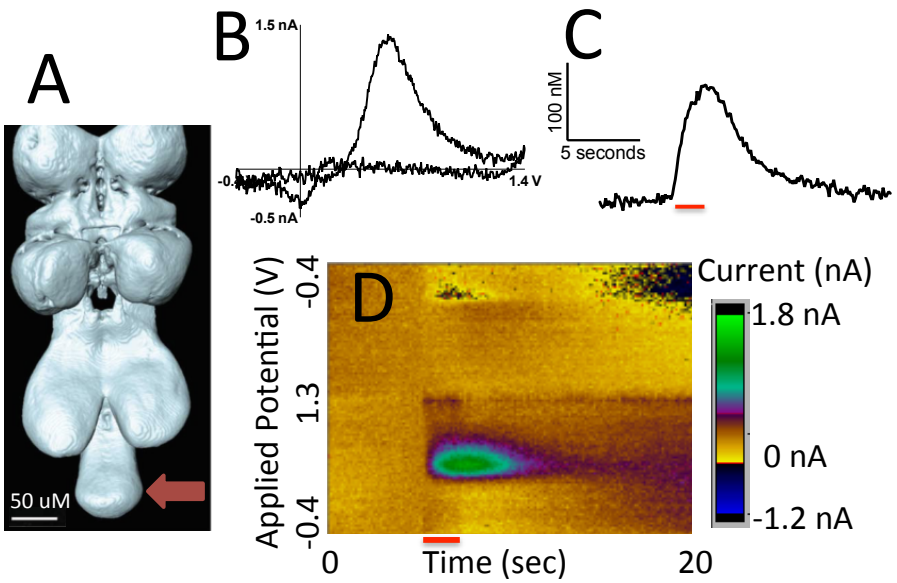

Figure 4.1 - Fast Scan Cyclic Voltammetry in adult *Drosophila* VNC. (A) 3D reconstruction of an adult *Drosophila* VNC, adapted from Boerner and Duch. Red arrow marks the abdominal ganglion. (B) Cyclic voltammagram showing the oxidation and reduction of dopamine. (C) Concentration of dopamine over time as 2 seconds of pulsed red light (red bar) causes CsChrimson-mediated neurotransmission. (D) Current in false color as the potential is ramped up and then back down (y-axis) over time (x-axis). Dopamine oxidation is seen in green and reduction is in dark blue.

In addition to the need for a smaller electrode, one of the major barriers to successful FSCV recording in adult *Drosophila* is the glial sheath. In order to make recordings from larval tissues, cuts must be made in order to allow the electrode to penetrate into the neuropil. (Borue et al., 2009; Vickrey et al., 2009) In the *Drosophila* CNS, there is a barrier homologous to the blood-brain barrier in humans known as the glial sheath consisting of flattened surface glia that encase neuropil structures. The glia form septate junctions similar to the astrocyte end feet that wrap myelinated axons in humans. (Freeman and Doherty, 2006) The typical carbon fiber microelectrode (CFME) used in FSCV experiments is cylindrical with a blunt end. In order to penetrate the tough glial sheath with minimal tissue damage, a sharper electrode must be designed.

Preliminary adult recordings were taken using a double-beveled disk electrode, which we named the dagger electrode, were taken in collaboration with the Jayaraman lab at Janelia Farm. The electrode was fabricated by taking a cylinder electrode, cutting it just above the glass seal, sealing the carbon fiber in with epoxy, beveling the electrode to a 45 degree angle point, and then rotating the electrode 180 degrees and beveling again to make a sharp point. A live, intact adult fly was immobilized with low melting point wax and the cuticle was removed from the top of the head (Figure 2A). A dagger electrode was inserted into the neuropil of the fly along with a small picosprizting pulled pipette (Figure 2B). Release was stimulated using ATP activation of $P2X_2$ channels, expressed in th containing cells. (Xiao and Venton, 2015) ATP was applied and dopamine release and uptake were monitored in both the mushroom bodies and central complex (Figure 2C-F).

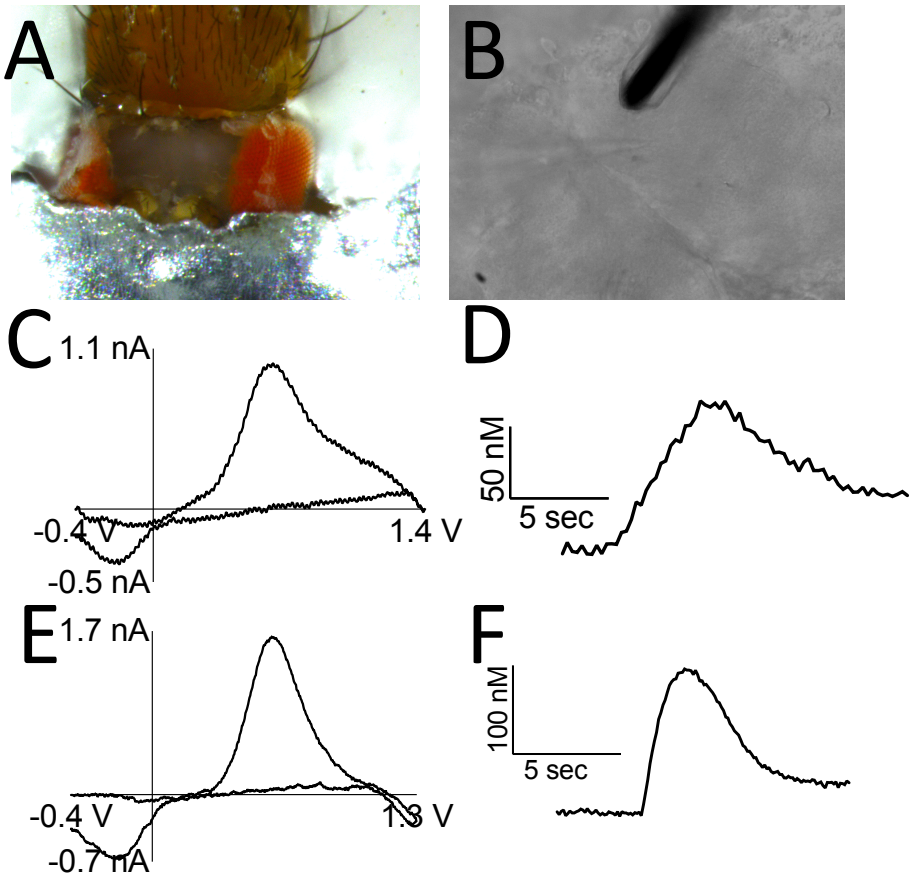

Figure 4.2 - Dopamine detection in the adult *Drosophila* central brain. (**A**) The adult fly was immobilized and the cuticle was microdissected from the top of the head. (**B**) The dagger electrode was inserted into the neuropil and dopamine release was stimulated using ATP picospritzed onto $P2X_2$-containing neurons. (C) Cyclic voltammagram of dopamine release in the mushroom body. (D) Concentration versus time trace in the mushroom body. (E) Cyclic voltammagram of dopamine release in the central complex. (F) Concentration versus time trace in the central complex. (**A+B**) Images by Romain Franconville.

The central complex and the mushroom bodies in the adult *Drosophila* are innervated by 600 known dopaminergic neurons, which are organized into 15 clusters of cells. (White et al., 2010; Bang et al., 2011) Processes from three different dopaminergic clusters project to the mushroom body neuropil. (Mao and Davis, 2009) The protocerebral anterior medial (PAM) neurons, which are poorly targeted by the TH driver, project to the medial portion of the horizontal lobes and are implicated in olfactory learning and memory (Figure 3). (Liu et al., 2012) The

paired posterior lateral 1 (PPL1) cluster of neurons project to the vertical lobes, junction, heel, and distal peduncle of the mushroom bodies, while the PPL2 neurons project primarily to the calyx of the mushroom bodies. (Mao and Davis, 2009) PPL1 consists of 12 neurons and plays a role in the reinforcement and retrieval of olfactory memories. (Claridge-Chang et al., 2009; Krashes et al., 2009) The central complex is an important region for behavior processing and sensory integration. (Kahsai and Winther, 2011) The central complex contains a neural network that mediates visual pattern recognition. (Liu et al., 2006; Pan et al., 2009) The main dopaminergic inputs to the central complex are the PPM3, PPL1 and T1 clusters. (Mao and Davis, 2009) These two regions of the adult *Drosophila* brain provide a model for studying the role of dopamine in the formation, retrieval, and integration of sensory information. Understanding the role of monoamine neurotransmitter in these processes could help in the design of psychotherapeutic agents to treat sensory integration disorders such as schizophrenia.

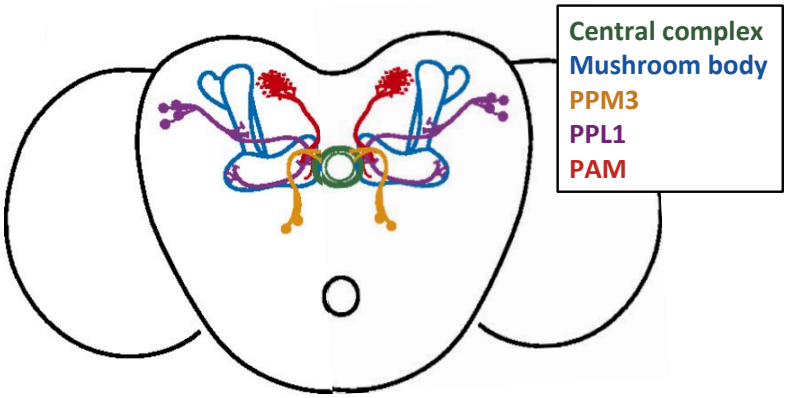

Figure 4.3 - Dopaminergic innervation of the adult *Drosophila* mushroom bodies and central complex. The PAM (red), PPL1 (purple), and PPM3 (gold) clusters of dopaminergic neurons project to the mushroom bodies and central complex. Adapted from Azanchi et al., 2013.

While preliminary recordings could be taken from the central brain of the adult *Drosophila* using the dagger electrode to penetrate through the glial sheath, the dagger electrode is still fairly large (~10 um diameter) compared to the areas we wish to record from. Therefore, in collaboration with the Bau group at University of Pennsylvania, carbon nanopipette electrodes (CNPE) were characterized for use in *Drosophila*. These extremely small, sharp electrodes are fabricated by pulling a quartz pipette, vapor depositing carbon on the inside, and then etching back the quartz to expose the desired length of carbon.(Rees et al., 2015) CNPEs that were only 200 nm in diameter and 7 um in length were used successfully to record dopamine from the larval ventral nerve cord (Figure 3). These methodological improvements combined with those described in Chapter 2 will facilitate the study of dopamine in the context of normal and PD aging and PD in *Drosophila*.

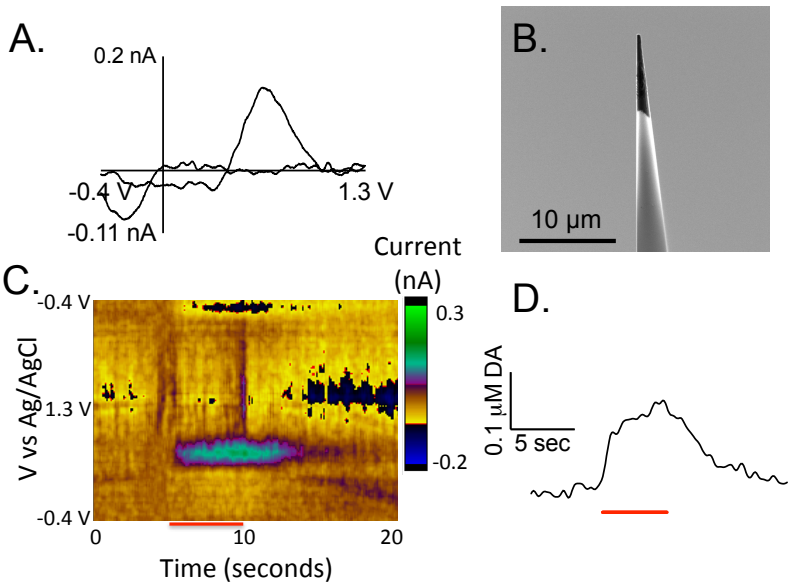

Figure 4.4 - Example CNPE measurement of endogenous dopamine evoked by a 5 second continuous red light stimulation. (A) Background-subtracted cyclic voltammagram of evoked dopamine. (B) SEM of a short CNP like the one used *in vivo*. (C) Color plot showing stimulated dopamine in a *Drosophila* larval

ventral nerve cord. Red light was applied from 5 to 10 seconds. (D) Extracellular concentration of dopamine over time as red light stimulates release (red line). Adapted from Rees et al 2015.

Measurements of dopamine in Parkinson models

The work described in Chapter 3 expands our understanding of the effects of RNF11 on dopamine neurotransmission by implicating RNF11 in the regulation of dopamine release and clearance. The next challenge is to study the effects of RNF11 in Parkinson disease model flies to understand the role of the observed downregulation of RNF11 in disease pathology. It is unclear how early in Parkinson's disease progression the dopaminergic neurons begin to malfunction in terms of their ability to release and uptake dopamine. There are multiple known genetic mutations that cause familial forms of the disease, including alpha-synuclein, *PINK1* and *parkin*, which can be modeled in the genetically tractable *Drosophila melanogaster*.(Whitworth, 2011)

PINK1 and *parkin* work together to maintain normal mitochondrial function. When they are mutated, the normal turnover of damaged mitochondria is impaired, leading to the mitochondrial dysfunction that is characteristic of the damaged and dying dopaminergic cells in Parkinson's disease. Additionally, *parkin* is known to impact the cell membrane expression of the dopamine transporter(Jiang et al., 2004), which clears dopamine from the extracellular space. Therefore there may be early changes in V_{max} in *parkin* mutant flies. Additionally, in older animals that have begun to lose their dopaminergic neurons due to *parkin* or *PINK1* mutations, the amount of dopamine available for release may be decreased.

PD can also be modeled in *Drosophila* by expressing human alpha-synuclein, which aggregates preceding cell death.(Varga et al., 2014) In mice overexpressing alpha-synuclein, dopamine release was decreased at every time point tested, with the earliest being 3-4 months of age (early mouse adulthood), preceding visible protein aggregation.(Janezic et al., 2013) However, dopaminergic signaling during the pre-symptomatic disease progression has not been well characterized. Building off of the advances described in Chapters 2 and 3, it should be possible to study the early changes that occur in dopaminergic neurotransmission in a variety of PD mutant and RNAi fly strains. By modulating PD genes in *Drosophila* containing CsChrimson in dopaminergic cells, it is possible to investigate the release and uptake of dopamine from the ventral nerve cord and medial protocerebrum structures (mushroom bodies and central complex) in larvae, young adults, and old flies.

PD can be modeled in flies through the expression of mutant disease proteins, the overexpression of endogenous proteins, or the knock down of proteins important to proper cellular function. Table 1, adapted from Whitworth (2011), summarizes some of the available PD fly models. Promising target proteins include Parkin and alpha-synuclein. By combining these models with RNF11 knockdown and overexpression, we can investigate RNF11 as a drug target in various forms of inherited and spontaneous PD. RNF11 modulation may allow for the continued symptom-free progression of Parkinson disease patients, as it modulates the ability of dopaminergic neurons to maintain extracellular levels of dopamine.

Figure 4.5 - Human genes linked to PD, their function, and fly homologs. Adapted from Whitworth (2011).

Gene/protein	Fly Homolog (CG#)	Putative Function
SNCA/α-synuclein	no homolog	Synaptic plasticity
Parkin	*parkin* (CG10523)	E3 ubiquitin-protein ligase
UCH-L1	*Uch* (CG4265)	Ubiquitin hydrolase/ligase
PINK1	(CG4523)	Mitochondrial kinase
DJ-1	*DJ-1α* (CG6646) *DJ-1β* (CG1349)	Oxidative stress sensor, chaperone?
Dadarin/LRRK2	(CG5483)	Kinase, GTPase
ATP13A2	No homolog	Lysosome
GIGYF2	(CG11148)	Insulin signaling
Omi/HtrA2	*HtrA2* (CG8464)	Serine protease
PLA2G6	*iPLA2-VIA* (CG6718)	Phospholipase
FBXO7	No homolog	Protein complex scaffolding
GBA	(CG31414, CG31148)	Glucocerebrosidase

The novel strategies discussed in this work could be combined with pharmacological interventions to help understand how different drug treatment regimens rescue dopaminergic neurotransmission at various stages of disease progression in the different mutant animals. *Drosophila* can provide a high throughput model for understanding pharmacology as the field moves towards increasingly personalized medicine.(Von Stockum et al., 2015) For example, deacetylase inhibitor trichostatin A (TSA) restores axonal transport in *Drosophila* leucine-rich repeat kinase 2 (LRRK2) Roc-COR mutants.(Godena et al., 2014) LRRK2 is found in the PARK8 locus and interacts with microtubules, affecting the transport of mitochondria in neurons.(Moon and Paek, 2015) By combining pharmacological interventions with the electrochemical and genetic approaches pioneered in this work, it will be possible to test how early deficits in dopamine neurotransmission can be ameliorated in PD patients and perhaps how disease progression can be slowed or halted using *Drosophila* as a model organism.

Final Conclusions

Overall, this dissertation provides an extension of the methods available to study dopamine in *Drosophila*. These methods were used to describe for the first time the role of RNF11 in the release and uptake of dopamine. These findings can now be extended to begin understanding of how dopaminergic neurons maintain normal gross function until a threshold level of them has died off. Future work using adult *Drosophila* can improve our understanding of this important process and help provide additional drug targets for the treatment of PD.

Chapter 4 References

Azanchi R, Kaun KR, Heberlein U (2013) Competing dopamine neurons drive oviposition choice for ethanol in Drosophila. Proc Natl Acad Sci U S A 110:21153–21158.

Bang S, Hyun S, Hong S-T, Kang J, Jeong K, Park J-J, Choe J, Chung J (2011) Dopamine signalling in mushroom bodies regulates temperature-preference behaviour in Drosophila. PLoS Genet 7:e1001346.

Boerner J, Duch C (2010) Average shape standard atlas for the adult Drosophila ventral nerve cord. J Comp Neurol 518:2437–2455.

Borue X, Cooper S, Hirsh J, Condron B, Venton BJ (2009) Quantitative evaluation of serotonin release and clearance in Drosophila. J Neurosci Methods 179:300–308.

Bouabid S, Tinakoua A, Lakhdar-Ghazal N, Benazzouz A (2015) Manganese Neurotoxicity: behavioral disorders associated with dysfunctions in the basal ganglia and neurochemical transmission. J Neurochem.

Claridge-Chang A, Roorda RD, Vrontou E, Sjulson L, Li H, Hirsh J, Miesenböck G (2009) Writing memories with light-addressable reinforcement circuitry. Cell 139:405–415.

Crickmore MA, Vosshall LB (2013) Opposing dopaminergic and GABAergic neurons control the duration and persistence of copulation in Drosophila. Cell 155:881–893.

Freeman MR, Doherty J (2006) Glial cell biology in Drosophila and vertebrates. Trends Neurosci 29:82–90.

Godena VK, Brookes-Hocking N, Moller A, Shaw G, Oswald M, Sancho RM, Miller CCJ, Whitworth AJ, De Vos KJ (2014) Increasing microtubule acetylation rescues axonal transport and locomotor deficits caused by LRRK2 Roc-COR domain mutations. Nat Commun 5:5245.

Janezic S et al. (2013) Deficits in dopaminergic transmission precede neuron loss and dysfunction in a new Parkinson model. Proc Natl Acad Sci U S A 110:E4016–E4025.

Jiang H, Jiang Q, Feng J (2004) Parkin increases dopamine uptake by enhancing the cell surface expression of dopamine transporter. J Biol Chem 279:54380–54386.

Kahsai L, Winther AME (2011) Chemical neuroanatomy of the Drosophila central complex: distribution of multiple neuropeptides in relation to neurotransmitters. J Comp Neurol 519:290–315.

Krashes MJ, DasGupta S, Vreede A, White B, Armstrong JD, Waddell S (2009) A neural circuit mechanism integrating motivational state with memory expression in Drosophila. Cell 139:416–427.

Liu C, Plaçais P-Y, Yamagata N, Pfeiffer BD, Aso Y, Friedrich AB, Siwanowicz I, Rubin GM, Preat T, Tanimoto H (2012) A subset of dopamine neurons signals reward for odour memory in Drosophila. Nature 488:512–516.

Liu G, Seiler H, Wen A, Zars T, Ito K, Wolf R, Heisenberg M, Liu L (2006) Distinct memory traces for two visual features in the Drosophila brain. Nature 439:551–556.

Mao Z, Davis RL (2009) Eight different types of dopaminergic neurons innervate the Drosophila mushroom body neuropil: anatomical and physiological heterogeneity. Front Neural Circuits 3:5.

Monastirioti M (1999) Biogenic amine systems in the fruit fly Drosophila melanogaster. Microsc Res Tech 45:106–121.

Moon HE, Paek SH (2015) Mitochondrial Dysfunction in Parkinson's Disease. Exp Neurobiol 24:103–116.

Pan Y, Zhou Y, Guo C, Gong H, Gong Z, Liu L (2009) Differential roles of the fan-shaped body and the ellipsoid body in Drosophila visual pattern memory. Learn Mem 16:289–295.

Privman E, Venton BJ (2015) Comparison of dopamine kinetics in the larval Drosophila ventral nerve cord and protocerebrum with improved optogenetic stimulation. J Neurochem 135:695–704.

Rees HR, Anderson SE, Privman E, Bau HH, Venton BJ (2015) Carbon Nanopipette Electrodes for Dopamine Detection in Drosophila. Anal Chem 87:3849–3855.

Varga SJ, Qi C, Podolsky E, Lee D (2014) A new Drosophila model to study the interaction between genetic and environmental factors in Parkinson's disease. Brain Res 1583:277–286.

Vickrey TL, Condron B, Venton BJ (2009) Detection of endogenous dopamine changes in Drosophila melanogaster using fast-scan cyclic voltammetry. Anal Chem 81:9306–9313.

Von Stockum S, Nardin A, Schrepfer E, Ziviani E (2015) Mitochondrial dynamics and mitophagy in Parkinson's disease: A fly point of view. Neurobiol Dis.

Wessnitzer J, Webb B (2006) Multimodal sensory integration in insects--towards insect brain control architectures. Bioinspir Biomim 1:63–75.

White KE, Humphrey DM, Hirth F (2010) The dopaminergic system in the aging brain of Drosophila. Front Neurosci 4:205.

Whitworth AJ (2011) Drosophila models of Parkinson's disease., 1st ed. Elsevier Inc.

Xiao N, Venton BJ (2015) Characterization of dopamine releasable and reserve pools in Drosophila larvae using ATP/P2X2 -mediated stimulation. J Neurochem 134:445–454.

Yellman C, Tao H, He B, Hirsh J (1997) Conserved and sexually dimorphic behavioral responses to biogenic amines in decapitated Drosophila. Proc Natl Acad Sci 94:4131–4136.